

NACA TN 2996

10369

# NATIONAL ADVISORY COMMITTEE FOR AERONAUTICS

TECHNICAL NOTE 2996

APPRAISAL OF HAZARDS TO HUMAN SURVIVAL

IN AIRPLANE CRASH FIRES

By Gerard J. Pesman

Lewis Flight Propulsion Laboratory  
Cleveland, Ohio



Washington  
September 1953

AFMDC  
TECHNICAL P.  
AFL 201





0066088

1E

## NATIONAL ADVISORY COMMITTEE FOR AERONAUTICS

## TECHNICAL NOTE 2996

## APPRAISAL OF HAZARDS TO HUMAN SURVIVAL IN AIRPLANE CRASH FIRES

By Gerard J. Pesman

## SUMMARY

The factors which affect the survival of human beings in airplane accidents followed by fire were studied by conducting full-scale crashes of transport- and cargo-type airplanes. Studies of burning airplane hulks supplemented the information obtained from the crash fires. The time interval during which occupants could escape from a burning airplane was determined by using the time histories of cabin temperatures and toxic gas concentrations in conjunction with data that define the environmental conditions which can be tolerated by human beings. Other hazardous factors, such as flying detached airplane parts, explosions, and crushing of the airplane structure, were also studied.

## INTRODUCTION

The injuries and the fatalities resulting from aircraft accidents are the result of four general factors: impact decelerations, fire, structural missiles, and destruction of occupied compartments. Recent aeromedical research has shown that human beings can tolerate severe decelerative forces if adequately restrained and supported. The remaining causes of death and injury must be studied if the hazard to occupants during otherwise survivable accidents is to be reduced to an acceptable minimum. A limited study of these additional hazards was possible as part of the comprehensive full-scale crash fire research program being conducted by the NACA Lewis laboratory. The results of the study are presented in this report.

The data presented were obtained by crashing instrumented full-scale transport- or cargo-type airplanes in such a manner that a large fire resulted. Fires built around previously crashed but unburned aircraft provided supplementary data. Time histories of the environmental temperatures and gas concentrations in the passenger and crew compartments were obtained while the airplane was burning. The structural disintegration of the airplane and flying parts were recorded during the crash by motion-picture cameras. Additional information was obtained by a careful post-crash examination of the wreckage.

These data were used in conjunction with physiological tolerance criteria in order to determine the time interval during which an escape attempt could be made. This time interval, subsequently named the "escape time," gives an indication of the relative hazard imposed by each of the factors affecting survival in the fire. The "escape time" is considered to be more important than the interval during which people could be expected to survive inside the fuselage because occupants must escape through their own efforts in the majority of accidents. The data also indicate some means of either increasing the escape time or minimizing the hazard.

The hazards associated with factors such as structural destruction and flying parts cannot be evaluated in terms of an escape time. In these cases the hazard is described and possible remedial measures are discussed.

#### CRASH PROCEDURE, EQUIPMENT, AND INSTRUMENTATION

Two types of airplane normally used by the military services for both cargo and personnel transport were used for these studies. The first group of airplanes employed was of the low-midwing twin-engine type similar to twin-engine commercial transports. The second group was of the high-wing twin-engine packet type. All the airplanes used were supplied by the military services and were no longer of use.

The studies were conducted by guiding an unmanned airplane along a fixed path under its own power and allowing it to strike preconstructed barriers that damaged the propellers, engines, landing gear, and fuel tanks. The airplane was guided by slaving the front landing wheel or wheels to a steel monorail placed in the center of a paved runway. This runway was long enough to allow the airplane to reach a speed of 85 to 95 miles per hour, approximately take-off speed. Removal of the main landing wheels by the barriers caused the airplane to slide along the ground on its belly while the additional damage to propellers, engines, and fuel tanks created the conditions conducive to fire. The crashes therefore simulated a take-off accident in which the likelihood of serious fire was high but the structural damage was moderate. The outboard fuel tanks were approximately three-fourths filled so that about 1000 gallons of fuel were involved in each crash. The fuel used was either standard 100/130 grade aviation gasoline or a low volatility fuel having a Reid vapor pressure of 0.1 pound per square inch. Figures 1 to 5 show various features of the crash site, crash operation, and damage inflicted on the airplane.

The data were recorded by motion-picture cameras located around the crash-site perimeter and by instrumentation installed in a shock-mounted heat-resistant box in the airplane. A complete description of the facilities and methods used for the crashes is given in reference 1.

Since all the required survival information concerning fire could not be obtained from the crashes, supplemental fire studies were made when necessary. Airplanes that did not burn when crashed were used for these studies. The major openings in the fuselage resulting from the crash were closed so that an essentially undamaged cabin was simulated. The fuel spillage on the ground and from the wing tanks was arranged to simulate that occurring in the full-scale crashes. Motion pictures of the cabin interior and airplane exterior were taken during the fire.

Other supplemental studies were also made. The equipment used in these cases is described briefly in the discussion.

Evaluation of the hazard associated with skin burning required computation of the rate with which heat would be transmitted to the exposed skin of airplane occupants. The heat is transferred to the occupants by convection from the hot gases and by radiation from the hot fuselage walls. The heat that could be transferred to an occupant's skin was computed from the temperature histories of matte-black copper sphere calorimeters placed at passenger locations within the fuselage. These spheres were approximately the same diameter as a human head. Since the head is not protected by clothing and will be more rapidly affected than clothed parts, heat transfer to the head will govern the escape time.

An airplane occupant exposed to a crash fire can also be injured by inhaling hot gases that enter the cabin, and can be poisoned by these same gases. These hazards were evaluated from time histories of the cabin atmosphere temperature and gaseous composition.

The temperature of the cabin atmosphere was measured by thermocouples shielded from the heat radiated by hot fuselage walls. The atmosphere in the cabin and the pilot's compartment was sampled periodically during the fire and subsequently analyzed. Carbon dioxide and oxygen concentrations were measured by the standard Orsat procedure. Carbon monoxide concentrations above 1 percent were also measured by the Orsat method. Smaller concentrations of carbon monoxide were measured by the Bureau of Standards colorimetric method (ref. 2). The estimate of aldehyde concentration was made by the sulfite-fuchsin colorimetric method.

#### ANALYSIS OF DATA

##### Thermal Injury

Of the various injuries that result from the exposure of human beings to abnormal temperature conditions, only skin injury and respiratory system damage were considered in this study. For the short

intervals considered typical of crash fire circumstances (less than 15 min), other forms of thermal injury, such as heat prostration, require heat source temperatures above those resulting in skin injury (fig. 3 of ref. 3).

Physiological criteria: skin injury. - On the basis of available physiological data, two criteria can be established that will limit the escape time when an airplane occupant's skin is exposed to heat. The first criterion is based upon the pain that is associated with the beginning of skin injury and that can be tolerated by people; the second is based upon data defining the thermal conditions that will inflict a second-degree burn on exposed skin surfaces.

Studies of infrared radiation on human skin (ref. 4) have shown that a skin surface temperature of 42° to 45° C (5° to 8° C above normal body temperature) is accompanied with "unbearable pain." This pain is sufficiently severe that, "According to lay reports, the feeling of facial pain may be strong enough to delay one from taking preventive measures to escape the fire" (ref. 4). If environmental temperatures inside the fuselage during a crash fire rise until the occupants feel pain of this magnitude, further escape attempts on the part of some individuals can be completely disorganized by panic.

The relation between heat absorbed by the skin and the time during which absorption occurs that causes unbearable pain is shown in figure 6. This figure is a modification of figure 3 presented in reference 4.

An investigation of thermal skin injury reported in reference 5 showed that skin burning, injury to the skin tissue, begins when the skin surface temperature is raised to 44° C (fig. 7). If this minimum skin surface temperature is maintained, progressively more severe injury occurs, the extent of the injury depending upon the duration of the exposure. Below 44° C the rate of cellular repair is equal to the rate of injury and no cumulative injury occurs. Because of the similar temperature values for pain and the beginning of skin injury, pain is a good indication that skin injury will occur if the application of heat continues. A skin surface temperature of 42° to 45° C (107.6° to 113° F) can then be used as one criterion limiting the escape time. The method of determining this escape time is described in appendix A.

Since some individuals can tolerate pain more readily than others without panic and could probably escape from a burning airplane even though exposed skin surfaces were severely burned, a second criterion for limiting the escape time is possible. This second criterion is based upon the combination of skin surface temperature and the duration of exposure to this temperature that produces a minimal second-degree burn. A minimal second-degree burn is one in which all cells in the

epidermal layer have been killed by heat. The relation between skin surface temperature and exposure time causing a second-degree burn is shown by the solid line on figure 7. This figure shows that if the skin surface temperature is  $44^{\circ}$  C ( $111^{\circ}$  F), an exposure of about 6 hours is required to produce a second-degree burn. If the skin surface is maintained at  $55^{\circ}$  C ( $131^{\circ}$  F), an exposure of only 20 seconds is required for a second-degree burn; while at a skin surface temperature of  $70^{\circ}$  C ( $158^{\circ}$  F), a second-degree burn will be inflicted in 1 second. The information presented in this figure makes possible the calculation of escape time as limited by a second-degree burn. With possible complicating factors neglected, a second-degree burn of face, head, and neck is considered survivable by medical authorities. The escape times based upon this criterion will be presented for comparison with the escape times as limited by pain and the beginning of skin injury. The method of calculating the second-degree burn escape time from a time history of calorimeter bulb temperature is also shown in appendix A.

Physiological criteria: respiratory system injury. - Since airplane occupants may inhale hot gases that could inflict respiratory system injury, a tolerance criterion must be established for this hazard also.

The results of studies reported in reference 6 show that the human body can tolerate ambient-air temperatures of  $240^{\circ}$  F without injury for periods of over 20 minutes. These exposures included breathing the ambient atmosphere in the heated chamber. This reference also reports an industrial case in which an engineer entered drying equipment at  $300^{\circ}$  F protected by several burlap bags. In this case his body was protected by the insulating capacity of the burlap bags but no such protection was mentioned for the respiratory system. No injury resulted. A case of human exposure reported in reference 4 in which body and face were exposed to air at  $390^{\circ}$  F for a short time resulted in only minor external burns at points where evaporative cooling from skin perspiration could not occur. Examination of experimental animals whose respiratory systems were subjected to hot gases showed that air hot enough to burn the skin of the face can be inhaled without causing damage to the windpipe or lungs (refs. 3 and 7). These data, however, do not indicate a sharply defined respiratory threshold temperature. Since the highest human respiratory system exposure without injury was  $390^{\circ}$  F, this temperature has been arbitrarily chosen as a threshold value to permit a gross comparison of the relative hazard of skin injury and respiratory damage.

Temperature histories and associated escape times. - Histories of the ambient and calorimeter temperatures in passenger and crew compartments during the various crashes together with the escape times as determined by the criteria described in the previous paragraphs are shown on figure 8. The pain and second-degree-burn escape times are indicated by appropriate labels. Pertinent data concerning type of airplane, type of

fuel, and wind velocity relative to the airplane are also included on each graph. For convenience in making comparisons from crash to crash, the escape times have also been tabulated in table I.

These temperature histories represent the thermal conditions that resulted from crashes in which fire occurred on both sides of the airplane. In three of the four crashes large volumes of fuel mist formed when fuel tanks were ruptured while the airplane was moving rapidly (fig. 9). When this fuel mist was ignited while the airplane was sliding, large mist fires developed. Figure 10 shows the extent of such a mist fire. These mist fires burn away in 15 to 20 seconds, leaving fires burning from fuel on the ground, on the wetted airplane structure, and pouring from the tanks. The size and extent of these fires are shown by the upper photographs of figure 11. In from 2 to 5 minutes these fires subsequently develop to the size shown by the lower photographs on this same figure.

Because the mist fires rise away from the airplane and also burn out in a few seconds, the air and calorimeter temperatures inside the fuselage do not increase. This effect is shown by inspection of the first 20 seconds of each temperature history (fig. 8). These cabin environment temperatures are not increased because the aluminum fuselage skin reflects most of the heat radiated by the fire; consequently, mist fires that touch the fuselage walls only momentarily while the airplane is sliding are not hazardous to the occupants.

The escape times tabulated in the third column of table I show that skin injury was imminent in as little as 53 seconds in the fuselage of the airplane used for crash 6. The escape time based on the second-degree-burn criterion, column 4, for the same airplane position is 59 seconds. These data show that, for the high rate of temperature rise which occurred at this airplane location ( $1200^{\circ}$  F/min), there was a 6-second difference in escape time as limited by pain and the inflicting of a second-degree burn. The intervals between the first feeling of pain and the inflicting of a second-degree burn for crashes 3 and 7, when the escape times are less than 100 seconds, are of the same order of magnitude as for the chosen example. It is apparent, therefore, that when a crash fire grows rapidly and the temperatures in occupied compartments rise with corresponding rapidity, little additional escape time can be gained beyond that indicated by the pain associated with the beginning of skin injury.

The time after impact at which the ambient temperature in personnel compartments reached the respiratory system threshold temperature of  $390^{\circ}$  F is given in column 5 of table I. The minimum time in which the ambient temperature reached the respiratory threshold was 60 seconds and the maximum time was 296 seconds. These results show that, in general, the respiratory threshold was reached in approximately the same time as

the skin burning threshold, 1 to 5 minutes. In one case (crash 6, pilot's compartment), the respiratory threshold was reached prior to the skin burning threshold. In this instance, hot gases were being carried into the pilot's compartment by wind and convection inside the fuselage. This comparison of the skin injury and respiratory injury escape times indicates that the magnitude of the difference is insufficient to warrant considering one type of injury more important than the other. Because of the rapidly rising ambient-air temperatures this result is applicable even though the respiratory injury escape time would be longer if more complete data on humans had indicated a higher tolerance to the inhalation of hot gases. Remedial measures would thus be required for both types of injury if additional escape time is to be provided.

The variation in escape time with position in a particular airplane during a fire and from one crash fire to another depends on the position of the passenger with respect to the main bulk of the fire, the wind direction and velocity, the area over which fuel is spilled during a crash, and the terrain on which the airplane comes to rest. The terrain determines where fuel will flow after it spills from the ruptured fuel tanks, which in turn determines where fire will be located with respect to the fuselage. The shorter escape times available in crash 3 as compared with crash 1 are the result of wind speed, wind direction, and terrain. During crash 1 the wind was fairly brisk (14 mph) and from such a direction that it carried the flame away from the passenger compartment in the fuselage. The airplane also came to rest on level ground with the result that spilled fuel remained pooled under the wings and the area of the fire did not increase rapidly. During crash fire 3 there was little wind so that the flames from both sides of the fuselage tended to merge, forming a canopy of flame around and over the fuselage. The airplane also came to rest on an upslope, causing fuel to run back so that the resulting fire more completely enveloped the fuselage. As a result, the escape time in the fuselage during crash 3 was little more than half that in the same location for crash 1 - 90 seconds as compared with 163 seconds, respectively.

The effect of the occupant's position in the airplane with respect to the major bulk of the fire is shown by the data from crash 6. In this fire the wind direction was such that the passenger compartment in the fuselage was almost completely bathed in flame while the front end and pilot's compartment were not involved (fig. 12). Subsequent growth of the fire both outside and inside the fuselage gradually involved the pilot's compartment and front end of the airplane. As a result the escape time as limited by pain was only 53 seconds in the fuselage as compared with 144 seconds for the pilot's compartment.

Passengers seated near windows that face a fire will be subjected to more intense radiation than those protected by the fuselage walls, and the available escape time will be correspondingly decreased. The

relative magnitude of this effect is shown by the comparison of the calorimeter bulb temperatures given in figure 13. Although both calorimeter bulbs were exposed to the fire in the forward end of the cabin, the bulb facing the window could also receive radiation directly from the fire on the left side of the airplane. As a result this bulb indicated a temperature of 700° F within 110 seconds after the fire started, while the bulb protected by the fuselage walls did not reach 700° F until 160 seconds had elapsed.

The plastic materials sometimes used for window panes soften rapidly when heated and melt so that passengers will be exposed directly to flame, hot gases, and smoke. Figure 14 shows two stages in the disintegration of such window materials.

Although these results indicate that the minimum escape time as limited by thermal injury is about 50 seconds, different crash circumstances may further reduce this minimum value. When there is direct contact between flame and the fuselage skin while the airplane is moving rapidly, the fuselage skin burns through quickly. Figure 15 shows the damage resulting from direct flame contact with the fuselage skin for  $7\frac{1}{2}$  seconds while the airplane was sliding to a stop. The fuel-air mixture was arranged to be practically stoichiometric in this case; thus the flame temperatures were above those of the smoky flame existing during convectionally aspirated fires. The damage shown is typical of the entire flame contact area. Under such circumstances, occupants seated near fuselage walls could be burned by flame when the fuselage skin burns through; thus the minimum escape time would be less than 50 seconds.

Effect of insulation on escape time. - Since commercial transport aircraft are equipped with sound and thermal insulation it was necessary to determine whether the thermal escape times in an insulated cabin would be essentially different from those listed in table I for uninsulated cabins. In order to obtain a valid comparison, two identical enclosures (the rear clam-shell doors from previously crashed cargo-type airplanes) were used. One of these enclosures was left uninsulated, the other was provided with 2 inches of glass wool held in place with a thin insulation and fabric pad. These enclosures were faced into the wind in such a position that fire would be similar around each enclosure. Pans containing equal quantities of fuel were placed in front of each enclosure and then ignited simultaneously. The ambient air and calorimeter temperature histories inside each enclosure were recorded.

The temperature histories for the insulated and uninsulated shells are shown in figure 16. This figure shows that in the initial stages of the fires the temperatures inside the insulated enclosure remained below those in the uninsulated enclosure. Seven and one-half minutes after the fires were started the insulated enclosure burned through. The temperatures inside this enclosure then increased rapidly and were equal to

those in the uninsulated enclosure 8 minutes after the fires were started. Thereafter, until the test was terminated, the insulated enclosure temperatures remained above those in the uninsulated enclosure. The uninsulated skin burned through 12 minutes after the test was started. Uninsulated skin melts away more slowly than insulated because heat from the fire can reradiate from the opposite skin surface.

As a result of these temperature conditions the thermal escape time for the insulated enclosure was about 8 minutes; whereas for the uninsulated enclosure, the escape time was  $8\frac{1}{2}$  minutes. These escape times show that the glass wool insulation presently used in commercial transport aircraft will not increase the escape time appreciably and may decrease the available time slightly. The glass wool insulation also offers little obstruction to the passage of flame and gases because it tends to shrink and fall away from its supports when exposed to direct flame contact. The shrinkage resulting from such flame contact is shown by figure 17.

Effect of fuel volatility on escape time. - When studying the effect of fuel volatility on escape time, two general fuel spillage conditions are recognized as being significant: one in which a large quantity of fuel mist is evolved, and one in which the fuel flows from ruptured fuel tanks to the ground in a predominantly liquid stream.

In two crashes in which the ignition of large volumes of low-volatility (0.1 lb Reid vapor pressure) fuel mist occurred, the resulting fires developed with the same rapidity as those crashes in which gasoline mists of comparable size were ignited. Figures 10 (gasoline fire, test 6) and 18 (low-volatility-fuel fire, test 7) show the fire resulting when gasoline and low-volatility fuel mists, respectively, were ignited under essentially similar circumstances. These photographs were taken at approximately the same time after ignition occurred and show that the fires had grown to approximately the same size in the same time interval.

Comparison of the escape times for crashes 6 and 7 (table I) shows that the escape time in the pilot's compartment for a gasoline fire (crash 6) was 144 seconds as compared with only 93 seconds in the same location for a low-volatility-fuel fire (crash 7). This result appears to indicate that the escape time is longer for gasoline. When comparing the escape time for the fuselage, however, the escape time associated with the gasoline fire was only 53 seconds, whereas the escape time for the low-volatility-fuel fire was 92 seconds. Further inspection of the data shows that these apparently contradictory results are explained by the difference in wind direction for the two crashes. During crash 6 the wind was more nearly perpendicular to the fore and aft axis of the fuselage so that the main fuselage was enveloped in flame while the

pilot's compartment was not. For this reason there was a difference of about 90 seconds in the escape time between the two positions. The wind conditions during crash fire 7, on the other hand, were such that the pilot's compartment and fuselage were both enveloped in flame and the escape times were nearly equal. Comparison of the data from these crashes thus gives no indication of significant escape-time advantage to be gained from decreasing the fuel volatility when large volumes of fuel mist are ignited and a large flash fire follows. The large quantity of heat released by the fuel-mist fire raises the temperature of the fuel tank environment above the flash temperature of the low-volatility fuel and most of the advantage expected from reduced fuel volatility is lost.

When fire involves fuels of different volatility spilled on the ground in liquid form, however, there is a difference in the rate of fire development, and thus a difference in escape time. In figure 19 are shown the time - fuselage skin temperature relations for three fires in which the fuel was allowed to pour to the ground from ruptured tanks of an unburned wrecked airplane hulk. The fuel was ignited by a torch on the ground. The development of the fire was recorded by motion pictures, and the time history of the airplane skin temperatures, by instruments. Wind conditions and fuel spillage rate were essentially similar in all tests. In order to preserve the hulk for successive fires, fire extinguishing was started at the time fire had reached the under surface of the wing, as indicated on the curves.

Comparison of the rate of fuselage skin temperature rise for fires involving gasoline and low-volatility fuel at nearly the same initial fuel temperature (fires 1 and 2, respectively, fig. 19) shows that the low-volatility-fuel fire developed less rapidly than the gasoline fire. A corresponding increase in escape time would result. During the gasoline fire the fuselage skin temperature increased about  $80^{\circ}$  F per minute, whereas the rate for low-volatility fuel was  $45^{\circ}$  F per minute. The gasoline fire developed so rapidly that it reached the under surface of the wing in about 50 seconds. A time interval of almost 200 seconds was required for the low-volatility-fuel fire to reach the same relative size. The final fuselage skin temperature resulting from the gasoline fire was less than for the low-volatility-fuel fire only because the gasoline fire was of shorter duration.

When the initial temperature of the low-volatility fuel was increased (fire 3, fig. 19), the escape-time benefit to be gained by using low-vapor-pressure fuel decreased. During fire 3 the initial fuel temperature was approximately  $85^{\circ}$  F as compared with  $60^{\circ}$  F for fire 2. Shortly before the fire was extinguished, the rate of temperature rise of the fuselage skin was practically equal in the two experiments:  $75^{\circ}$  F per minute for the low-volatility-fuel fire as compared with  $80^{\circ}$  F per minute for the gasoline fire. Furthermore, comparison of the times at which the fire had reached the underside of the wing indicates that the

85° F low-volatility-fuel fire had reached the same stage of development in 75 seconds that the gasoline fire had reached in 60 seconds. While it is difficult to generalize from one experiment, the results appear to show that increasing the initial fuel temperature decreases the escape-time advantage of the lower volatility fuel.

#### Toxic Gases

The consumption of cabin oxygen in the fire and the generation of toxic combustion products present a survival hazard in addition to the heat released. Carbon monoxide, carbon dioxide, aldehydes, fuel fumes, and smoke from burning fuel and oil are generally considered to be the most plentiful and hazardous of the combustion products that may be produced. Other toxic gases can be formed from the burning of doped fabrics, interior trim, and electrical insulation. The gases in this latter group were not encountered in this study.

Physiological criteria: carbon monoxide and oxygen deficiency. - The presence of carbon monoxide and subnormal oxygen concentration both result in anoxia (anoxemia); therefore the effects of these two gases will be considered together. Carbon monoxide produces anoxia by combining with the hemoglobin to form carboxyhemoglobin and thus reduce the oxygen-carrying capacity of the blood. The physiological effects of increasing the carboxyhemoglobin concentration in the blood stream are shown in table II. This table shows that a carboxyhemoglobin concentration of 30 percent results in impaired judgment and fainting if any considerable exertion is attempted, while concentrations between 40 and 50 percent result in fainting and collapse on slight exertion. Since any escape attempt may involve exertion comparable with light work, a concentration of 35 percent carboxyhemoglobin in the blood stream was chosen as limiting the escape time.

The factors which determine carbon monoxide absorption rate are presented in reference 8. In this reference, it is shown that the percentage of carboxyhemoglobin in the blood stream depends upon the carbon monoxide concentration, the duration of the exposure, and the volume of air inhaled per unit time by exposed persons as determined by their activity. The volume of air inhaled per unit time is usually called the "pulmonary ventilation rate," but will be designated the ventilation rate in this discussion. The carbon monoxide concentration and duration of exposure are factors affected by the circumstances of the accident and resulting fire. The ventilation rate depends upon the type of work being done. For this analysis, it has been assumed that the ventilation rate would be equal to that resulting from light work. Reference 8 also shows that a decrease in the oxygen concentration has little effect upon the rate of carbon monoxide absorption rate except for changes caused in the ventilation rate by decreases in oxygen concentration. The rate of

carbon monoxide absorption was therefore corrected for the increased ventilation rate. The details of these calculations and corrections are shown in appendix B.

Physiological criteria: carbon dioxide. - The relatively short exposures to carbon dioxide of less than 10 to 15 minutes duration result in anoxia, irritation of the eyes and respiratory system, increased breathing rate, faintness, and finally, unconsciousness. The physiological data reported for carbon dioxide (ref. 9) show that the time of useful consciousness depends upon the concentration of carbon dioxide and duration of exposure but do not indicate a sharply defined threshold concerning the effect of abnormal concentration. Curves of this threshold of consciousness as interpreted by various investigators are shown in figure 20.

Since curve 2 (fig. 20) indicates the conditions that can be tolerated by most individuals and is little more severe than the limits chosen by Spealman or King (ref. 10), this curve was chosen as the basis for escape time calculations, although the results may indicate shorter escape times than would actually exist. The escape times were determined by the graphical method recommended in appendix 1 of reference 9. This graphical method is so arranged that the quantity of carbon dioxide inhaled under the varying concentrations that occur during a fire is equated to the maximum that can be tolerated as indicated by the tolerance curve.

History of gas concentrations and associated escape times. - Because of the difficulty experienced in obtaining samples of the cabin atmosphere during the fire following a crash, it was necessary to obtain the information on the concentrations of toxic gases in the airplane by setting fire to the hulks of airplanes that did not burn when previously crashed. The fires were arranged to follow the same history as the crash fires observed.

Time histories of the carbon monoxide, carbon dioxide, and oxygen concentrations in the pilot and passenger compartments together with the associated escape times for these hulk fires are shown in figure 21. For comparison with these gas concentration histories, the composition of single samples of the cabin atmosphere obtained during three crash fires is shown in table III. These samples were obtained at various times after crash impact, as shown in the fourth column of the table.

Inspection of the gas concentration histories and of the isolated values given in table III shows that the composition of the cabin atmosphere can vary widely with time from crash to crash. During the two hulk fires (fig. 21) the carbon monoxide concentration reached a maximum value of approximately 4 percent. The crash fire data show, however, that higher carbon monoxide concentrations are possible, since one concentration of 12 percent of carbon monoxide was measured. Combustion studies indicate that such concentrations are possible when the oxygen supply is limited.

The maximum carbon dioxide concentration encountered was approximately 15 percent in the forward part of the cabin in hulk fire 1 and occurred at the time of lowest oxygen concentration (5 percent) for this particular position. The minimum oxygen concentration encountered was less than 1 percent and occurred at the same location and time at which the 12 percent of carbon monoxide was encountered.

The escape times established by the chosen criteria and based on the concentrations measured during the hulk fires are listed in table IV. For purposes of comparison, the escape times as limited by a second-degree burn are also included. The second-degree burn escape times for these hulk fires range from 55 to 319 seconds and are comparable with those obtained during the crash fires and listed in table I.

The escape times as limited by carbon monoxide poisoning exceeded 300 seconds in both hulk fires (table IV). The relatively large escape times, as compared with thermal injury, associated with carbon monoxide stem from the fact that carboxyhemoglobin is formed only when carbon monoxide replaces the oxygen as it is used by the body. Since about 35 percent of the oxyhemoglobin in the blood must be converted to carboxyhemoglobin before fainting occurs upon slight exertion, the escape time can be expected to exceed 1 minute even though carbon monoxide concentrations of the order of 12 percent, the maximum shown in table III, exist continuously. Although the escape times as limited by carbon monoxide poisoning are longer than those limited by thermal skin injury, the difference does not justify disregarding carbon monoxide as a hazard.

The physiological tolerance limit for carbon dioxide was reached only once during the 10-minute sampling period for these two fires. In this one case, the forward cabin of hulk fire 1, the carbon-dioxide escape time was 365 seconds as compared with 398 seconds for carbon-monoxide poisoning and 151 seconds for a second-degree skin burn (table IV). In no case did carbon dioxide limit the escape time; thus carbon dioxide is not considered so important a hazard as either carbon monoxide poisoning or thermal injury.

The free hydrocarbon concentrations shown in figure 21 indicate that fuel-air mixtures near the combustible range exist at times in some of the passenger and crew compartments. These concentrations are due to the rapid evaporation of fuel, hydraulic fluid, and oil. The destructive distillation of wood sometimes used in the floor structure can also produce hydrocarbon vapors. Under hydrocarbon concentration conditions shown, fire can spread in the occupied compartments with explosive rapidity when the fuel-air mixture reaches the combustible range. Figure 22 shows the flame from such an explosion escaping through the forward fuselage door.

Human exposure to hydrocarbon vapors in the smaller concentrations even though fire does not occur can result in anesthesia and is fatal if the concentration is large or the exposure is too long. Gasoline vapor concentrations of 2 to 3 percent are fatal for short exposures (ref. 11). The exact timewise limits are not specified, however; thus, the effect of the concentrations recorded in these fires cannot be evaluated.

Smoke and aldehydes. - Both smoke and certain of the combustion products which are irritating to the eye can interfere with vision and make escape difficult. Motion pictures of the cabin interior during a fire showed that even strongly illuminated objects 20 feet away could not be photographed 10 seconds after smoke began entering the cabin even though the opening admitting the smoke was only 2 feet in diameter. Since fuselage walls can burn through in as little as 1/2 minute under conditions in which the airplane is not in motion, smoke can begin to reduce visibility inside the fuselage a short time after fire starts.

The odor of certain gas samples indicated that aldehydes were present in passenger and crew compartments. Analysis of one sample indicated an aldehyde concentration of approximately 1/2 of 1 percent. In this concentration, aldehydes are very irritating to the eyes and respiratory system (ref. 11). An escape time as limited by the various aldehydes could not be calculated because of insufficient physiological data.

Escape avenues. - Motion pictures of the fires were studied to determine where escape avenues through the exterior flame are most likely to be located. In general, the avenues through which escape would be possible and the time interval during which these avenues remain open are determined by three major factors:

- (a) The circumstances of the fuel spillage, which, in turn, determine whether one or both sides of the airplane are involved in fire, the location of fire with respect to the fuselage, and whether the fire receives a strong initial impetus or builds up gradually
- (b) The design of the airplane, which determines the location of the bulk of fuel with respect to the occupants
- (c) The wind direction with respect to the fire and fuselage

During the fires studied, the fuel spillage circumstances were such that fire existed on both sides of the airplane. In some of the crashes, the fuel mist was ignited and provided a strong initial impetus so that the fires built up rapidly. The fuel was located outboard of the engine nacelles, and the wings were attached to the fuselage at a position along the longitudinal axis typical of present-day commercial transport

aircraft. The wind varied from a light breeze to one having a speed of about 15 miles per hour and usually had a tail wind component because of the necessary orientation of the crash site with respect to the prevailing wind direction. These conditions thus result in a fairly severe fire with respect to the possibility of escape.

The escape conditions for four typical crashes are shown in figure 23. During crash 1 (fig. 23(a)), escape was possible in one direction or another at all times during the 5-minute interval studied. The upwind escape route to the right rear was open continuously after the initially spilled fuel had burned away. The appearance of this escape avenue is shown in figure 24(a). During crash fire 3 (fig. 23(b)), an escape route to the left front (fig. 24(b)) was open continuously during the 5-minute interval. The upwind route to the left rear was open for only 1 minute because fuel spilling from the ruptured tanks and fuel system running down the slope upon which the airplane came to rest reenveloped the aft part of the fuselage and would have prevented further escape in this direction. The escape avenue existing during this 1-minute interval is shown in figure 24(c). During crash fire 6 (fig. 23(c)), an escape avenue to the right front existed continuously after the initial flash fire involving the fuel mist had burned away. During crash fire 7 (fig. 23(d)), except for the 10- to 15-second intervals indicated, escape was also possible out of either side to the rear after the fuel mist had burned away. Figures 24(d) and (e) show the escape avenues during these two crash fires. Although this analysis indicates that escape avenues exist in the majority of crash fires, this result must be qualified to some extent. Landings and take-offs are normally made into the wind; consequently, if an accident occurs and fire spreads rapidly to both sides of the airplane, flame would be carried past the main passenger compartment doors, effectively blocking escape toward the rear. Furthermore, passage through the forward end of the fuselage and thence through escape hatches and into a forward escape avenue is frequently obstructed by galley equipment, baggage storage, and crew accommodations plus possible damage to the forward end of the fuselage. Under such circumstances escape from many present transport airplanes would be difficult. This qualification, however, does not change the fact that escape avenues exist with sufficient frequency that measures for increasing the escape time inside the fuselage are justified.

Rigorous specific procedures to be followed in seeking an escape avenue cannot be formulated on the basis of these results. The study of various escape avenues discussed in the previous paragraphs indicates that, generally, the most likely location of escape avenues will be toward the upwind portions of the airplane unless fire exists on only one side of the fuselage. This result can also be extensively modified, however, by the fuel spillage pattern and the airplane design. An example of the effect of fuel spillage pattern is shown by a comparison

of the escape avenues for crash fires 6 and 7, in which the wind and terrain conditions were similar. The escape avenue for crash fire 6 (fig. 23(c)) is toward the right front, while for crash fire 7 (fig. 23(d)) escape was possible from either side of the rear end of the airplane, both upwind and downwind. Study of the motion pictures of these two fires shows that this difference in possible escape routes is the result of differences in fuel spillage pattern caused by variations in the extent of fuel tank damage. In the case of airplanes with the wing and fuel tanks well forward with respect to the fuselage, the most feasible escape route could be toward the rear because of the protection afforded by the fuselage, which together with the convective lifting of the flame would allow occupants to escape rearward and underneath the flame even though a headwind exists.

#### Missiles

The motion pictures of crashes and the post-crash examination of airplanes that were crashed without burning indicated the hazard imposed by detached airplane parts and explosion-propelled fragments. No data were obtained concerning the hazard resulting from normally unattached cabin equipment or equipment torn from its moorings within the airplane that become missiles under the effect of impact decelerations. All such equipment was salvaged from the airplanes before the crash.

Detached propeller parts. - The impact of hollow steel propeller blades with an obstacle with the engines at take-off power sometimes causes the entire blade to twist out of the hub, as shown by figure 25. In some instances detached blades passed through both cabin walls and then traveled 400 to 500 feet. Figure 26 shows the holes made in the upper part of the fuselage by two detached blades.

Forged aluminum blades generally do not twist out of the hubs but the tips break off and become missiles (fig. 27). It should be noted that the propeller section shown is a part broken from the blade after the tip had already been removed. A single blade may thus provide more than one missile. Occasionally an aluminum blade breaks at the shank. The flying blade fragments generally penetrate one fuselage wall and then ricochet from the opposite wall or other cabin structure. Figure 28 shows nine holes made in the wall of a fuselage by fragments from the right propeller.

Since the propellers of the airplanes used in this study rotate in a clockwise direction, the distribution of damage to the fuselage by propeller parts (fig. 29) indicates that parts broken from the propellers separate from the hub or parent blade in a half revolution or less after an obstacle has been struck. The direction of motion of such parts is thus determined by the direction of motion in the lower half of the

propeller. Turning propellers in such a direction that the motion of the blades below the center of rotation is away from the fuselage would reduce the probability of propeller fragments entering the airplane. The propeller fragments broken from the blade upon ground impact would then have an initial impulse directed away from the fuselage.

Landing gear parts. - Front landing-wheel strut and support structure broken in the crash impact can penetrate the fuselage. Figure 30 shows a hole approximately 2 by 3 feet torn in the floor 20 feet aft of the nose-wheel location by the broken front-wheel strut and guide slipper which is attached to the strut in place of the front wheel. These parts came through the floor at high velocity, struck the instrument box, and rebounded to the position near the front door shown in figure 31. Another example of floor damage caused by destruction of the front landing gear is shown by figure 32. Figure 33 shows the destruction of the bulkhead to which the landing gear is attached. This structure came to rest practically in the dummy's lap and the entire floor was raised approximately 3 feet. A person seated in this location would certainly not have been able to escape serious injury. It is expected that destruction similar to that shown in these figures would result if the front landing wheel and strut were to collide with a solid obstacle during a forced landing. The hazard from dislodged landing-gear parts is minimized if the crash occurs with the landing gear retracted.

Explosions. - The explosion of large quantities of fuel vapor - air mixtures that may be formed within the wings following damage to the fuel system may spread flaming fuel and wing parts over distances several times the wing length. Wing explosions may occur if the initial ignition is delayed a sufficient time for considerable mixing of fuel and air to occur in the wing. The violence of such explosions is shown by figure 34. These three photographs show an explosion and the resulting wing-structure damage when an explosive mixture in the wing panel outboard of the fuel tanks was ignited  $4\frac{1}{2}$  seconds after impact.

Once the wing fuel is burning the likelihood of explosions declines and the explosions of pockets of fuel-air mixtures that do occur are seldom of sufficient violence to project wing parts into the air or to scatter flaming fuel. Damage under these circumstances is usually limited to tearing of the wing skin. Figure 35 shows the effect of a wing explosion that occurred after the main fire had been burning for about 9 minutes.

The explosion of hydraulic equipment, such as struts, actuating cylinders, and accumulators, containing trapped liquids usually occurs after the fire is well developed. Because these members of the hydraulic system are massive, they can withstand the heat of an intense fire for several minutes before explosive failure occurs. The accumulated

parts of a hydraulic strut cylinder that exploded in a crash fire are shown in figure 36. A fragment of hydraulic strut cylinder wall that was propelled about 150 feet when the strut exploded is shown in figure 37. The danger to airplane occupants from this source is particularly significant because many components of the hydraulic system and occasionally large quantities of fuel are carried within the fuselage.

#### Structural Destruction of Occupied Compartments

The airplanes that did not burn were also carefully studied for information concerning the hazards to which occupants would be exposed when the structure surrounding and supporting the occupants is damaged. The damage that resulted in these crashes can be considered typical of a moderately severe wheels-up belly landing.

Floor-structure damage. - The floor structure of the low-midwing, twin-engine type airplane is not damaged when the landing is made on a solid surface like dry or frozen ground or on pavement. The fuselage skin supporting structure and the nacelle structures deform and absorb the landing shock, thus protecting the floor and upper fuselage structure. Figure 38 shows the exterior of such a fuselage and shows that there was no appreciable deflection of the floor line.

Aircraft in which the floor and the fuselage skin are attached to the same structural members are considerably damaged when subjected to belly landing conditions. The entire vertical impact and sliding friction forces are imposed on this structure. When the landing is made upon a solid surface like a paved runway or hard dry or frozen soil, structural distortion such as shown by figures 39 and 40 occurs. The side frame and floor support members bend, allowing the corner bent connecting these two members to rotate (fig. 39). The seats and seat belts for fuselage occupants are attached to this corner bent. The floor support members in the front end of the fuselage are usually bulged upward slightly (fig. 40). This small distortion is not dangerous to occupants.

If the landing surface is soft and yielding like mud and is several inches deep, the floor structure may be severely damaged. Loose material enters the floor structure through the front landing-gear opening or through breaks in the fuselage skin and packs into the spaces between the fuselage skin and floor, thus distorting and bulging the floor structure. Extreme examples of such damage are shown in figure 41. The floor was bulged upward from 2 to 3 feet and the corner bent was rotated from  $20^{\circ}$  to  $30^{\circ}$  from its original position. Further rotation of this corner bent occurs when the airplane is subjected to side loads that in turn impose further vertical loads on the structure. Such a situation is shown in figure 42. In this case the corner bent has been rotated

from 90° to about 120° from its original position and at the rear appears about to fold under the floor. The hazard to occupants under such circumstances would depend upon the extent to which the corner bent has been rotated and the location of the occupant with respect to the damage.

Lateral collapse of fuselage. - Lateral collapse of rectangular fuselage structures used in some cargo aircraft may occur if the fuselage is subjected to side loads such as would result if an airplane were involved in a ground-loop accident and the main landing gear collapsed.

Incipient fuselage collapse was noted in one crash in which the airplane was placed in a ground loop by removing only one of the main landing gear assemblies at the crash barrier. The other main landing gear was left undamaged.

The damage resulting from the lateral load on the fuselage is shown in figures 43(a) and (b). The vertical wall members were torn away from the ceiling members (fig. 43(a)), and several vertical wall members showed buckling and shearing (fig. 43(b)). In figures 43(c), (d), and (e) are shown a further collapse of the fuselage structure when a second airplane was ground looped about 120° from its original direction after both main landing wheels were removed. The vertical wall members were buckled as shown by figure 43(c), several of the vertical members were torn away from the ceiling members as can be seen in figure 43(d), and the fuselage wall was bulged and distorted as shown by figure 43(e). The instrument box, by supporting the fuselage ceiling (fig. 43(c)), prevented the fuselage from collapsing completely.

#### CONCLUDING REMARKS

The implications of the data and results presented in the preceding sections should be considered with respect to airplane construction and operation. Certain remedial measures may be suggested that would increase the time available for escape or make the escape less difficult. The results of this study indicate that approximately 50 seconds would be available for escape in all but the most severe fires, although in some cases passengers must move away from areas of burned-through fuselage skin in as few as  $7\frac{1}{2}$  seconds.

Of the possible protective measures that can be suggested, the data presented have shown that additional escape time cannot be provided by the present transport sound and thermal insulation. Therefore,

the substitution of other materials that could serve as an adequate flame and gas barrier as well as thermal and sound insulation should be considered.

In order to extend the escape time, such a proposed heat, gas, and sound barrier must satisfy definite requirements in addition to that of thermal and sound insulation. Study of the various modes whereby heat is transferred from the fire to the occupants shows that more than half the heat absorbed by the exposed human skin is transmitted by radiation; thus the barrier must reflect a large percentage of the infrared radiation from the fire. The barrier must also be essentially gas tight in order to exclude flame, hot toxic gases, and smoke. Molten metal from the melting fuselage skin must not drip through on the occupants; therefore, the insulation should be able to support the weight of the molten metal that drips on it. A barrier satisfying these requirements would also have the advantage of excluding the steam formed by the use of water in rescue operations. Since melting of the fuselage skin and horizontal stringers would leave only the main frames and bulkheads to support the barrier, it must have sufficient mechanical strength to support itself between the frames or bulkheads. The Bureau of Standards has conducted exploratory tests on various combinations of intumescent paint, insulation, and metal foil for barriers that might increase the fire resistance of the fuselage. The results indicate that the fire resistance of an aircraft fuselage can be modified, but the differences obtained with the materials used in this study were not of sufficient value to justify detailed consideration at this time.

A fire barrier alone, however, is not sufficient to protect the occupants completely and must be supplemented by other airplane modifications to prevent heat and gases from entering by other avenues. The window pane material must be fire resistant to prevent heat from destroying it and permitting hot gases and smoke to enter. Some means of excluding the radiant heat transmitted by the windows should also be provided. Flame, hot gases, and smoke can also be carried into the fuselage by convection through openings at the juncture of the wing and the fuselage structure and through heating and ventilating systems. This situation calls for adequate flame and gas barriers inside the structure between the wings and the occupied parts of the fuselage.

The rapidity with which the fuselage skin burns through if flame is in contact with the fuselage while the airplane is in motion shows that the passenger compartments and fuel tanks should be separated as far as practicable in a spanwise direction to prevent direct flame contact with the fuselage. Wide spanwise separation is not of itself sufficient, however, if fuel can drain down through the wing structure into the fuselage belly or wing center section and thus spread fire to the occupied compartments. A means of preventing such fuel drainage should be placed inside the wing structure inboard of the fuel tanks.

The action of pain as a limit for escape time has been discussed. There are two other circumstances in which pain can be a factor in hindering or preventing the escape of airplane occupants: Heat conducted from the exterior or absorbed by convection and radiation from the interior can raise the temperature of door and escape hatch handles to the point where passengers cannot touch them with bare hands. Since the pain resulting from touching metal at a temperature of about  $113^{\circ}$  F will be practically unbearable (ref. 4), little heat need be absorbed to at least hinder the manipulating of these parts. The second circumstance in which pain can hinder escape arises when occupants must face direct radiation from exterior flame while escaping. Exposure to the intense radiation may produce such facial pain that escape will not be attempted (ref. 4). Any protective material such as clothing, curtains, blankets, or rugs that could be used to shield an occupant's exposed skin from direct radiation for a few seconds would facilitate escape. The use of such material could be suggested to passengers by the crew members as part of the evacuation procedure.

#### SUMMARY OF RESULTS

The results of this study of human survival in airplane crashes followed by fire should be considered applicable only to accidents that are essentially similar to the crashes studied.

1. For the severe crash fires studied, the survival times as limited by pain or skin burning ranged from 50 to 300 seconds. This variation in survival time depends primarily on the area of zones around the airplane wetted by the burning fuel, the slope of the terrain near the airplane, and the wind direction with respect to the relative positions of the fire and the airplane. During these crash fires, all fuel was carried outboard of the nacelles. In experiments in which fuel spillage occurred inboard of the nacelles at the forward part of the airplane, there was direct contact between the flames from this fuel and the fuselage skin. In these circumstances the fuselage skin burned through in about  $7\frac{1}{2}$  seconds. This situation would give minimum survival times appreciably less than 50 seconds.

2. Because the escape times determined in this study for the hazards of skin burning, respiratory injury, and toxic gases do not differ greatly, protection must be provided against all three if a significant increase in escape time is to be made.

3. The thermal and sound insulation presently used in transport airplanes will not increase the escape time appreciably and may decrease the escape time slightly.

4. Decreasing the fuel volatility will extend the escape time when the fuel is spilled in essentially liquid form but is of little benefit when large quantities of fuel mist are formed by fuel spillage from a rapidly moving airplane.

5. Propeller fragments launched by impact of rotating propellers with the ground would have a reduced probability of entering the airplane if the rotating blades moved away from the fuselage in their travel below the axis of rotation. The propeller fragments broken from the blade upon ground impact would then have an initial impulse directed away from the fuselage.

Lewis Flight Propulsion Laboratory  
National Advisory Committee for Aeronautics  
Cleveland, Ohio, May 1, 1953

## APPENDIX A

METHOD OF COMPUTING ESCAPE TIME BASED ON PAIN AND SECOND-DEGREE  
BURNS AS LIMITING CRITERIA

Prepain escape time. - The severe pain accompanying extensive skin burns can prevent human beings from functioning rationally when exposed to fire and thus prevent possible escape from a burning airplane. Pain can therefore be used as a criterion for establishing a limit to the time available for escape.

Experiments conducted with human beings exposed to radiating heat sources show the relation between the intensity of infrared radiation and duration of a continuous exposure to this radiation that causes unbearable pain (ref. 4). A summary of these data as they apply to the problem of computing the time available for escape from a burning airplane is plotted in figure 6 (prepain curve). This figure is a modification of figure 3 from reference 4. The heat absorbed by the skin during a continuous exposure is plotted against the time at which unbearable pain occurs instead of infrared radiation intensity against time as in the original figure.

The use of figure 6 for determining the prepain-escape time requires that the heat absorbed time curve for a particular crash and passenger position be plotted on the figure. The escape time is the time at which the heat absorbed curve reaches the lower pain tolerance curve.

In these crash fire studies, the rate with which heat is absorbed by the skin by radiation from flames and hot surfaces and by convection from the air is obtained by calculation from the temperature history of the copper bulb calorimeter in the following manner. The net rate of radiant heat absorption per unit area of skin  $(dq/dt)_R$  is given by the well-known expression

$$\left(\frac{dq}{dt}\right)_R = R - (seT^4)_{\text{skin}}$$

where  $R$  is the heat radiated per unit time for all zones to which the skin is exposed and  $(seT^4)_{\text{skin}}$  is the heat radiated by the person's skin. The heat absorption rate to the skin by convection with the atmosphere is given by the equation

$$\left(\frac{dq}{dt}\right)_C = K (T_{\text{air}} - T_{\text{skin}})$$

Therefore, the total rate of heat absorption by the skin is given by

$$\left(\frac{dq}{dt}\right)_{\text{total}} = R - (seT^4)_{\text{skin}} + K (T_{\text{air}} - T_{\text{skin}}) \quad (1)$$

In this equation

$\left(\frac{dq}{dt}\right)_{\text{total}}$  heat absorbed by skin, cal/(sq cm/min)

R radiant heat absorption by skin, cal/(sq cm/min)

s Stefan-Boltzmann constant,  $8.2 \times 10^{-11}$  cal/(sq cm/min/ $^{\circ}\text{K}^4$ )

e emissivity

T temperature of skin surface,  $^{\circ}\text{K}$

K convective heat-transfer coefficient, cal/(sq cm/min/ $^{\circ}\text{C}$ )

$T_{\text{air}}$  ambient air temperature,  $^{\circ}\text{C}$

The term R in equation (1) represents the only unknown if the skin temperature is assumed constant. It can be shown that this assumption introduces little error within the range of skin temperatures being considered and is therefore justified. Since the absorptivity of human skin and of the calorimeter bulb are essentially equal, the value of R is the same for the calorimeter and human skin. The value of R can then be computed from the recorded calorimeter temperature history by using the relation expressed in equation (2). The radiant energy to which the calorimeter bulb is exposed is partly absorbed by the bulb in raising its temperature, partly reradiated to the surroundings, and partly lost by convection to the surrounding air if the bulb is above air temperature. Expressed mathematically,

$$R = Wc \left(\frac{dT}{dt}\right)_{\text{cal}} + (seT^4)_{\text{cal}} + K (T_{\text{cal}} - T_{\text{air}}) \quad (2)$$

In this equation

W weight of calorimeter bulb per unit area, g/sq cm

c specific heat, cal/g

$T_{\text{cal}}$  calorimeter temperature,  $^{\circ}\text{C}$

$e_{\text{cal}}$  emissivity of calorimeter bulb surface

Since the radiation to which either the calorimeter bulb or a human being's skin would be exposed is equal and the general dimensions of the bulb and of a human head are similar, the value of  $R$  obtained for the calorimeter can be considered to apply to a human head. The final equation for the rate of heat absorption by the skin is, from equations (1) and (2),

$$\left(\frac{dq}{dt}\right)_{\text{absorbed}} = W_c \left(\frac{dT}{dt}\right)_{\text{cal}} + (seT^4)_{\text{cal}} - (seT^4)_{\text{skin}} + K (T_{\text{cal}} - T_{\text{skin}}) \quad (3)$$

The values of the various constants in equation (3) were established as follows:

The weight per unit area of the copper sphere calorimeter was 0.4 gram per square centimeter. The first term of the equation thus becomes  $0.0368 \frac{dT_{\text{cal}}}{dt}$  when the weight per unit area is multiplied by the specific heat of copper.

In the second term of equation (3), the emissivity of the flat-black lacquer surface of the copper calorimeter is 0.96 to 0.98 (ref. 12). The second term thus becomes

$$8.2 \times 10^{-11} \times 0.97 T_{\text{cal}}^4$$

or

$$7.95 \times 10^{-11} T_{\text{cal}}^4$$

The emissivity of human skin for the third term of the equation is 0.9, based upon references 3 and 13. Since normal human body temperature is  $37^\circ \text{C}$  and it can be shown that disregarding the skin temperature increase introduces a negligible error, the third term becomes

$$-8.2 \times 10^{-11} \times 0.9 (37 + 273)^4 = -0.7 \text{ cal/(sq cm/min)}$$

The value of 0.0026 for the convective heat-transfer coefficient  $K$  in the fourth term is based upon data presented in reference 12. This heat-transfer coefficient takes into account the general dimensions of the calorimeter bulb, which, in turn, approximates a human head, and natural convection air flow. This coefficient also changes the temperature difference term to a  $5/4$ -power function. The fourth term then becomes

$$0.0026 (T_{\text{cal}} - 37)^{5/4}$$

Assembling the individual terms gives the final equation used for these calculations as

$$\left(\frac{dq}{dt}\right)_{\text{absorbed}} = 0.0368 \left(\frac{dT}{dt}\right)_{\text{cal}} + 7.95 \times 10^{-11} \times T_{\text{av cal}}^4 - 0.7 + 0.0026 (T_{\text{av cal}} - 37)^{5/4} \quad (4)$$

By integration of equation (4) with time, the total heat absorbed by a square centimeter of exposed skin can be obtained. A time interval  $dt$  varying from 2 to 10 seconds was chosen for making the numerical integration, the time interval magnitude varying inversely as the rate of change of temperature. The values of  $T_{av\ cal}$  and  $T_{av\ cal}^4$  correspond to the average values existing during the successive time intervals  $dt$  chosen for the numerical integration. The values of heat absorbed at the end of the successive time intervals plotted on the same coordinates with figure 6 give the prepain-escape time at the intersection of the heat absorption curve with the lower prepain curve, as shown by the example for crash 1, left front fuselage.

Second-degree burn escape time. - Human beings can survive extensive skin burns unless relatively large portions of the body surface are involved. For those individuals who can function rationally regardless of the pain while sustaining second-degree burns over areas of the body limited to exposed skin such as face, arms, and legs, additional escape time may be available.

Escape times based on minimal second-degree burns can be computed from a knowledge of the skin temperature history. The skin temperature history is obtained by plotting on figure 44 the heat absorbed by the skin, provided by integration of equation (4) in the manner just described, and noting the times at which this curve crosses each of the constant skin-temperature lines. This skin temperature history is then used in conjunction with the integral

$$\Omega = 3.1 \times 10^{98} \int_0^t e^{-\frac{75,000}{T_t + 273}} dt \quad (5)$$

from reference 14 to determine the escape time. A minimal second-degree burn has been inflicted when the integrated value of the equation is equal to unity. In this equation  $t$  is the time in seconds, and  $T_t$  is the skin temperature at the epidermal-dermal interface. The stepwise integration of equation (5) requires that the skin temperature  $T_t$  correspond to the selected time interval  $dt$  in order to evaluate the  $e$  function. For convenience in evaluating this  $e$  function, definite increases in skin temperature were selected and the corresponding time interval was obtained from figure 44. From the stepwise integration of equation (5) a value of  $t$  is then obtained at which the value of  $\Omega$  is equal to unity. This value of  $t$  is the escape time as limited by a second-degree burn. An example of this procedure is presented later in the discussion.

Figure 44 was developed from the data presented in table VI of reference 15 in combination with the prepain data presented by figure 6.

Table VI lists the histories of epidermal-dermal interface temperatures resulting from the exposure of young pigs to various circumambient and circumradian temperatures. From the various circumambient and circumradian temperatures listed it is possible to calculate the quantity of heat that must be absorbed per unit area of skin surface to raise the skin to the temperature listed in the table. With the quantity of heat absorbed and the skin temperature-time relations it is possible to plot curves that indicate the quantity of heat that must be absorbed at a steady rate during any particular time interval to maintain a given skin temperature. Such a figure based upon the data of table VI alone, however, is not directly applicable to human beings because humans can tolerate more heat than pigs. Human beings perspire, whereas pigs do not; and the evaporation of this perspiration affords considerable protection against excess heat.

A correction for the perspiration effect can be obtained by comparing the above data obtained from the study of pigs with the prepain data from reference 6. The above data show the heat that will be absorbed in bringing pig skin up to and maintaining it at 45° C (line B in fig. 45). Reference 4 provides this same information for human skin (line A in fig. 45). The protective effect of perspiration is then the algebraic difference between the two sets of data (line C on fig. 45). The slope of the line representing the heat absorbed by perspiration (line C) shows that up to about 3 minutes a protection of 0.4 calorie per square centimeter per minute is provided by the evaporation of perspiration. The inflection point at about 3 minutes corresponds roughly to the earliest time at which copious perspiring begins when a person enters a hot environment (ref. 16). Thereafter the slope of this line increases to approximately 0.9 calorie per square centimeter per minute. These values for the protection afforded by perspiration, 0.4 to 0.9 calorie per square centimeter per minute, agree reasonably well with the values quoted in reference 3, 0.5 to 1.0 calorie per square centimeter per minute. Accordingly, line C was used as a base line and the heat absorbed data from the pig experiments (ref. 15) plotted above it to form figure 44. This figure thus includes the heat absorbed by the skin plus that required to evaporate the perspiration.

In order to illustrate the use of figure 44 for determining the skin temperature history for use in equation (5), the calorimeter temperature history for the left forward fuselage position (crash 1) in figure 8 was chosen as an example. The skin-temperature history is obtained by plotting the time history of heat absorbed by the skin for any particular passenger position in figure 44. The values of heat-transfer rate for the example chosen, calculated by equation (4), show that heat transfer to the skin began 137 seconds after impact; thus time zero on figure 44 corresponds to 137 seconds on the calorimeter temperature history (fig. 8). The subsequent history of total heat absorbed by the skin up to any particular time is then plotted in figure 44 as

shown. The intersections of the heat absorbed curve with the various constant-temperature lines provide the skin-temperature history as tabulated here:

Chart time, sec	Skin temperature, °C
18	40
64	45
78	50
84	55
91	60

The second step in the procedure is to use this skin-temperature history in conjunction with equation (5) to determine the escape time. The initial time for the calculation with equation (5) is the time at which the skin temperature reaches  $44^{\circ}\text{C}$  and cumulative skin injury begins, 54 seconds in this case. The integrated value of equation (5) equals 1, 87 seconds after heat transfer to the skin begins; thus in this instance a minimal second-degree burn would have been inflicted  $87 + 137 = 224$  seconds after impact; the value of escape time listed in table I.

Because there are no well-defined physiological data to indicate in what way the effects of heat application on skin temperature are additive in an environment of rapidly changing temperature such as obtained in a crash fire, it is difficult to establish the error involved in computing human skin temperature histories by the stepwise procedure employed here. Comparison of human skin temperatures measured in experiments in reference 6 with those computed by this stepwise procedure for the constant temperature environments established in their experiments shows the computed skin temperatures to be slightly higher than the measured values. Since the protective body mechanisms such as blood circulation and perspiration do not respond immediately to the rapidly fluctuating thermal environments which exist in crash fires, skin temperatures can be expected to rise faster under these circumstances than would be the case in an equivalent elevated temperature that is uniform with time. This difference in computed and measured skin temperatures therefore agrees with the expected variation for the crash-fire problem and no attempt was made to adjust the computational procedure to give skin temperature histories in closer agreement with the experimental values obtained in reference 6.

## APPENDIX B

CALCULATION OF ESCAPE TIME AS LIMITED BY CARBON-MONOXIDE POISONING  
AND OXYGEN DEFICIENCY

The varying carbon-monoxide concentrations encountered in personnel compartments during aircraft fires make it necessary to use a stepwise calculation procedure to determine the escape time. This appendix describes the details of the calculation procedure used.

When human beings are exposed to atmospheres containing carbon monoxide the portion of the hemoglobin that has combined with carbon monoxide to form carboxyhemoglobin and thus is not capable of transporting oxygen is given by the following equation, taken from reference 8:

$$\text{COH}_b = K \times \text{CO} \times t$$

where

$\text{COH}_b$  percent of carboxyhemoglobin formed

CO percent of carbon monoxide

t exposure time in min

In this equation the absorption constant K depends upon the volume of air required per minute by the exposed person. This volume, generally termed the "pulmonary ventilation rate" by physiologists, will be termed "ventilation rate" throughout this discussion.

The constant K is equal to 3 for persons at rest, 5 for light activity, 8 for light work, and 11 for heavy work. For these studies, it was assumed that the pilots were engaged in light work, pulse 110 and ventilation rate 18 liters per minute, and an absorption factor of 8 was used for the calculations. Passengers would not be so active as the crew; therefore they could tolerate the same carbon monoxide concentrations for a somewhat longer time interval.

Since both carbon monoxide poisoning and low oxygen partial pressures result in anoxia and since the larger carbon monoxide concentrations are accompanied by decreased oxygen concentrations in an aircraft fire, these two factors are considered simultaneously. It is shown in reference 8 that the carbon monoxide absorption rate is independent of lowered oxygen pressure provided allowance is made for the increase in ventilation rate caused by low oxygen pressure.

The correction required to account for a variation in ventilation rate caused by decreased oxygen pressure can be determined from data presented in reference 8. This reference presents human data from which a relation between altitude and ventilation rate can be obtained. This relation was then converted to a relation between oxygen concentration at sea level and ventilation rate, and is plotted as line A-A in figure 46. The relation between ventilation rate, as determined by work level, and the corresponding absorption factor is presented as line B-B, which is based upon data also available in reference 8. The absorption coefficients given by line B-B were obtained at a normal sea-level oxygen concentration of 21 percent. In the crash tests the oxygen concentration decreased as noxious gases mixed with the cabin air and some of the oxygen was consumed in the fire. No physiological data covering this circumstance exist; hence it is necessary to combine the effects of oxygen concentration on ventilation rate, as shown by line A-A, with the effect of ventilation rate on the absorption coefficient, as shown by line B-B. For this reason an assumption has been made that the effect of diminishing oxygen concentration is the same for light work as it is at rest. Line C-C is accordingly drawn parallel to line A-A through the sea-level value of ventilation rate for light work (18 liters per min). The corrected absorption factor for any particular oxygen concentration is thus found from figure 46 by finding a point on B-B vertically below the point on C-C corresponding to a given oxygen concentration.

Because of the nonlinear change in the carbon monoxide and oxygen concentrations encountered in the crash fires, a stepwise method of calculating the increase in carboxyhemoglobin was required. Since the linear equation for carboxyhemoglobin concentration

$$\text{COH}_b = 8 \times \text{CO} \times t$$

shows no influence of existing carboxyhemoglobin in the blood on the absorption rate, each increment in a stepwise computation should be additive. The calculation procedure thus is to determine the average carbon monoxide and oxygen concentrations during a time interval in which the gas concentrations vary at a reasonably uniform rate, determine the absorption factor corresponding to the average oxygen concentration from figure 46, and then calculate the incremental carboxyhemoglobin concentration. The increments can then be added to obtain the total carboxyhemoglobin content at the end of each time interval.

A time history of total accumulated carboxyhemoglobin content in the blood is then plotted against time to obtain the time history of carbon monoxide poisoning. The time at which the total carboxyhemoglobin content reaches 35 percent, the selected limit, is considered to be the limit of the escape time. A sample calculation is shown in the following paragraph.

The sample calculation is based upon the time history of gas concentrations in the pilot's compartment during the first bulk fire (fig. 21). This time history shows that during the first half minute the average carbon monoxide concentration was practically zero and no gas could be absorbed. During the next half-minute period the average carbon monoxide concentration was 0.02 percent. During this same time interval the average oxygen concentration was 18.3 percent. Figure 46 shows that the absorption factor corresponding to an 18.3 percent oxygen concentration is 8.3. The amount of  $\text{COH}_b$  formed is then

$$\Delta\text{percent } \text{COH}_b = 8.3 \times 0.01 \times \frac{1}{2} = 0.04 \text{ percent}$$

The accumulated  $\text{COH}_b$  is thus 0.04 percent.

The increment of  $\text{COH}_b$  for the next time interval is

$$\Delta\text{percent } \text{COH}_b = 8.5 \times 0.03 \times \frac{1}{2} = 0.13$$

The accumulated  $\text{COH}_b$  by the end of this interval is then  $0.04 + 0.13 = 0.17$  percent. These accumulated values are then plotted against time and the time at which the accumulated  $\text{COH}_b$  reached 35 percent is considered to be the limit of escape time.

#### REFERENCES

1. Black, Dugald O.: Facilities and Methods Used in Full-Scale Airplane Crash-Fire Investigation. NACA RM E51L06, 1952.
2. Shepherd, Martin: Rapid Determination of Small Amounts of Carbon Monoxide. Analytical Chem., vol. 10, 1947, pp. 77-81.
3. Moritz, A. R., Henriques, F. C., Jr., Dutra, F. R., and Weisiger, J. R.: Studies of Thermal Injury. IV. An Exploration of the Casualty-Producing Attributes of Conflagrations; Local and Systemic Effects of General Cutaneous Exposure to Excessive Circumambient (Air) and Circumradian Heat of Varying Duration and Intensity. Archives of Pathology, vol. 43, 1947, pp. 466-488.
4. Buettner, Konrad: Effects of Extreme Heat on Man. Jour. Am. Medical Assoc., vol. 144, no. 9, Oct. 28, 1950, pp. 732-738.
5. Moritz, A. R., and Henriques, F. C., Jr.: Studies of Thermal Injury. II. The Relative Importance of Time and Surface Temperature in the Causation of Cutaneous Burns. Am. Jour. Pathology, vol. 23, Sept. 1947, pp. 695-720.

6. Blockley, W. V., and Taylor, C. L.: Studies of Human Tolerance for Extreme Heat. Memo. Rep. Eng. Div. Ser. No. MCREXD-696-113A, U.S.A.F. Air Materiel Command, Wright-Patterson Air Force Base, Nov. 1, 1948.
7. Moritz, Alan R., Henriques, Frederick Co., Jr., and McLean, Regina: The Effects of Inhaled Heat on the Air Passages and Lungs. Am. Jour. Pathology, vol. 21, pt. 1, 1945, pp. 311-331.
8. Forbes, W. H., Sargent, F., and Roughton, F. J. W.: The Rate of Carbon Monoxide Uptake by Normal Men. Am. Jour. Physiology, vol. 143, 1945, pp. 594-608.
9. White, Clayton S.: Estimated Tolerance of Human Subjects to Various CO<sub>2</sub> - Time Concentrations. Rep. No. 2, Proj. No. 200, Dept. Aviation Medicine, Lovelace Clinic, July 27, 1948. (Aviation Consultant's Rep. to Douglas Aircraft Co., Inc.)
10. King, Barry Griffith: High Concentration - Short Time Exposures and Toxicity. Jour. Ind. Hygiene and Toxicology, vol. 31, no. 6, Nov. 1949, pp. 365-375.
11. Henderson, Yandell, and Haggard, Howard W.: Noxious Gases and the Principles of Respiration Influencing Their Action. Second ed., Reinhold Pub. Corp. (New York), 1943.
12. McAdams, William H.: Heat Transmission. Second Ed., McGraw-Hill Book Co., Inc., 1942.
13. Bueettner, Konrad: Effects of Extreme Heat on Man. III. Surface Temperature, Pain, and Heat Conductivity of Living Skin in Experiments with Radiant Heat. Rep. No. 3, Air Univ., USAF School Aviation Medicine, Randolph Field (Texas), Nov. 1951. (Proj. No. 21-26-002.)
14. Henriques, F. C., Jr.: Studies of Thermal Injury. V. The Predictability and the Significance of Thermally Induced Rate Processes Leading to Irreversible Epidermal Injury. Archives of Pathology, vol. 43, 1947, pp. 489-502.
15. Henriques, F. C., Jr., and Moritz, A. R.: Studies of Thermal Injury. II. The Conduction of Heat to and Through Skin and the Temperatures Attained Therein. A Theoretical and an Experimental Investigation. Am. Jour. Pathology, vol. 23, 1947, pp. 531-549.

16. Glickman, Nathaniel, et al.: Physiological Adjustments of Human Beings to Sudden Change in Environment. Heating, Piping and Air Conditioning, vol. 19, no. 7, July 1947, pp. 101-115.

TABLE I. - ESCAPE TIME AVAILABLE BASED ON SKIN BURNING AND RESPIRATORY DAMAGE THRESHOLDS

Crash	Position in airplane	Severe pain and skin injury begin, sec after impact	Minimal second-degree burn, sec after impact	Respiratory limit ( $390^{\circ}$ F), sec after impact	Airplane	Wind direction and speed	Fuel
1	Left front fuselage	180	224	251	C-46		Gasoline
	Right front fuselage	220	260	292			
	Left rear fuselage	174	306	296			
	Right rear fuselage	163	180	288			
3	Pilot's compartment	182	203	182	C-46		Gasoline
	Front fuselage	92	101	151			
	Rear fuselage	90	100	138			
6	Pilot's compartment	144	150	60	C-82		Gasoline
	Fuselage	53	59	131			
7	Pilot's compartment	93	97	112	C-82		Low-volatility fuel
	Fuselage	92	95	93			

TABLE II. - PHYSIOLOGICAL EFFECTS OF VARIOUS CARBON MONOXIDE  
HEMOGLOBIN PERCENTAGES

[Based on similar table in ref. 11]

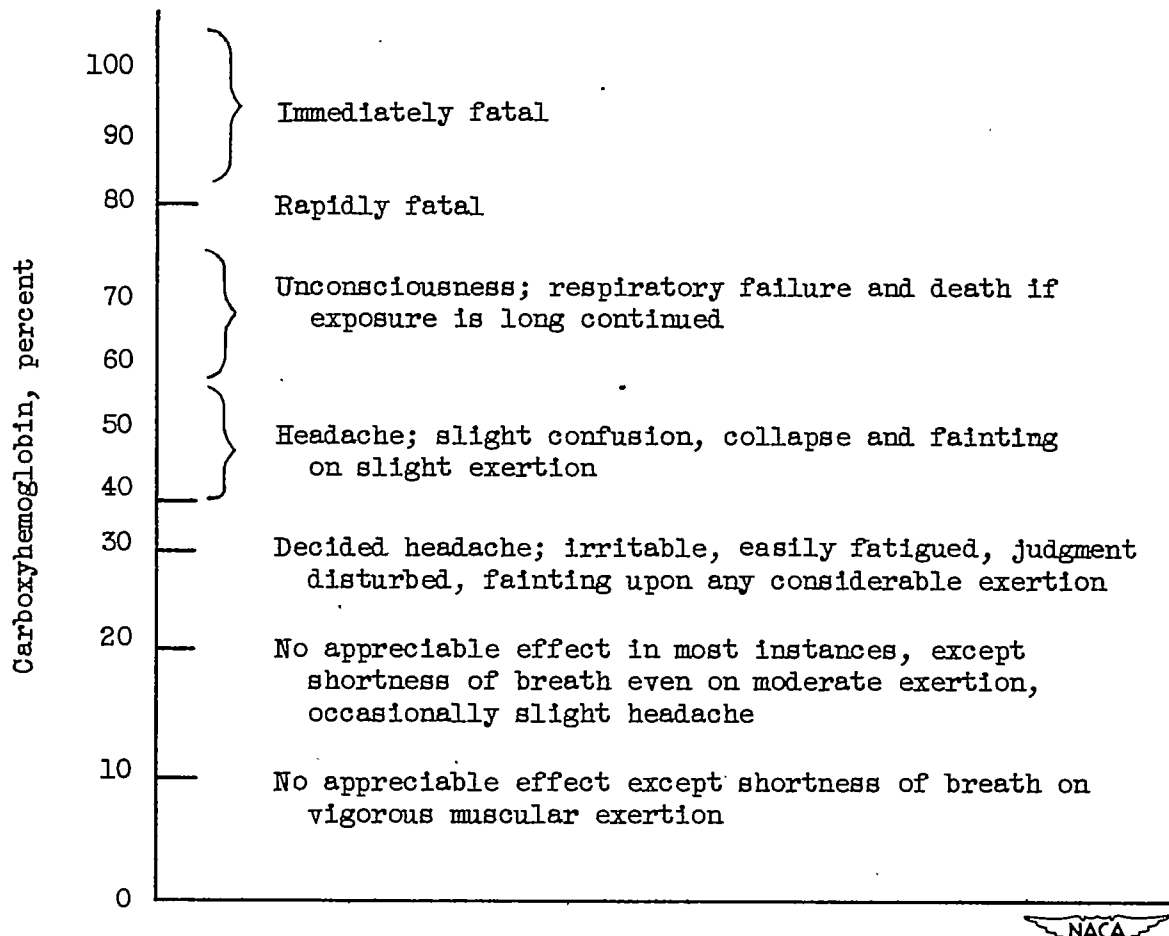
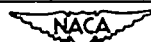


TABLE III. - REPRESENTATIVE CONCENTRATIONS OF NOXIOUS GASES  
 PRODUCED BY FIRE AND FOUND IN COMPARTMENTS OF  
 AIRPLANES DURING CRASH FIRES

Crash	Airplane	Compart- ment	Time after impact, sec	Constituents, percent			
				CO	CO <sub>2</sub>	O <sub>2</sub>	<sup>a</sup> CH <sub>4</sub>
1	Low midwing	Pilot	300	12	2.5	<1	3
		Passenger	300	0.1-0.5	0.6	19.5	0.1 or less
6	High wing	Pilot	120	0.015	0.7	20.0	
		Front passenger	180	0.1	2.2	17.4	
		Rear passenger	60	0.1	trace	20.6	
7	High wing	Front passenger	180	0.1	1.25	17.5	
		Rear passenger	60	0.1	3.4	13.0	



<sup>a</sup>Hydrocarbons other than CH<sub>4</sub> were detected in small concentrations in one test.

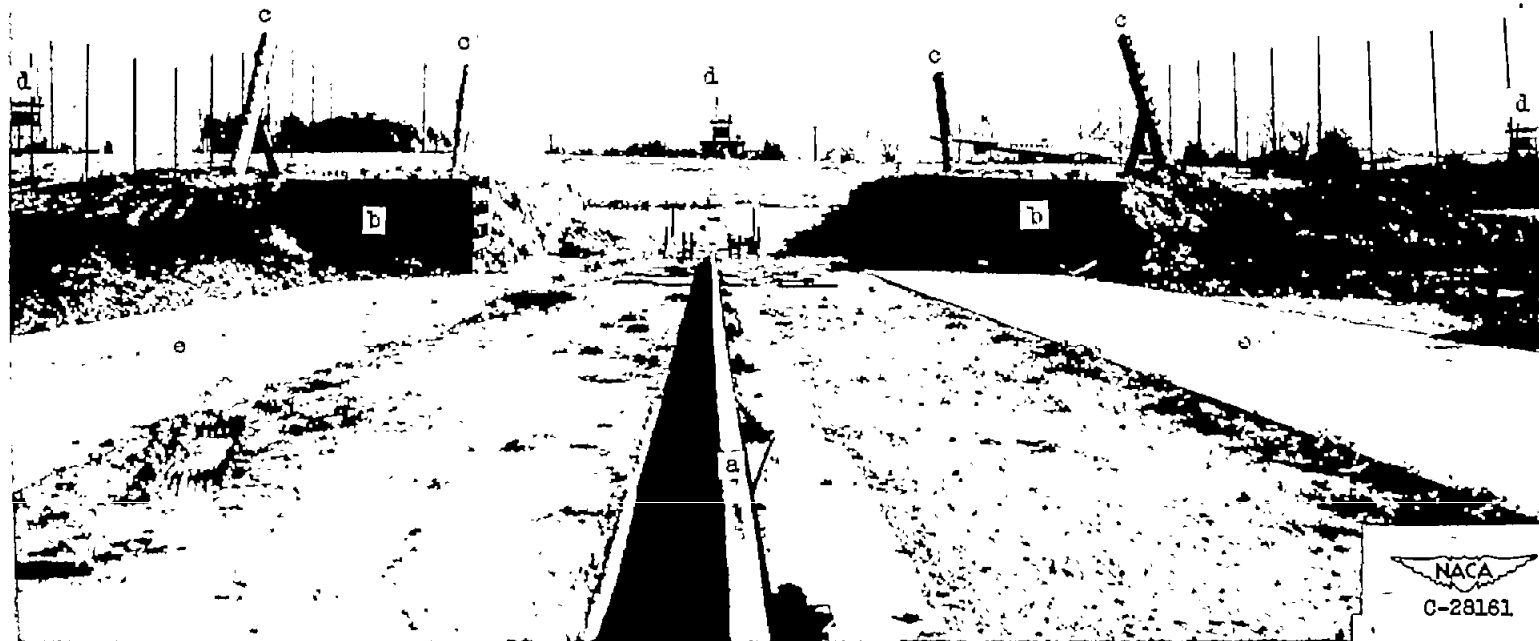
TABLE IV. - ESCAPE TIMES FOR TWO FIRES BUILT AROUND  
PREVIOUSLY CRASHED BUT UNBURNED AIRPLANES

Hulk fire	Position	Escape time, sec		
		Carbon monoxide- oxygen depletion	Minimal second- degree skin burn	Carbon dioxide
1	Pilot's compartment	397	319	(a)
	Forward cabin	398	151	365
	Aft cabin	(a)	257	(a)
2	Pilot's compartment	398	55	(a)
	Forward cabin	305	65	(a)
	Aft cabin	(a)	106	(a)



<sup>a</sup>Escape time limit not reached.

- a Guide rail
- b Timber-and-dirt barrier to damage propellers and landing gear
- c Spike-studded poles to tear open fuel tanks
- d Stands for motion-picture cameras
- e Paved runways for main landing gear wheels



NACA  
C-28161

Figure 1. - Crash site showing end of guide rail, propeller and wheel barriers, fuel-tank pole barriers, and camera stations.

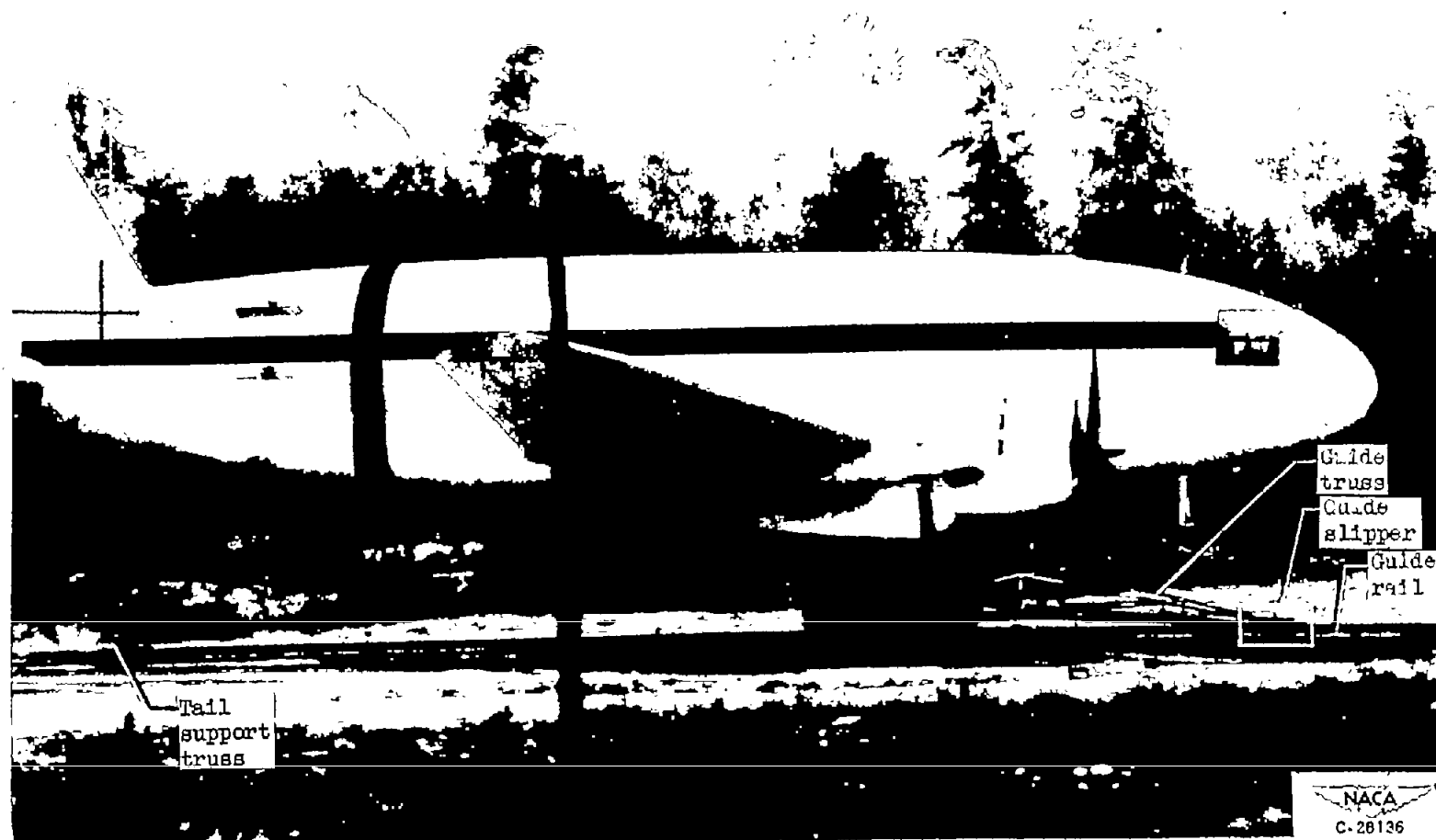


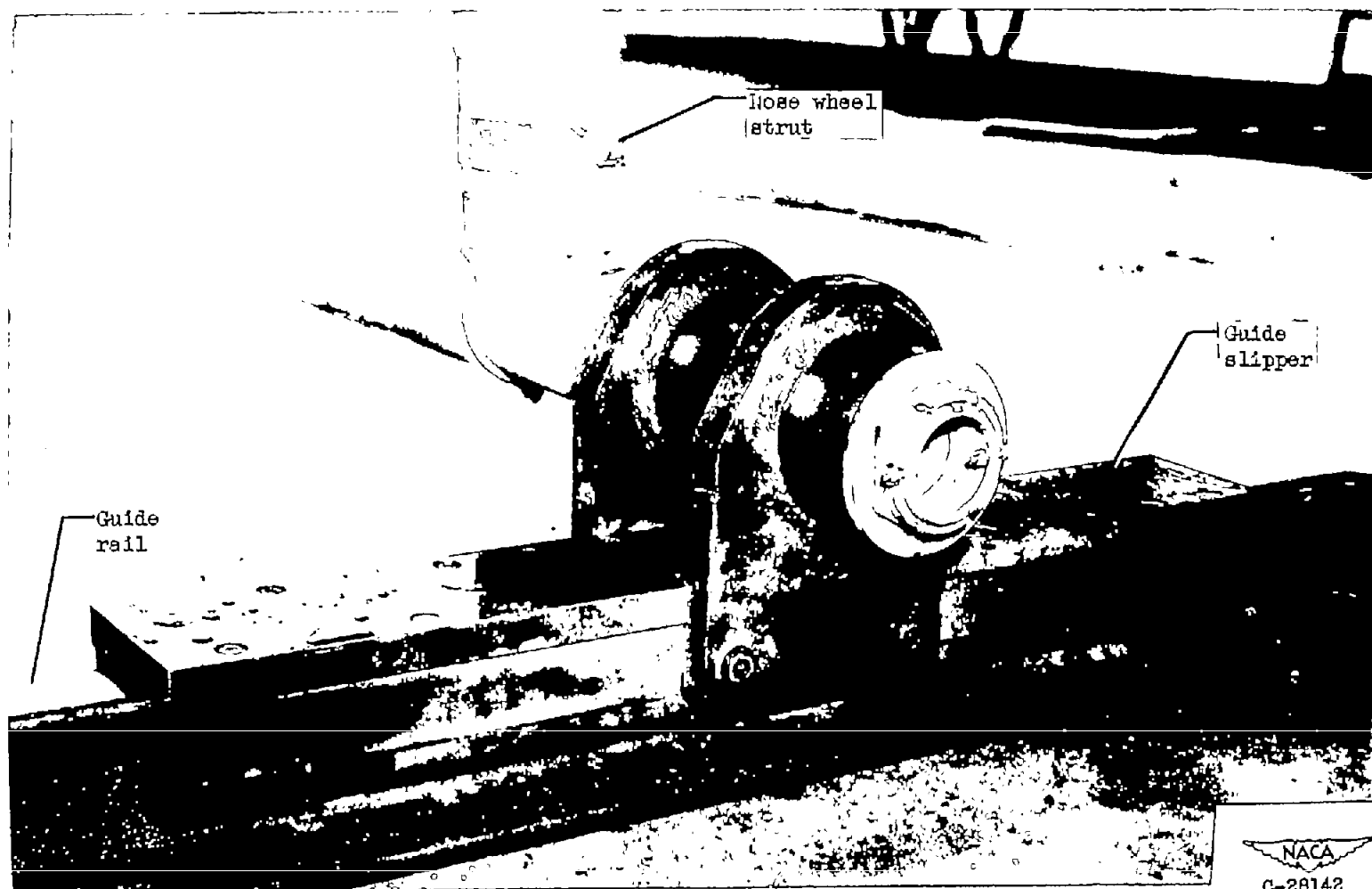
Figure 2. - Airplane with conventional landing gear traveling along guide rail showing guide slipper, guide truss attached to main landing gear, and tail support truss that slides along top of guide rail.



Figure 3. - Airplane with tri-cycle landing gear traveling along crash strip showing guide slipper attached to strut and replacing nose wheel.

NACA TM 2996

NACA  
C-28145



NACA  
C-28142

Figure 4. - Close-up view of guide slipper attached to strut in place of nose wheel. Guide slipper grips over top bead of rail to prevent airplane nose from lifting.

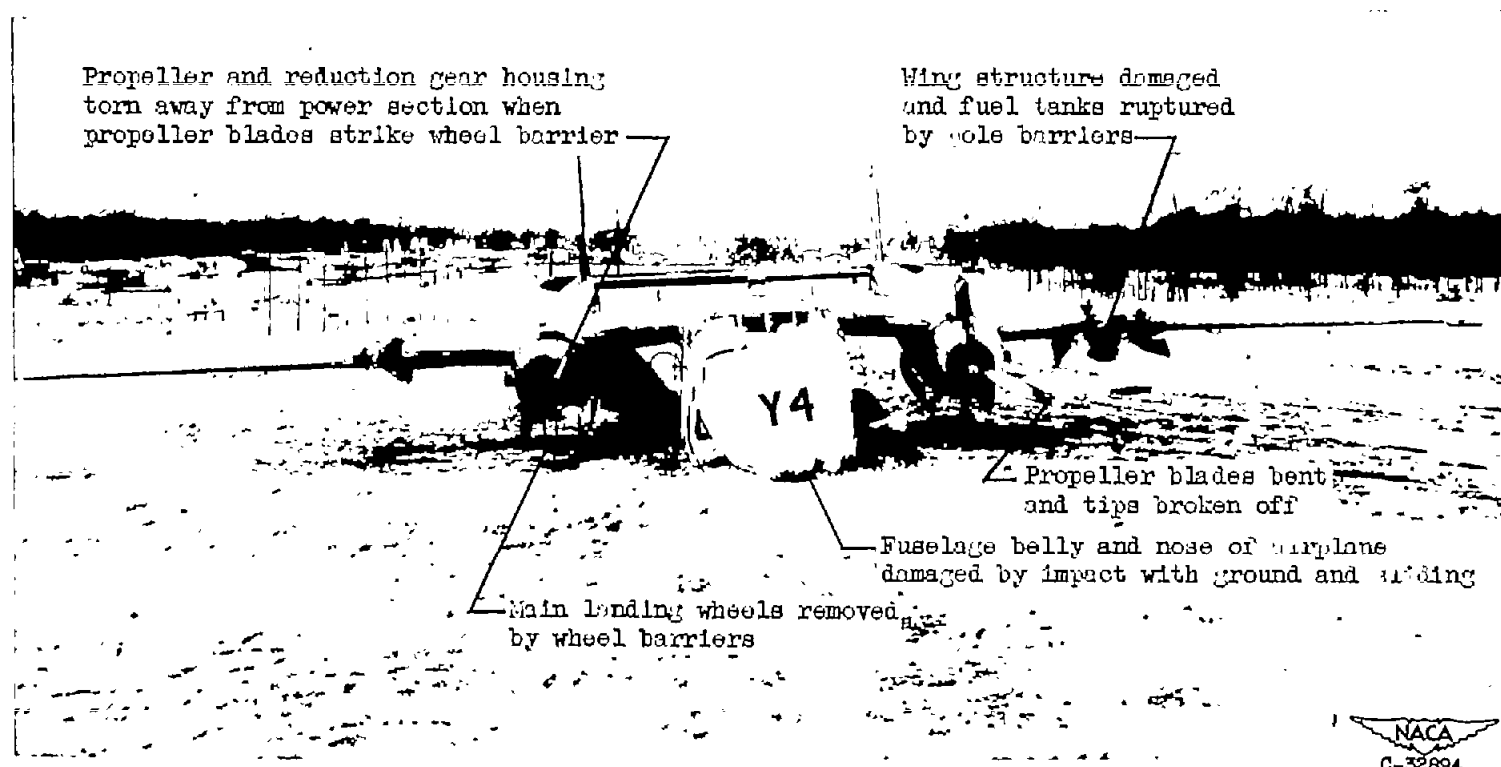


Figure 5. - Damage inflicted to airplane and engines by wheel barriers, fuel tank barriers, and contact with ground.

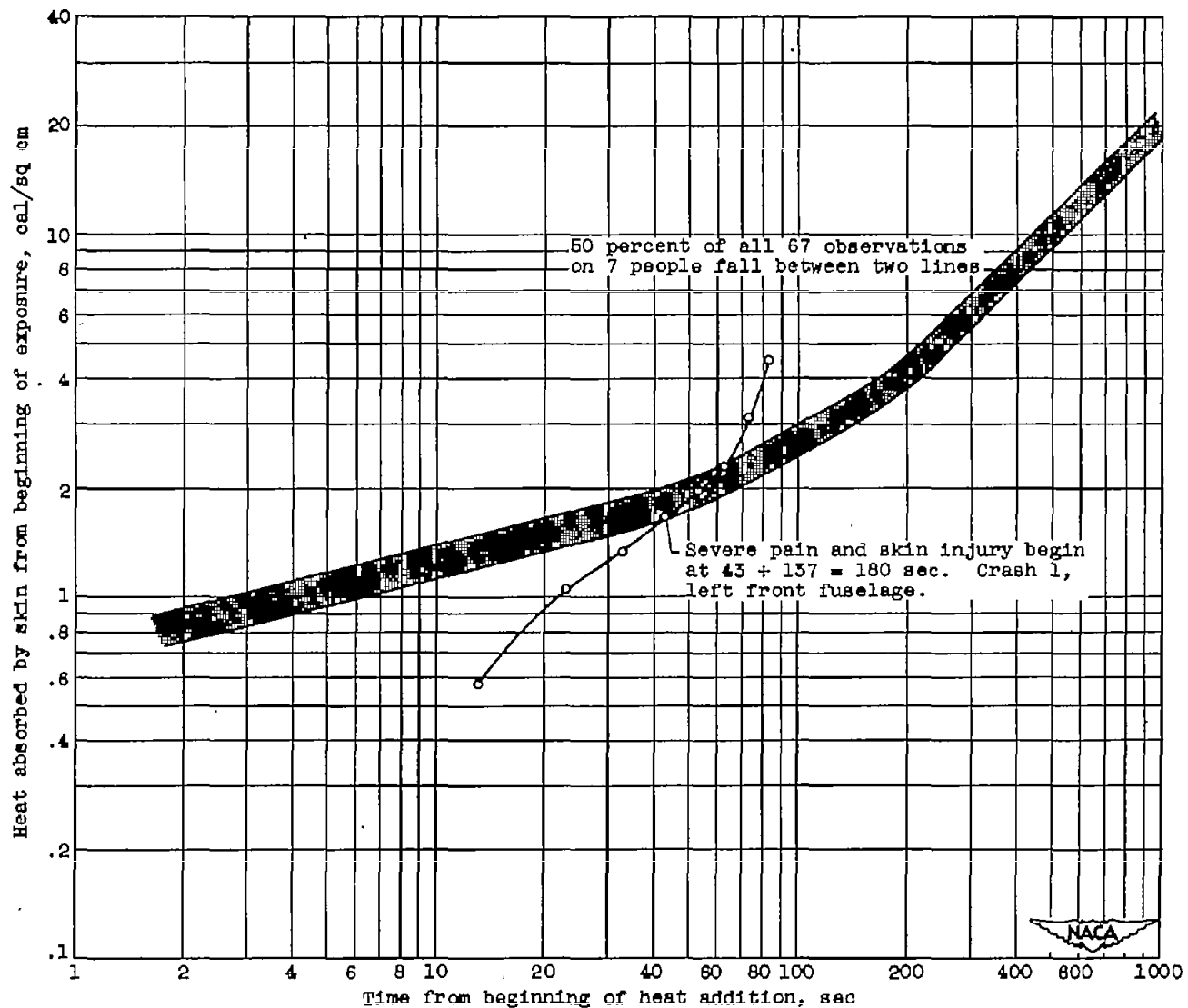


Figure 6. - Time until unbearable pain occurs if dorsal side of forearm is exposed to infrared radiation and absorbs indicated amount of heat. (Converted from fig. 3 of ref. 4.)

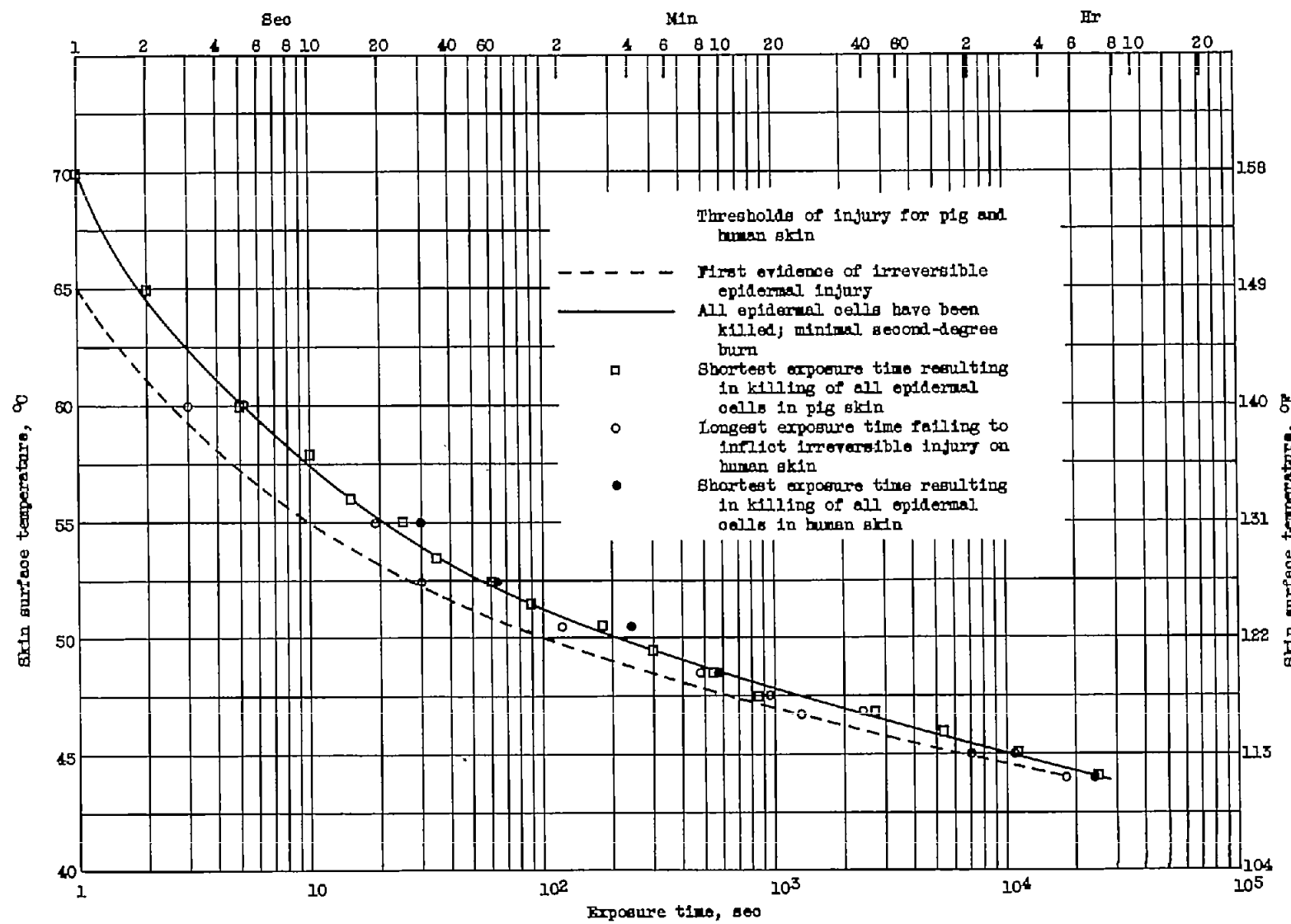
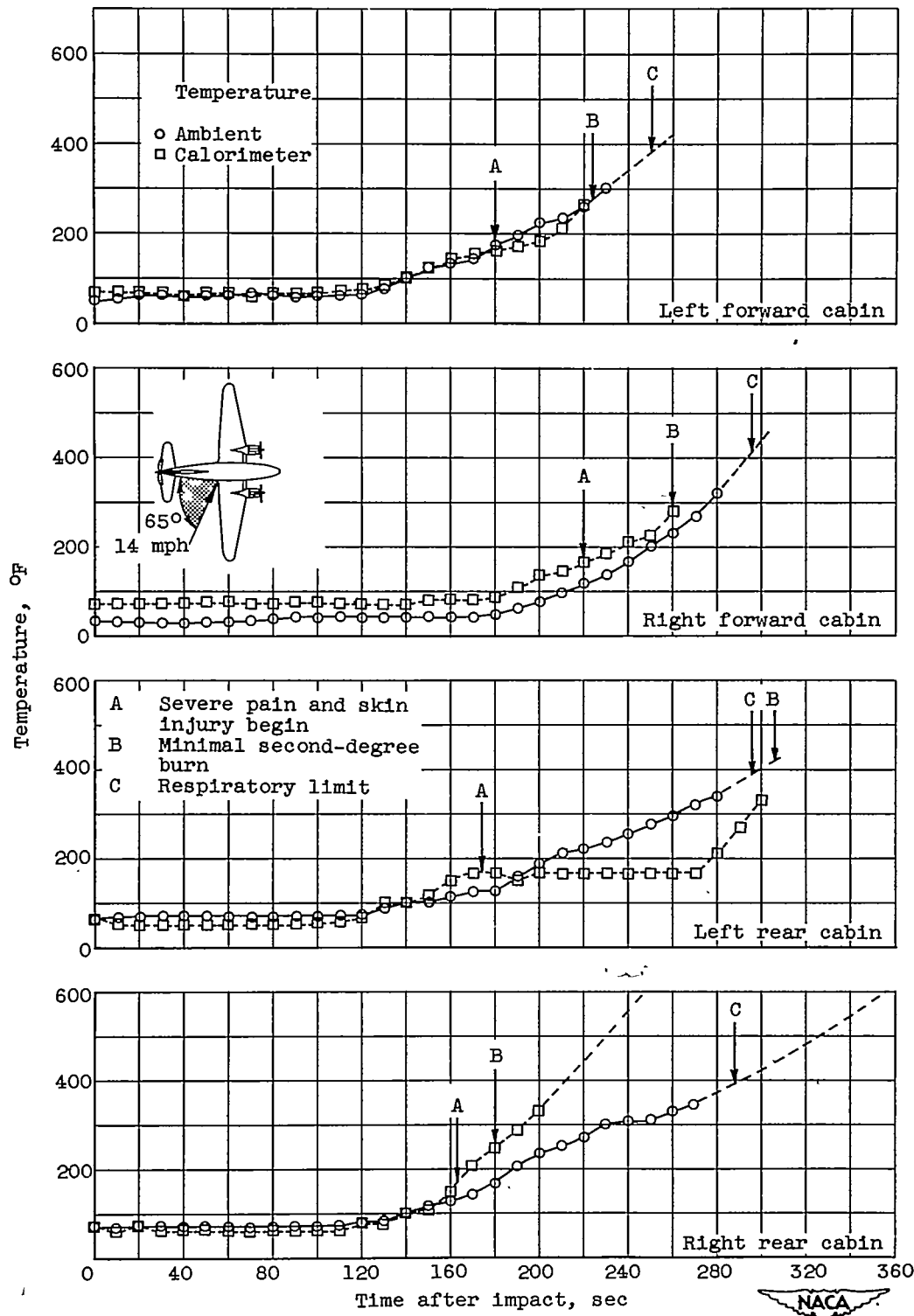
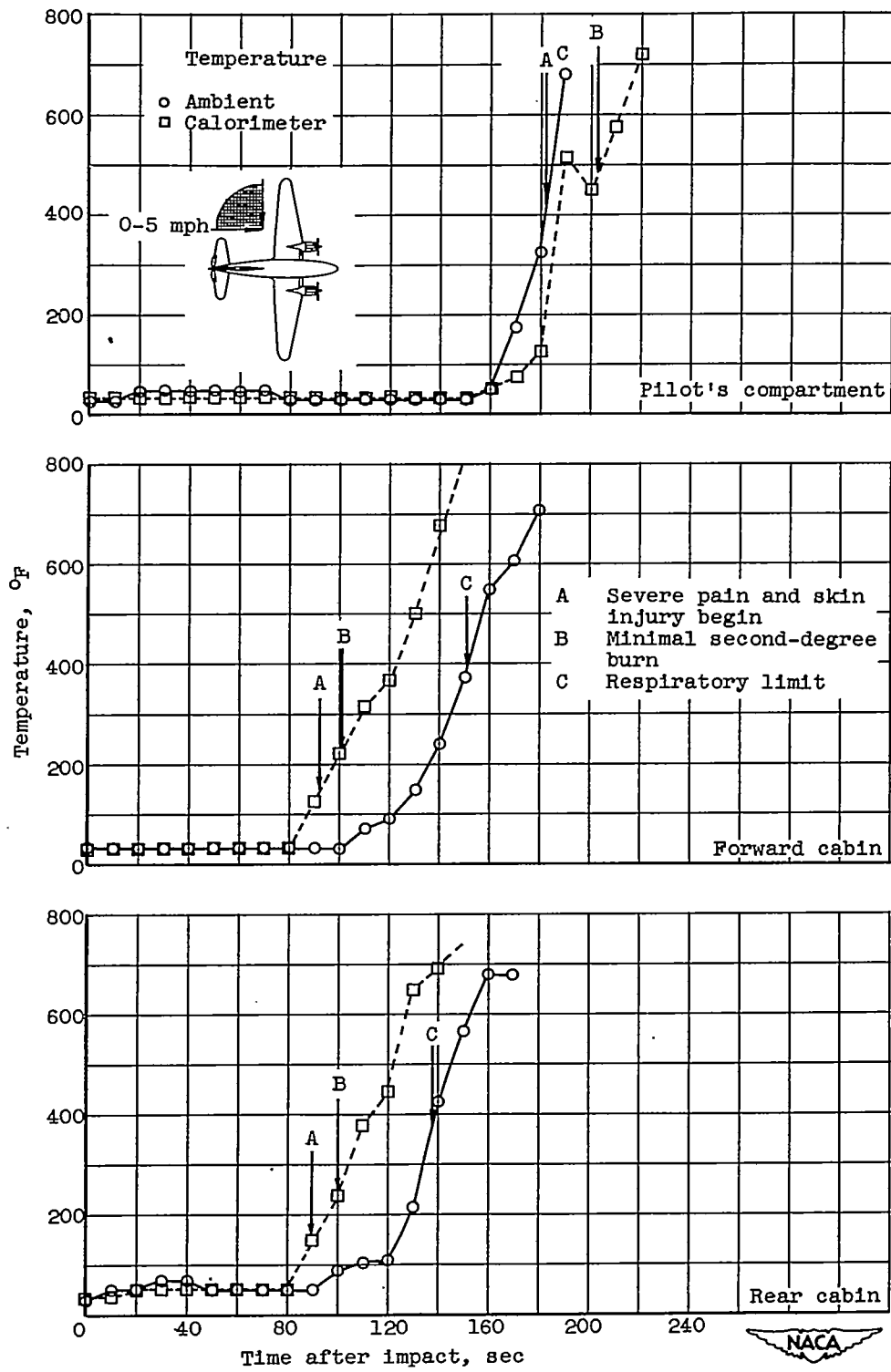


Figure 7. - Time-surface temperature thresholds for skin burning. (Reproduced from ref. 5.)



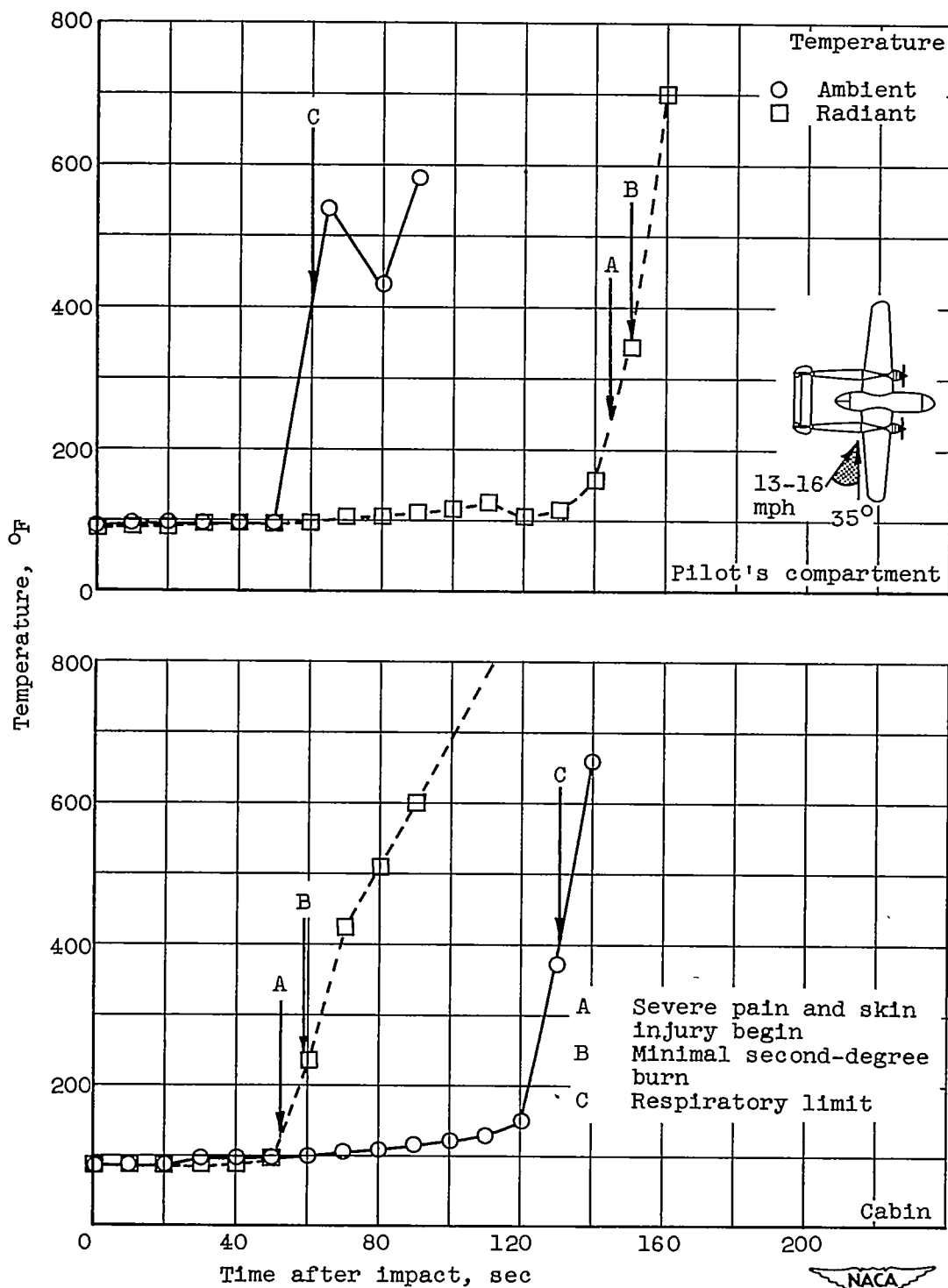
(a) Crash 1; low midwing transport-type airplane; fuel, gasoline.

Figure 8. - Time histories of ambient and calorimeter temperatures in various compartments during several crashes.



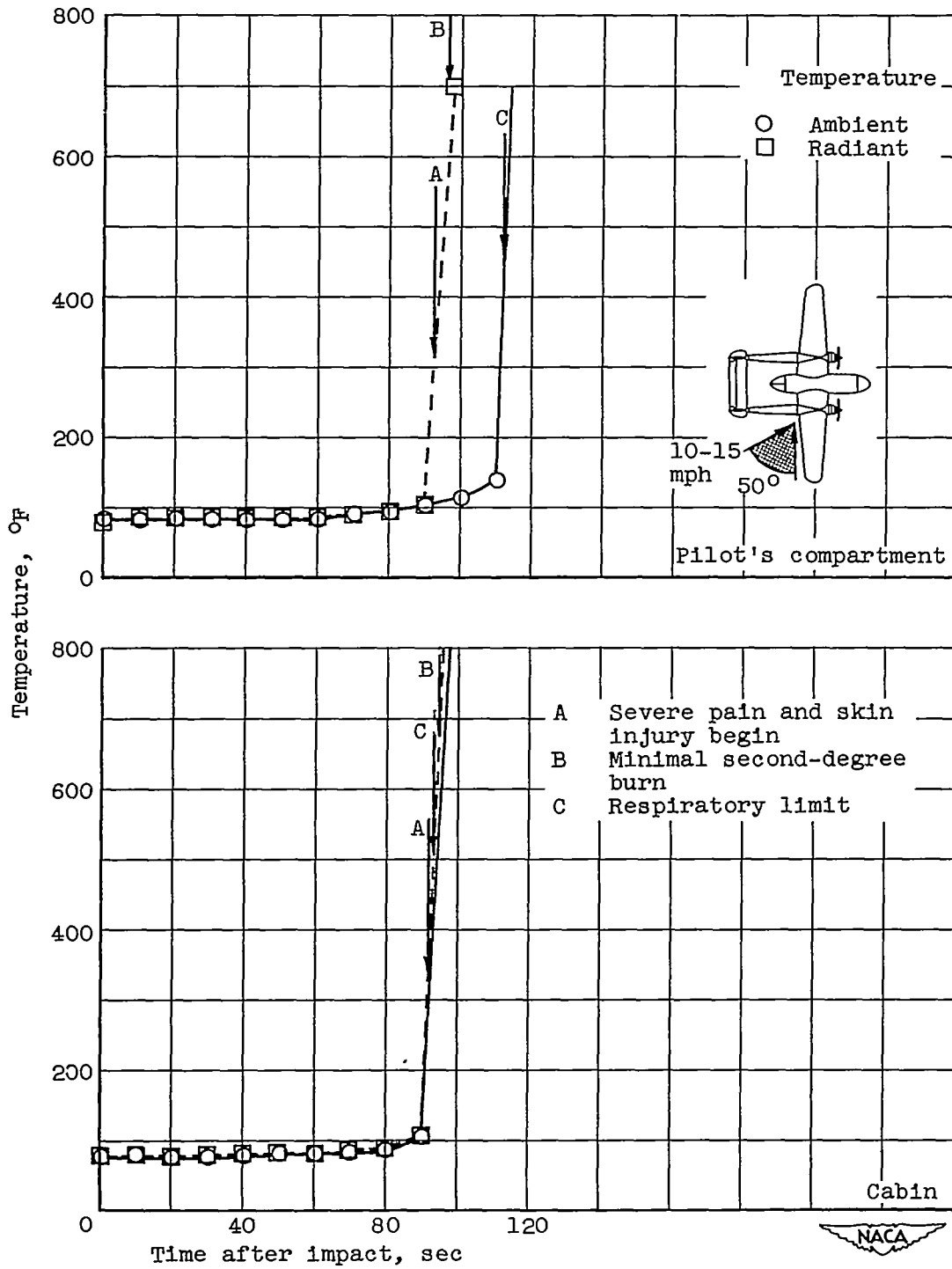
(b) Crash 3; low midwing transport-type airplane; fuel, gasoline.

Figure 8. - Continued. Time histories of ambient and calorimeter temperatures in various compartments during several crashes.



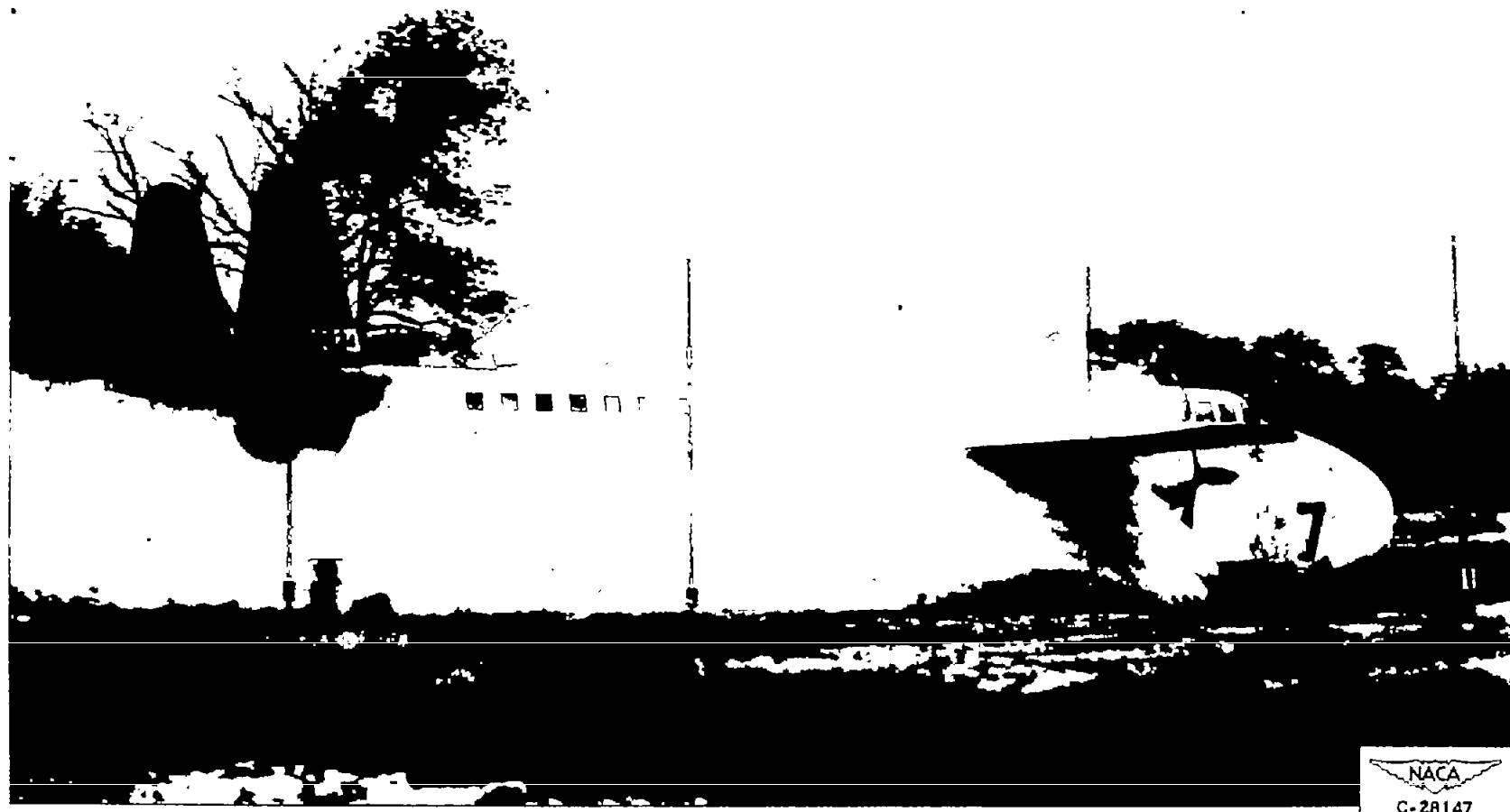
(c) Crash 6; High wing cargo-type airplane; fuel, gasoline.

Figure 8. - Continued. Time histories of ambient and calorimeter temperatures in various compartments during several crashes.



(d) Crash 7; high wing cargo-type airplane; fuel of low volatility.

Figure 8. - Concluded. Time histories of ambient and calorimeter temperatures in various compartments during several crashes.



NACA  
C-28147

Figure 9. - Typical fuel mist formed when either gasoline or low volatility fuel tanks are ruptured while airplane is in motion. Fuel mist appears as white cloud around and behind wing surfaces. No fire existed at time this photograph was taken.



Figure 10. - Fire resulting from ignition of cloud of gasoline mist.



NACA  
C-32895



NACA  
C-32896

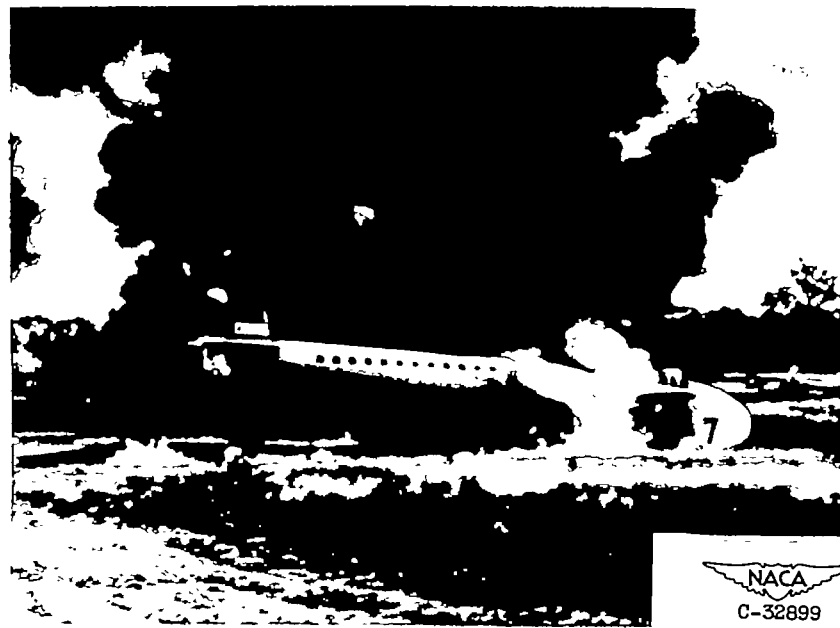
(a) Crash 1.

Figure 11. - Photographs showing development of fire during escape time. Upper photograph shows initial fire or fire shortly after airplane stopped sliding; lower photograph shows fire at end of calculated escape time.



(b) Crash 3.

Figure 11. - Continued. Photographs showing development of fire during escape time.  
Upper photograph shows initial fire or fire shortly after airplane stopped sliding;  
lower photograph shows fire at end of calculated escape time.



NACA  
C-32899



NACA  
C-32900

(c) Crash 7.

Figure 11. - Concluded. Photographs showing development of fire during escape time. Upper photograph shows initial fire or fire shortly after airplane stopped sliding; lower photograph shows fire at end of calculated escape time.



NACA  
C-33011

Figure 12. - Location of fire and wind direction such that fuselage is bathed in flame but pilot's compartment not enveloped.

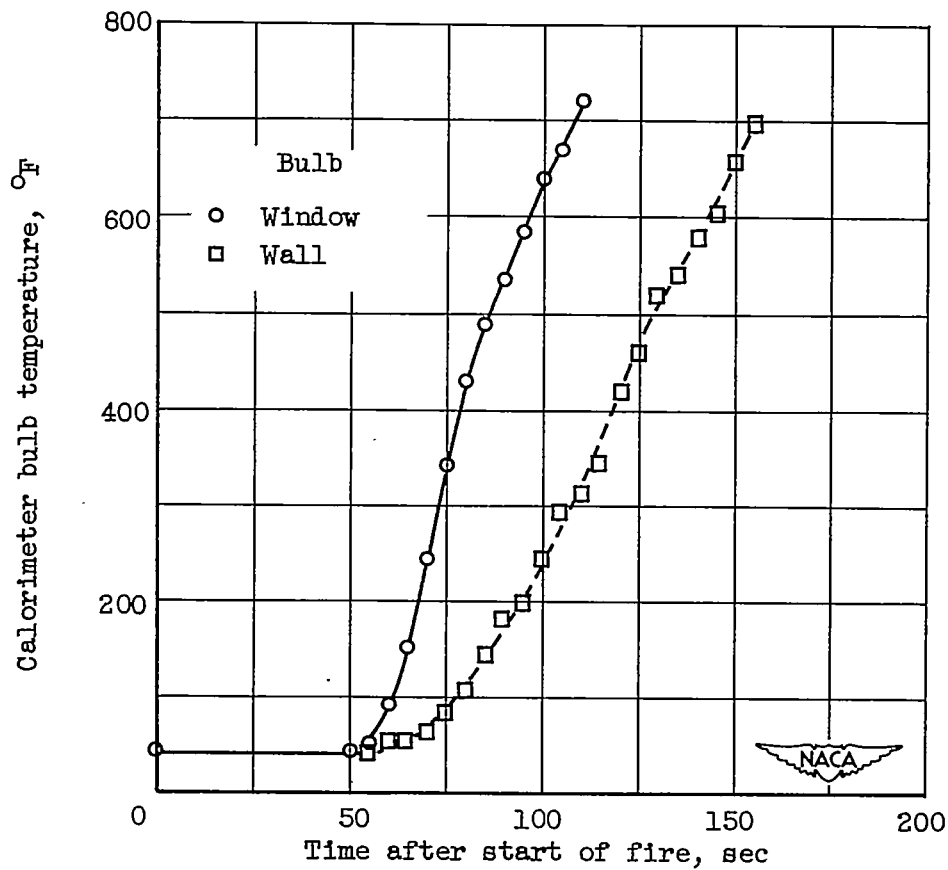


Figure 13. - Temperature histories of calorimeter bulb facing window exposed to fire and bulb facing insulated fuselage wall.



(a) Pane beginning to melt.



(b) Pane completely melted.

Figure 14. - Two stages in disintegration of plastic window pane when subjected to fire.



NACA  
C-52903

Figure 15. - Damage to fuselage skin resulting from  $7\frac{1}{2}$  second contact with fire while airplane was in motion.

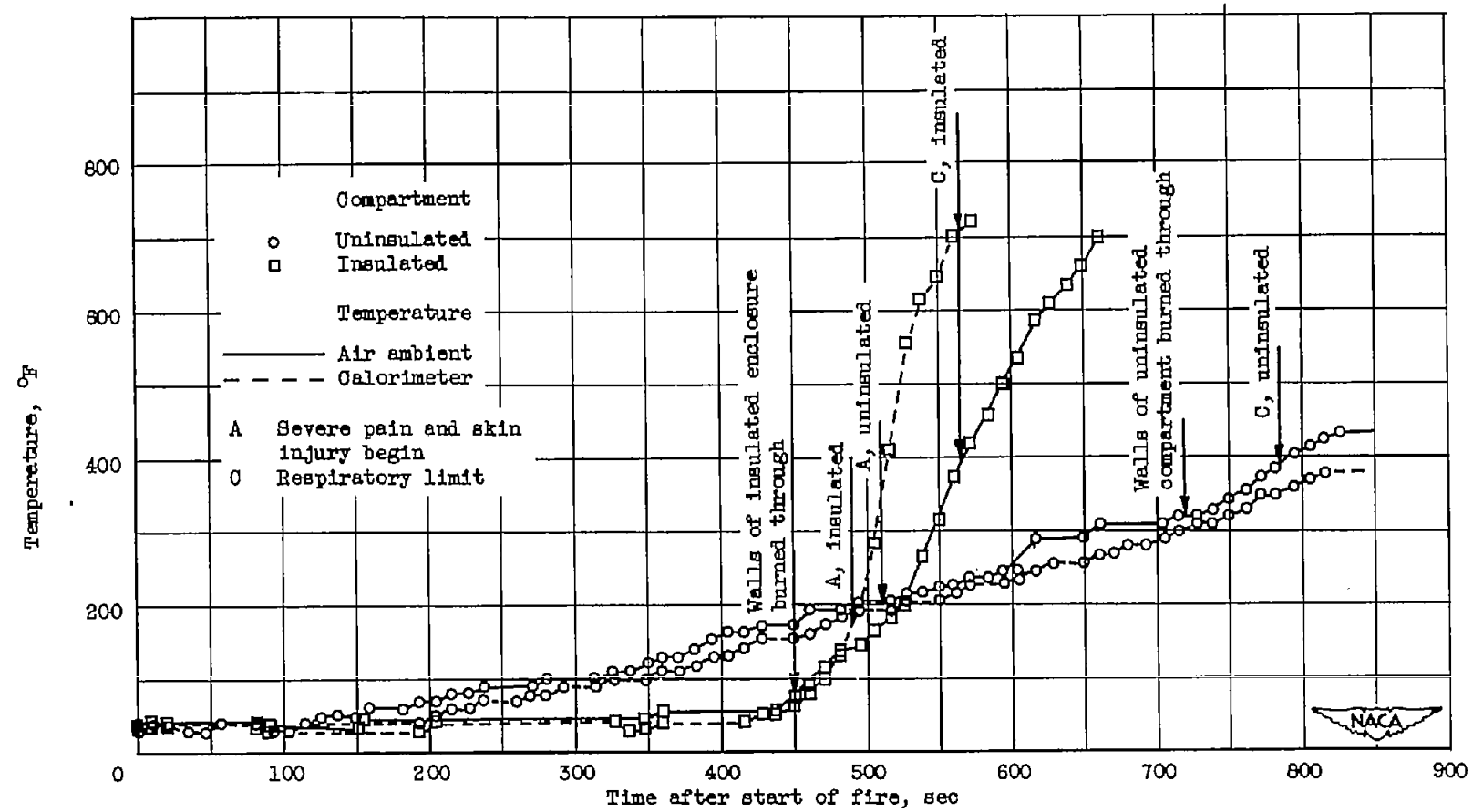
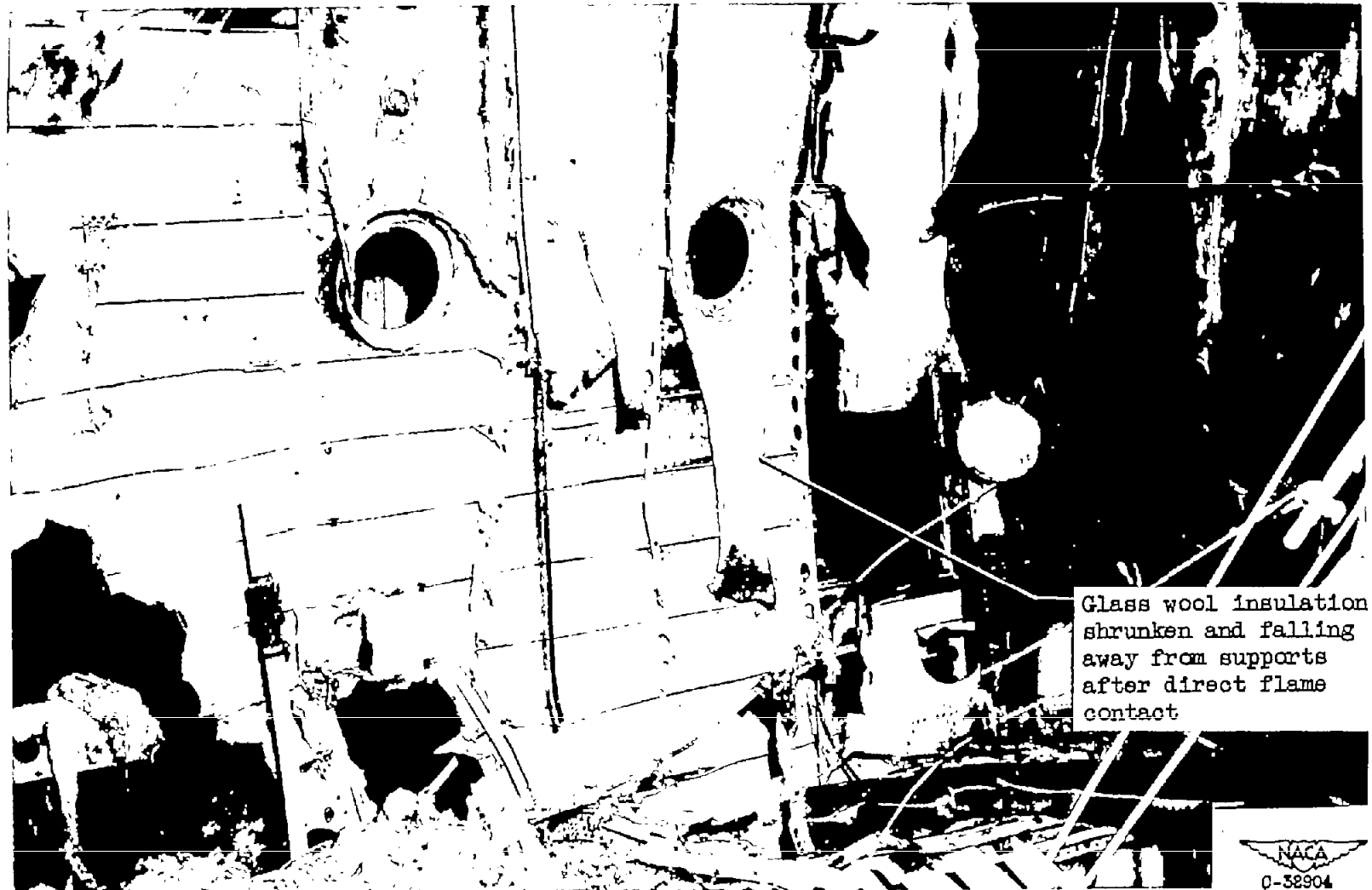


Figure 16. - Comparison of temperature histories and escape times in insulated and uninsulated enclosures.



NACA  
0-32904

Figure 17. - Effect of direct flame contact upon some glass-wool types of thermal and sound insulation.



Figure 18. - Fire resulting from ignition of cloud of low-volatility fuel mist.

NACA  
C-28149

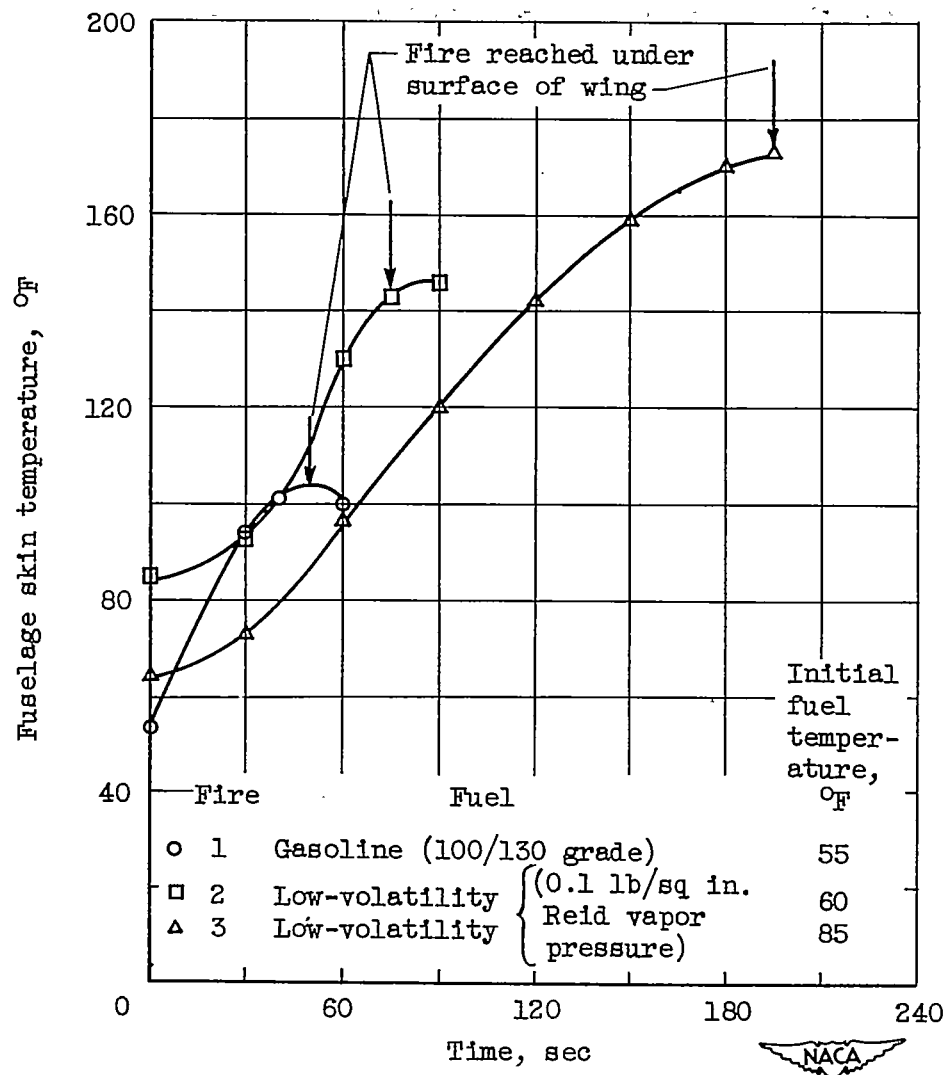


Figure 19. - Increase in fuselage skin temperature with time for three essentially similar fires but with fuel at various vapor pressures and initial temperatures.

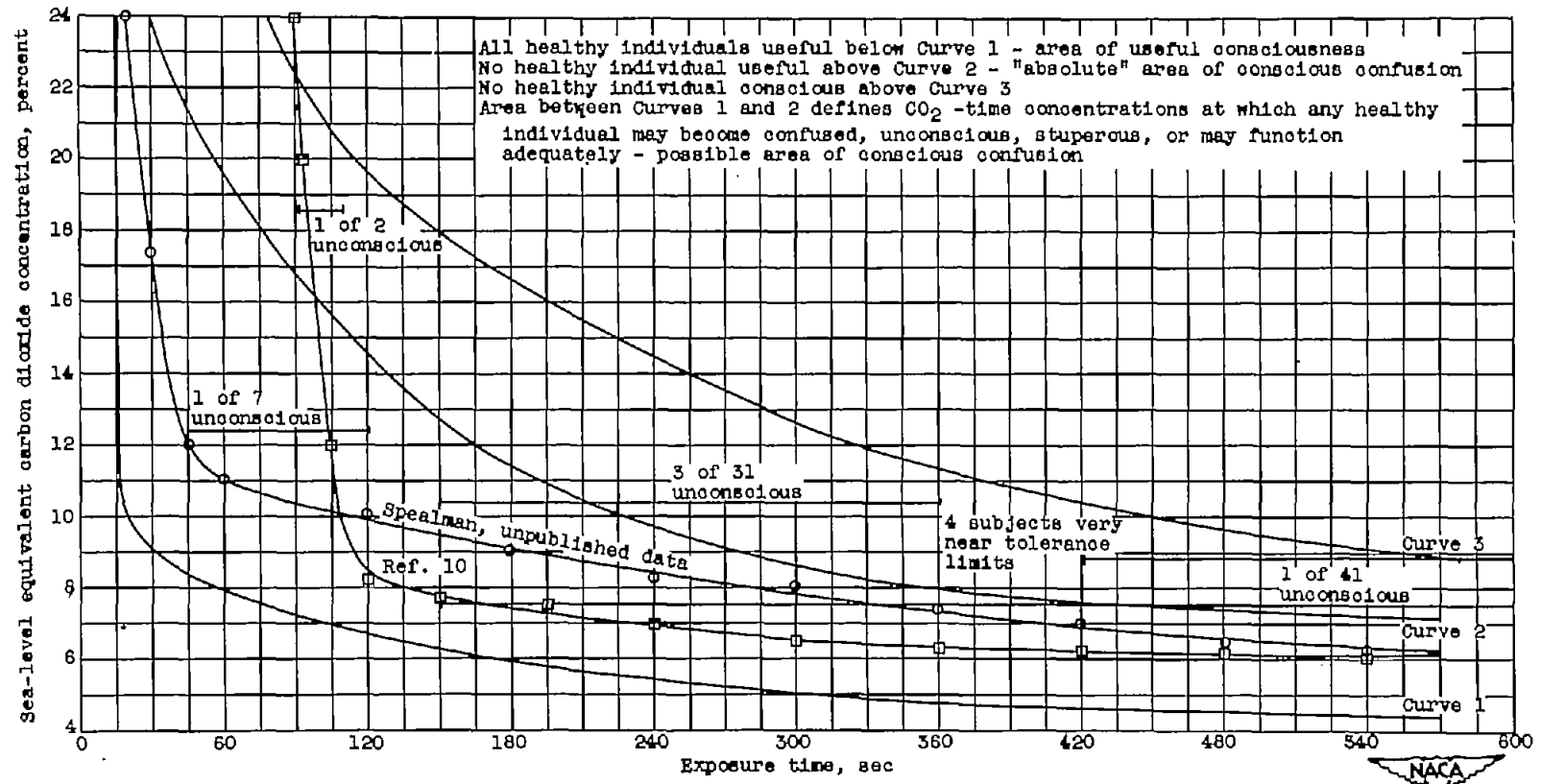
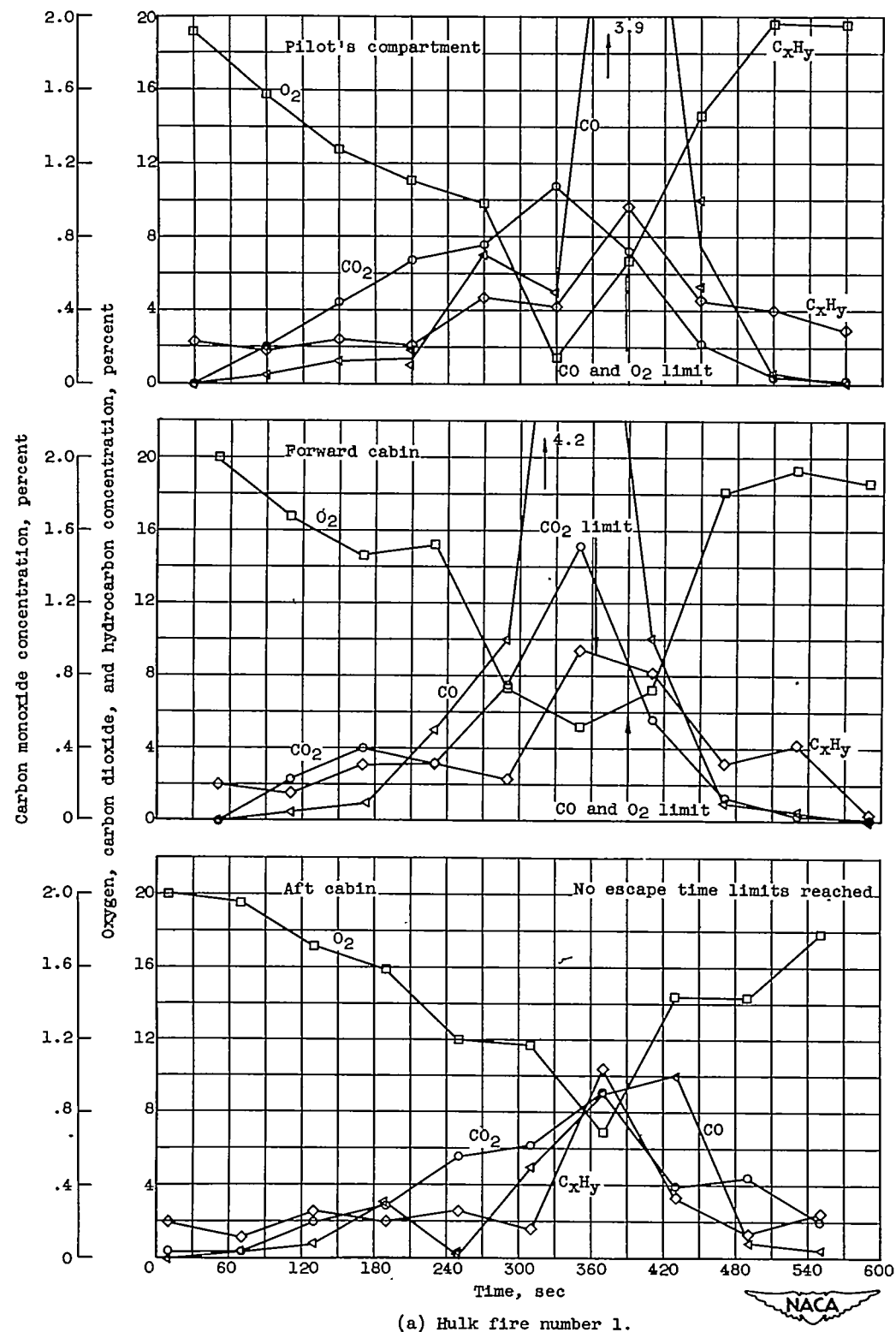


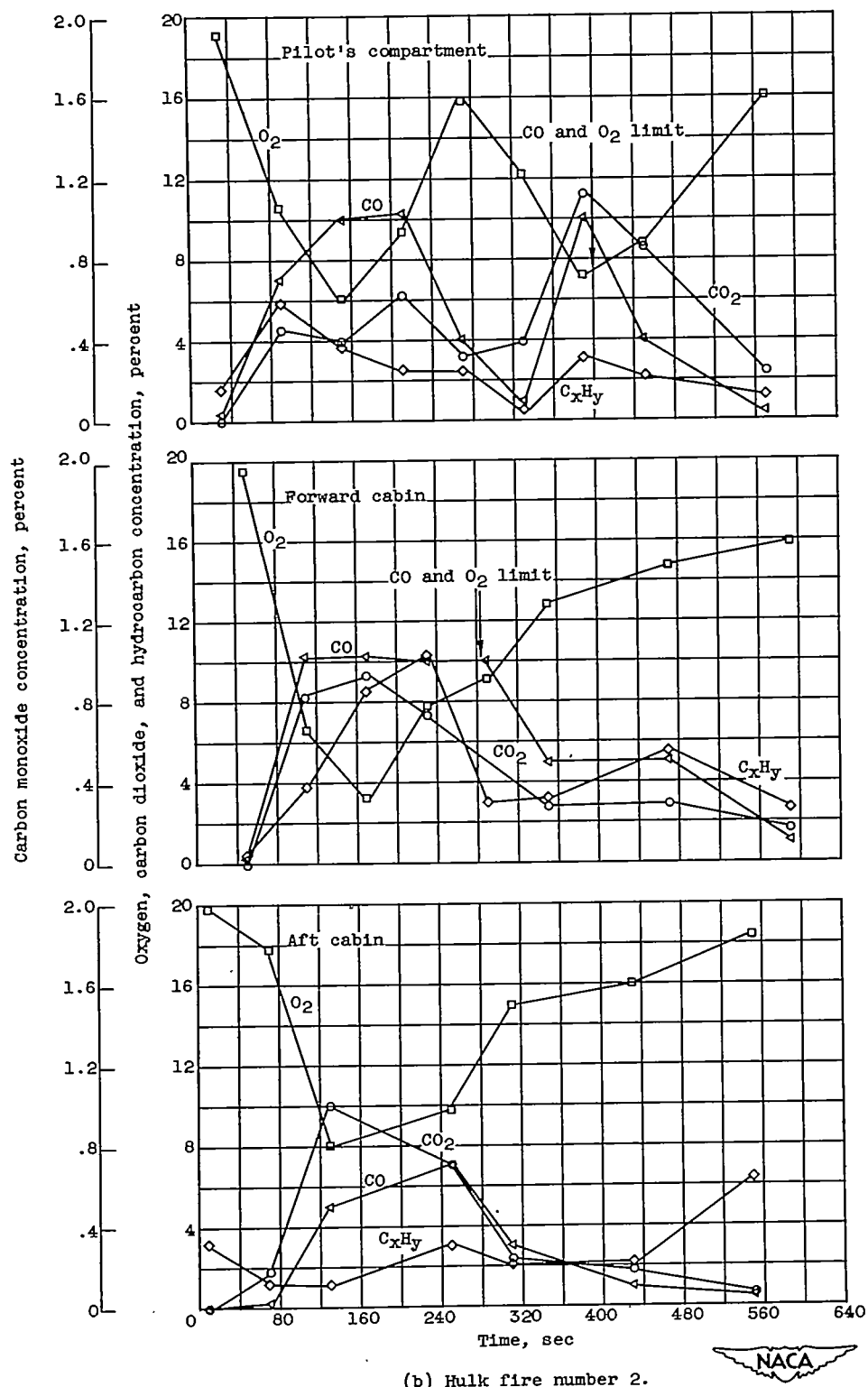
Figure 20. - Threshold curves of carbon-dioxide concentration and duration of exposure tolerable by healthy human beings.  
 (Curves 1, 2, and 3 from ref. 9.)



(a) Hulk fire number 1.



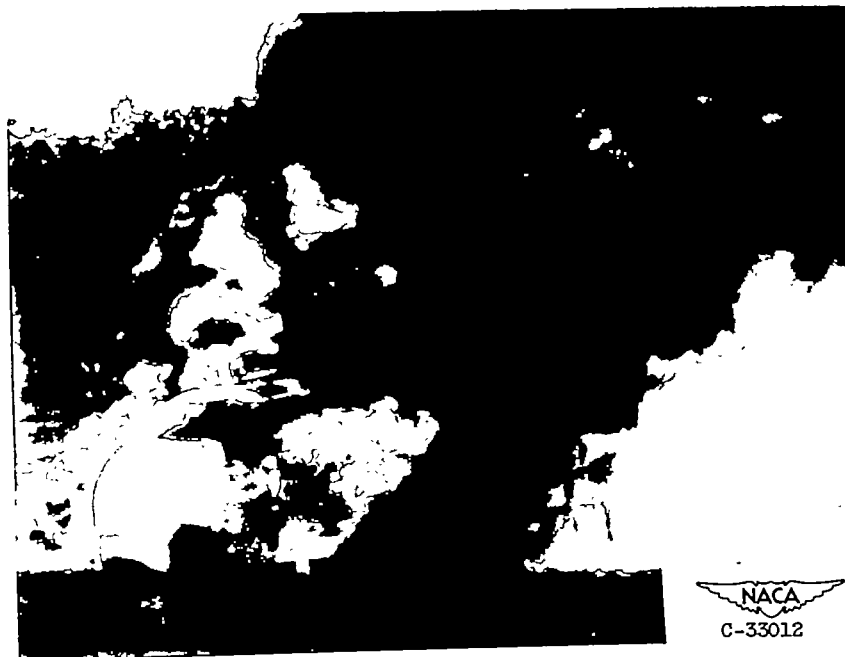
Figure 21. - Time histories of gas concentrations at various positions in burning airplane hulks.



(b) Hulk fire number 2.

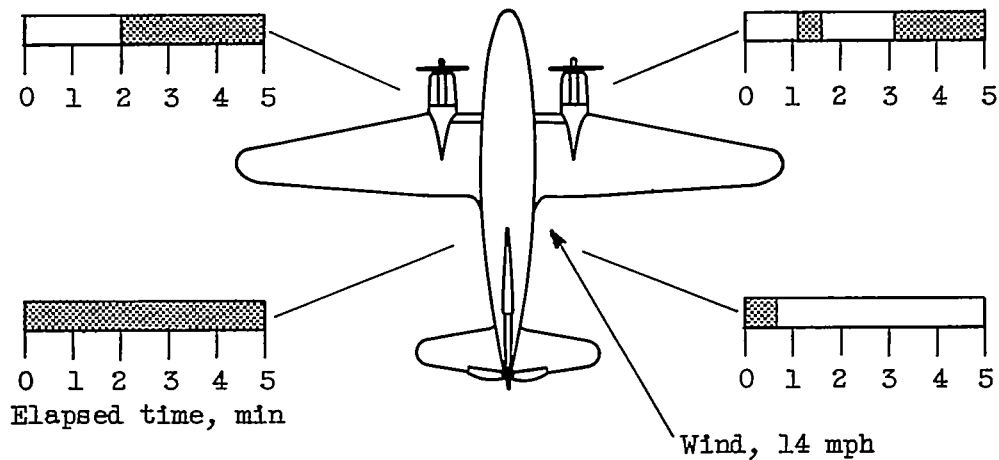


Figure 21. - Concluded. Time histories of gas concentrations at various positions in burning airplane hulks.

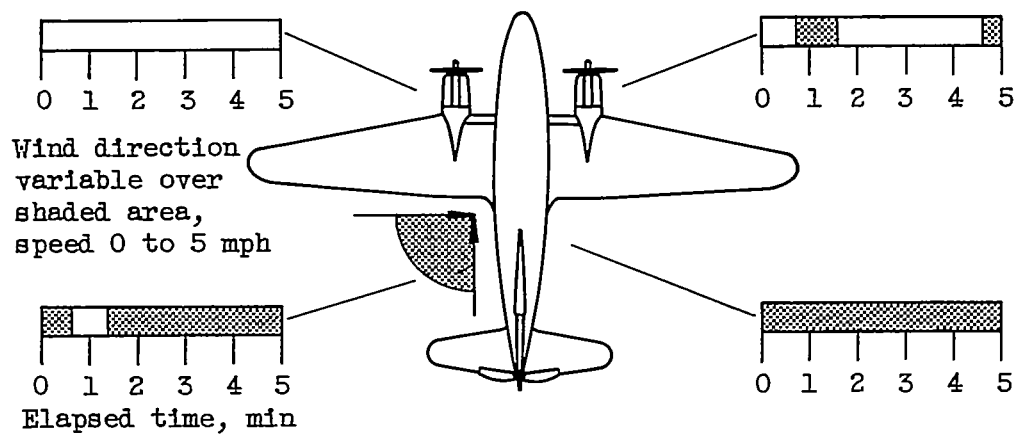


NACA  
C-33012

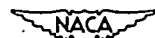
Figure 22. - Flame from explosion of hydrocarbon vapor in fuselage escaping through forward fuselage door.



(a) Crash 1; low midwing airplane.

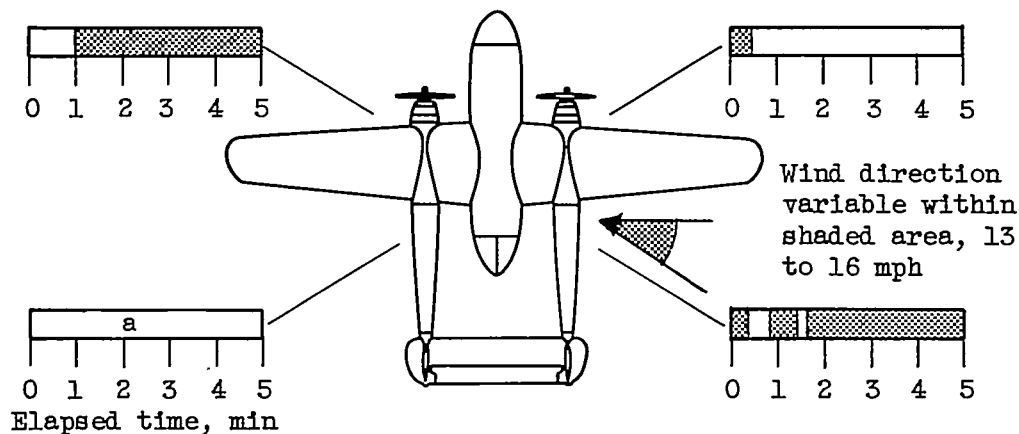


Escape possible  
 Escape impossible



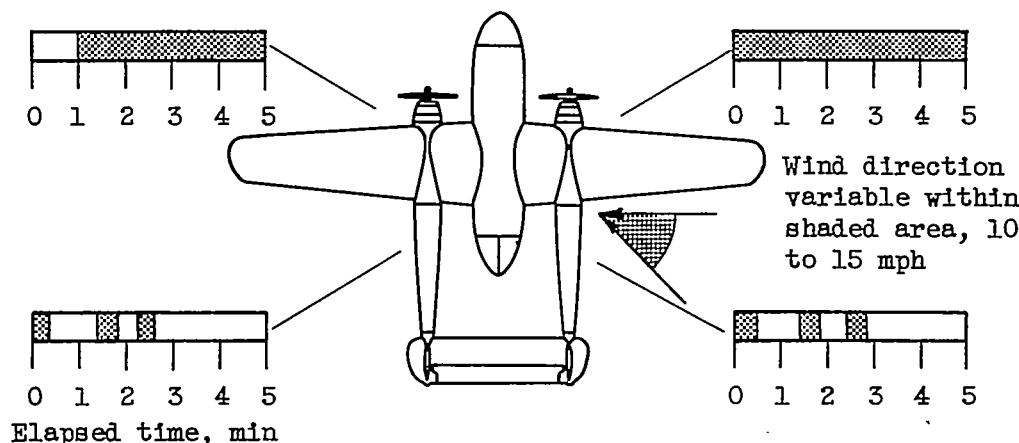
(b) Crash 3; low midwing airplane.

Figure 23. - Time histories of escape possibility from various quarters of several transport airplanes involved in crash fire.



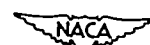
<sup>a</sup>Data not obtained.

(c) Crash 6; high wing airplane.



Escape possible

Escape impossible



(d) Crash 7; high wing airplane.

Figure 23. - Concluded. Time histories of escape possibility from various quarters of several transport airplanes involved in crash fire.



NACA  
C-28139

- a) Escape avenue to right rear of airplane open approximately 30 seconds after impact and after fuel mist flash fire had burned away; wind from right rear; crash 1.



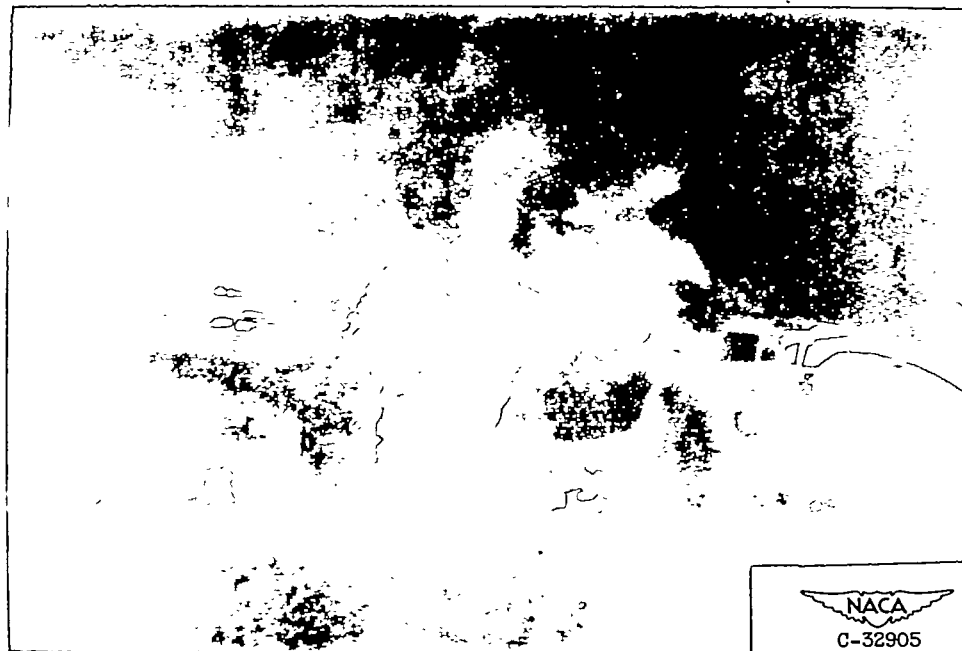
NACA  
C-33010

- (b) Escape avenue to left front; wind from left rear quarter, variable at 0 to 5 miles per hour; crash 3.

Figure 24. - Escape avenues.

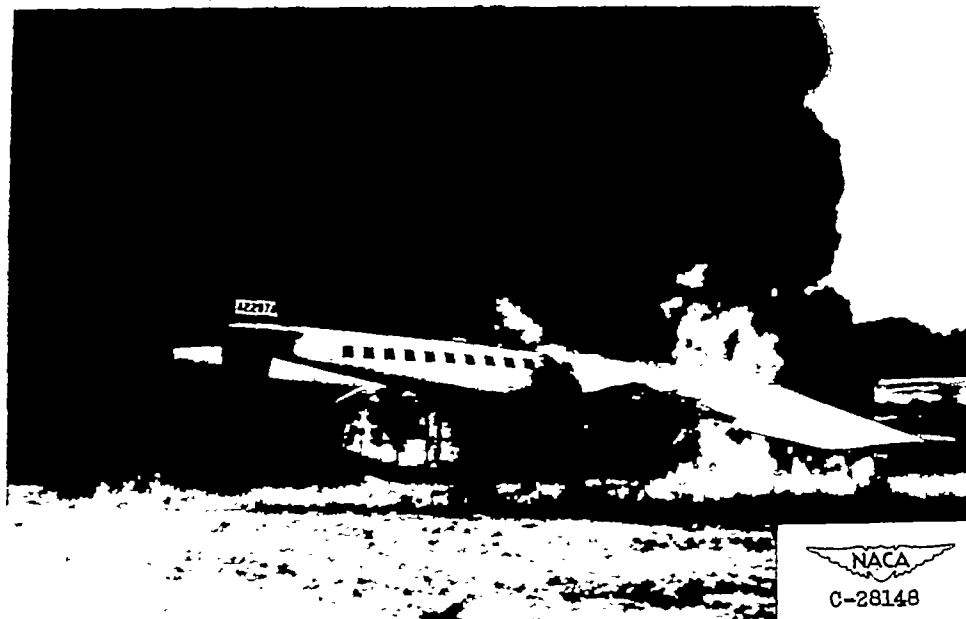


(c) Escape avenue to left rear after major part of spilled fuel had burned away; wind from left rear, 0 to 5 miles per hour; crash 3.



(d) Escape avenue to right front; wind from right rear, 13 to 16 miles per hour; crash 6.

Figure 24. - Continued. Escape avenues.



NACA  
C-28148

(e) Escape avenue to right rear after fuel mist fire burned away; wind from right rear, 10 to 15 miles per hour; crash 7.

Figure 24. - Concluded. Escape avenues.



NACA  
C-28197

Figure 25. - Typical damage to steel propeller blade caused by impact with crash barrier.

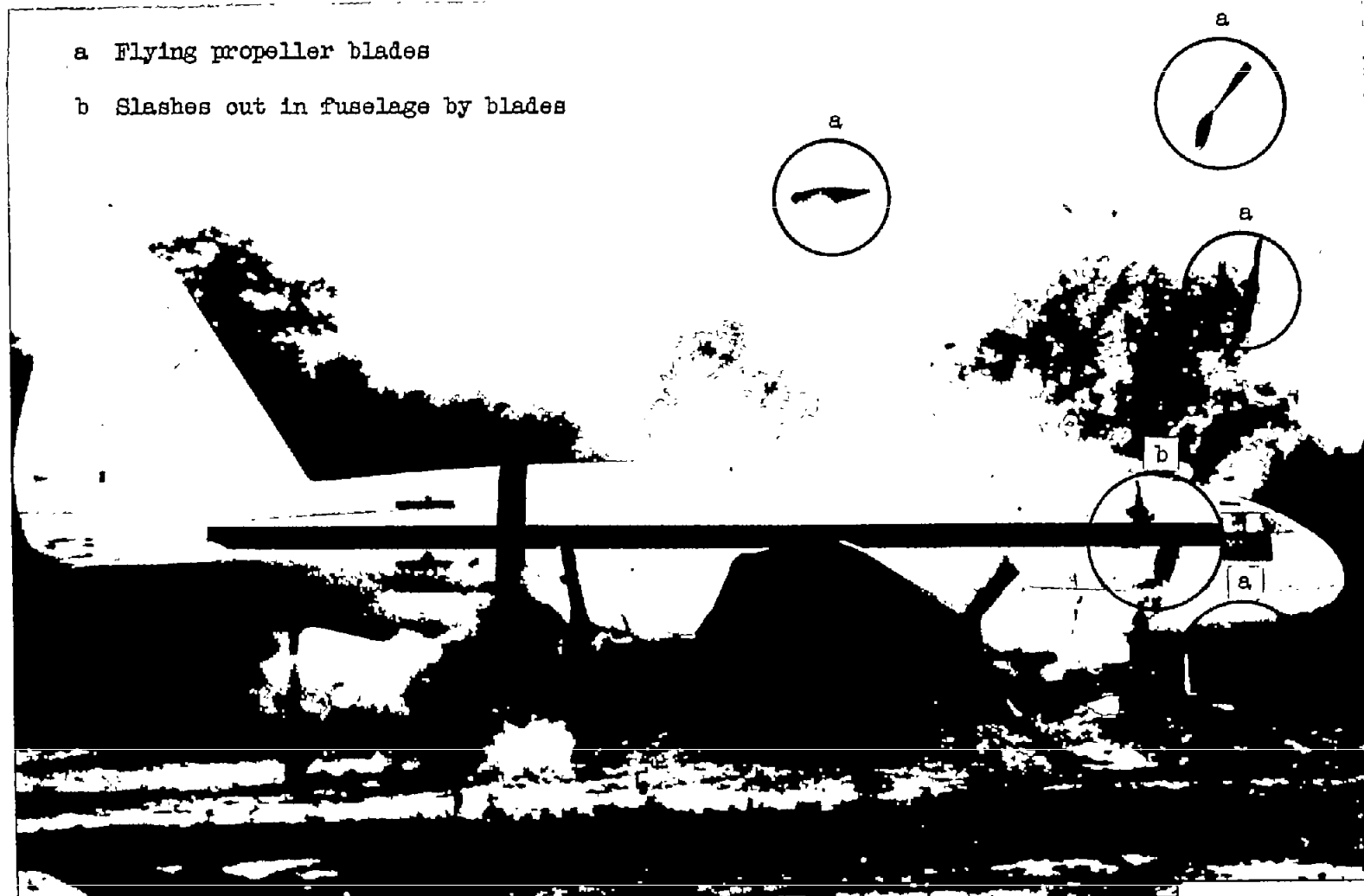


Figure 26. - Typical example of damage to fuselage by flying propeller blades.

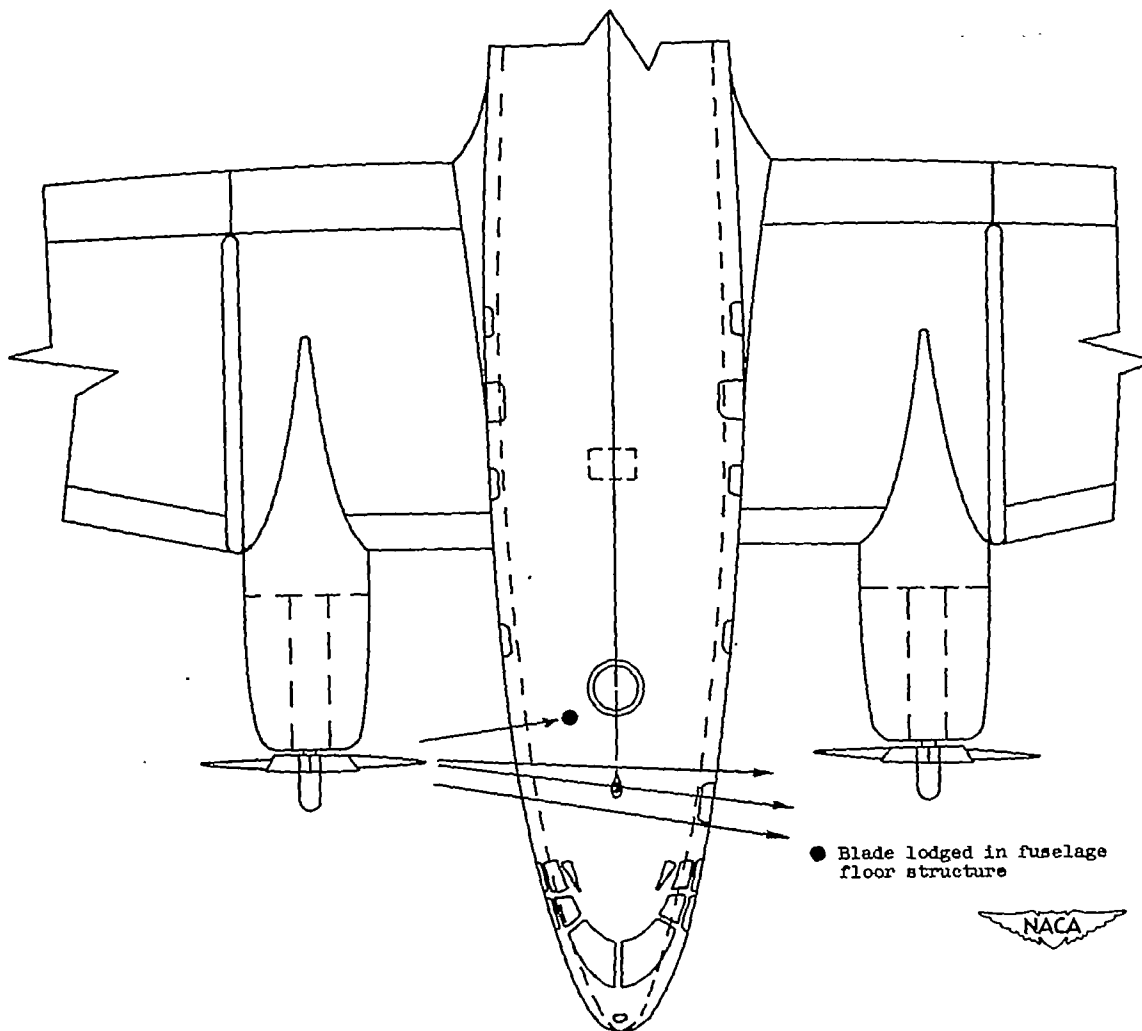
NACA  
C-28159



Figure 27. - Section of broken forged aluminum propeller blade caused by impact of blade with an obstacle.

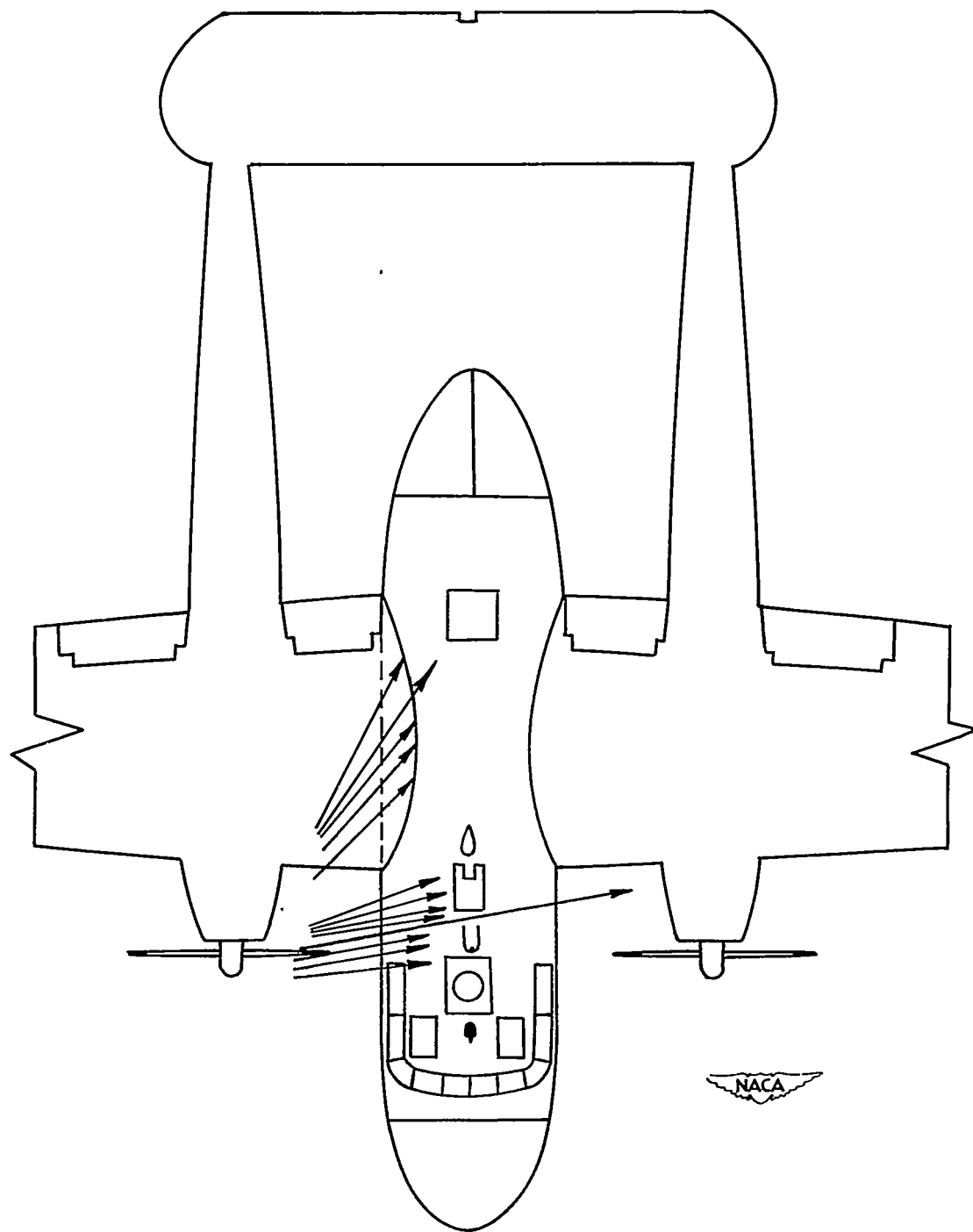


Figure 28. - Typical damage caused by flying fragments of forged aluminum propeller blades.



(a) Penetration by steel propeller blades during four crashes.

Figure 29. - Penetration of fuselage by propeller fragments.



(b) Penetration by forged aluminum propeller fragments during 14 crashes.

Figure 29. - Concluded. Penetration of fuselage by propeller fragments.



NACA  
C-28152

Figure 30. - Hole made in floor when front landing-gear strut and guide slipper were detached by contact with obstacle at crash barrier and penetrated floor structure.



Figure 31. - Position of front landing-wheel strut after penetrating floor and rebounding from rear of cabin.



NACA  
C-28157

Figure 32. - Damage resulting when front landing-gear structure penetrates floor.

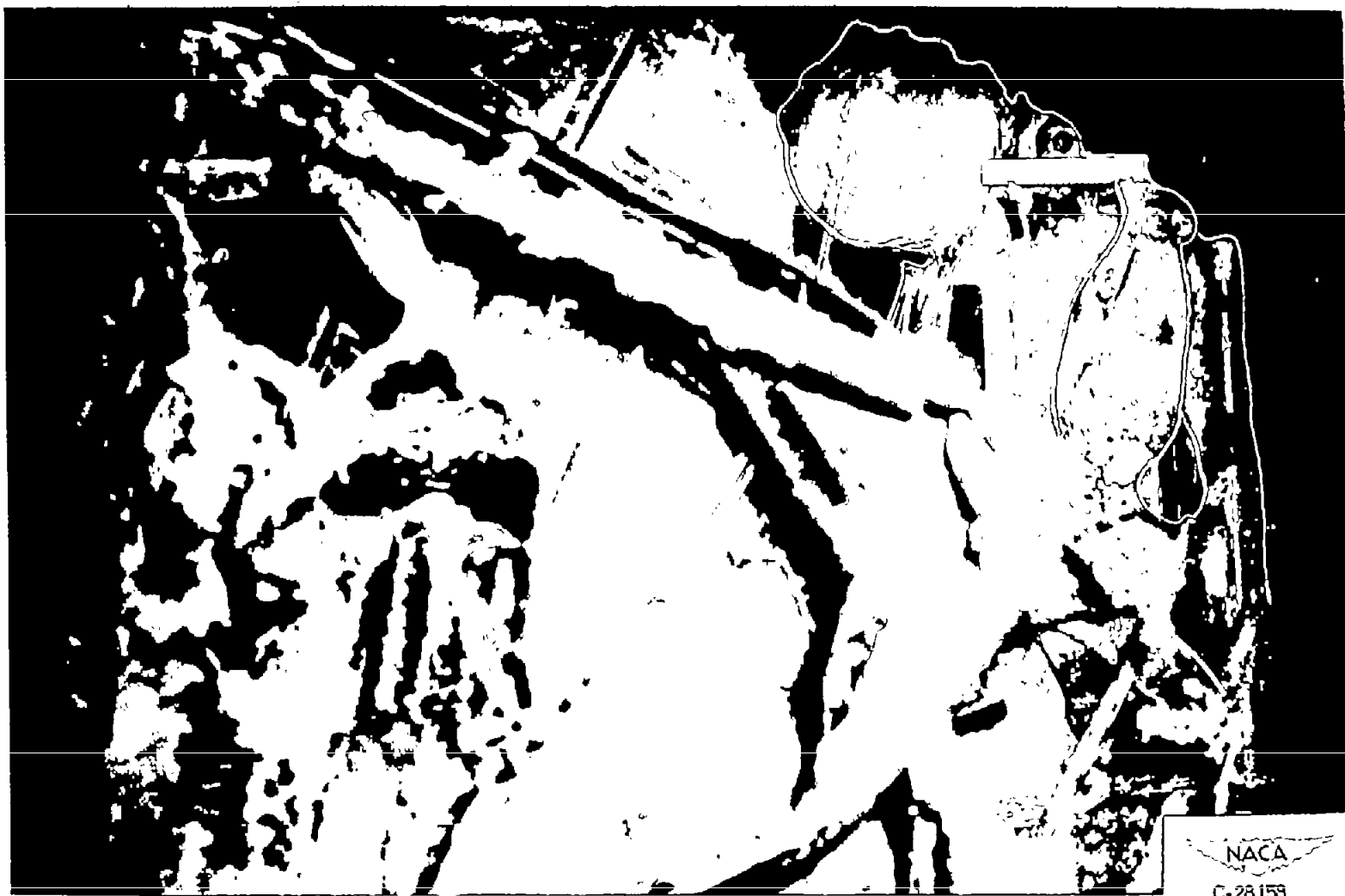
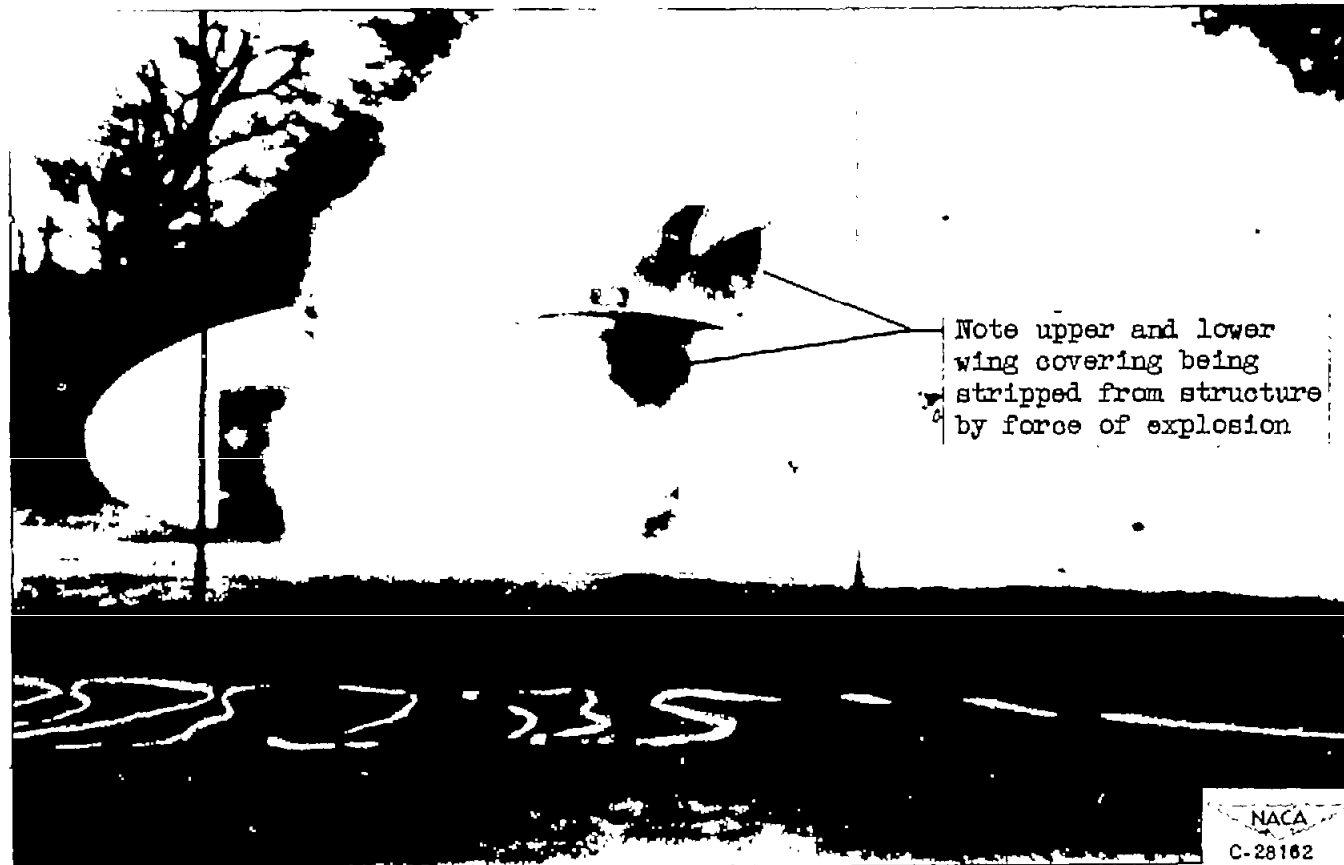
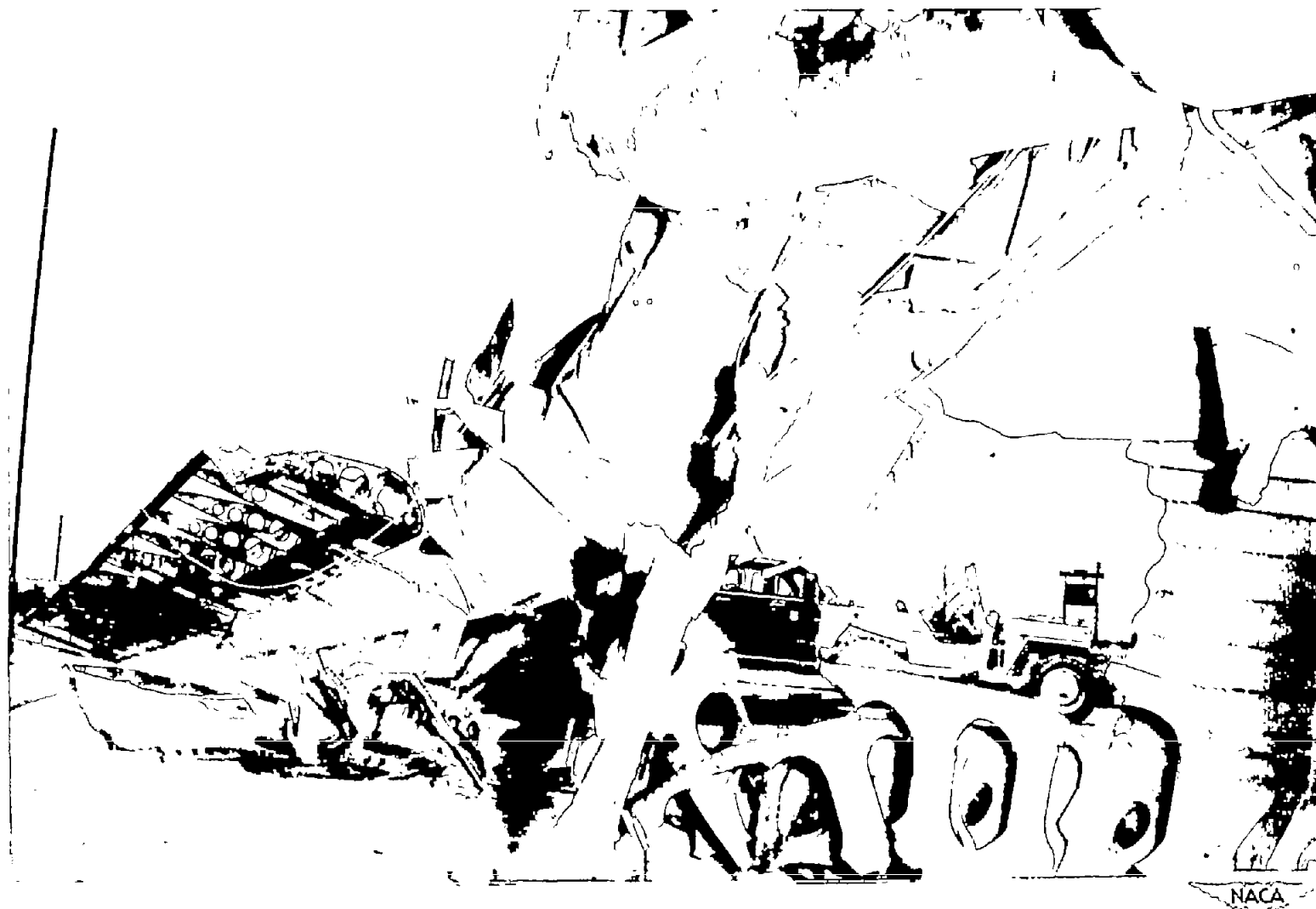


Figure 53. - Destruction of front landing-gear bulkhead and structure. Proximity to dummy shows possibility of injury to occupants seated in front part of fuselage.



(a) Ignition  $4\frac{1}{2}$  seconds after impact.

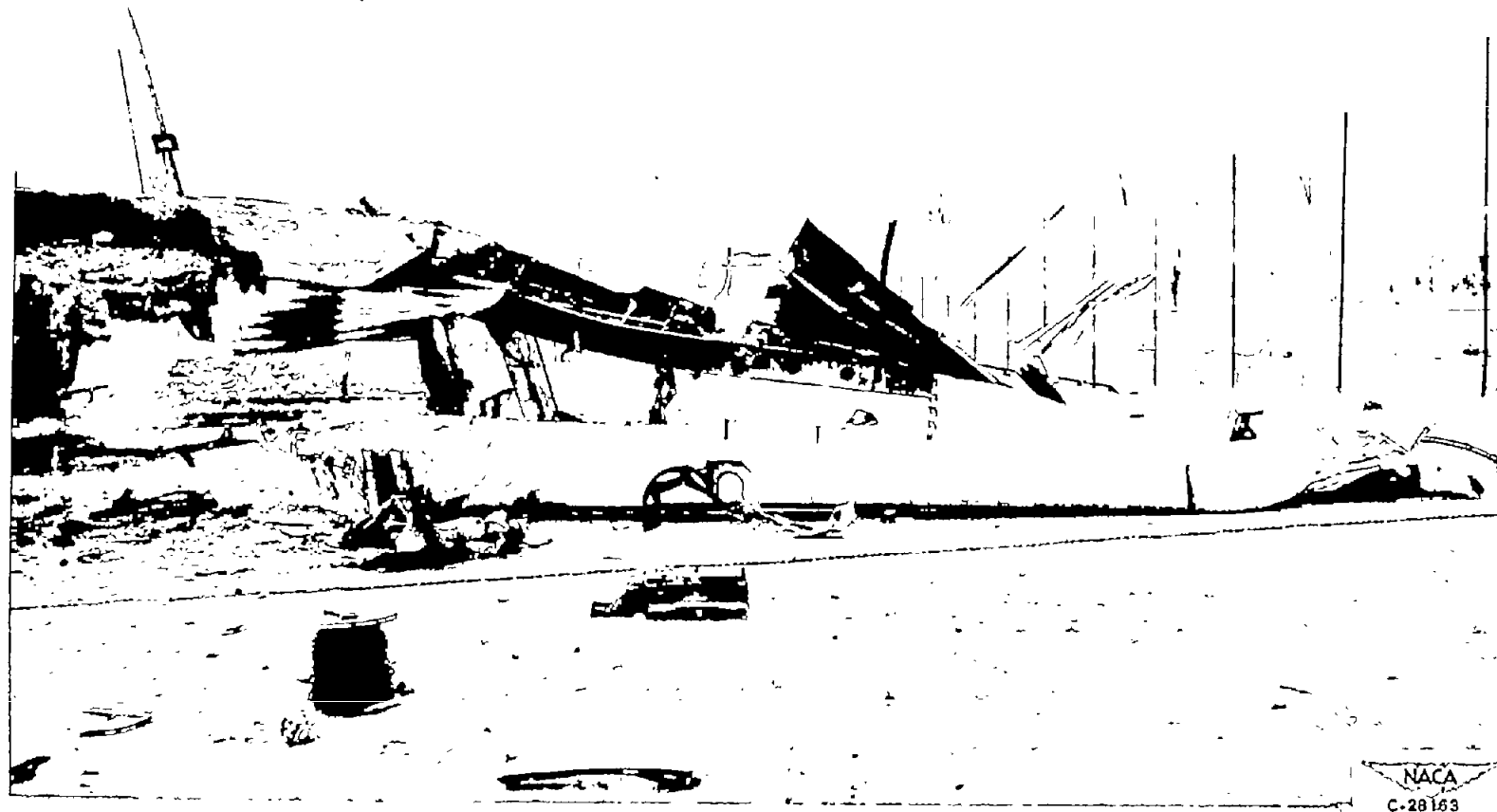
Figure 34. - Wing explosion resulting from ignition of fuel-air mixture accumulated in wing while airplane was sliding to a stop.



(b) Rear view of damage to wing structure.

Figure 34. - Continued. Wing explosion resulting from ignition of fuel-air mixture accumulated in wing while airplane was sliding to a stop.

NACA  
C-28164



(c) Front view of damage to wing structure.

Figure 34. - Concluded. Wing explosion resulting from ignition of fuel-air mixture accumulated in wing while airplane was sliding to a stop.

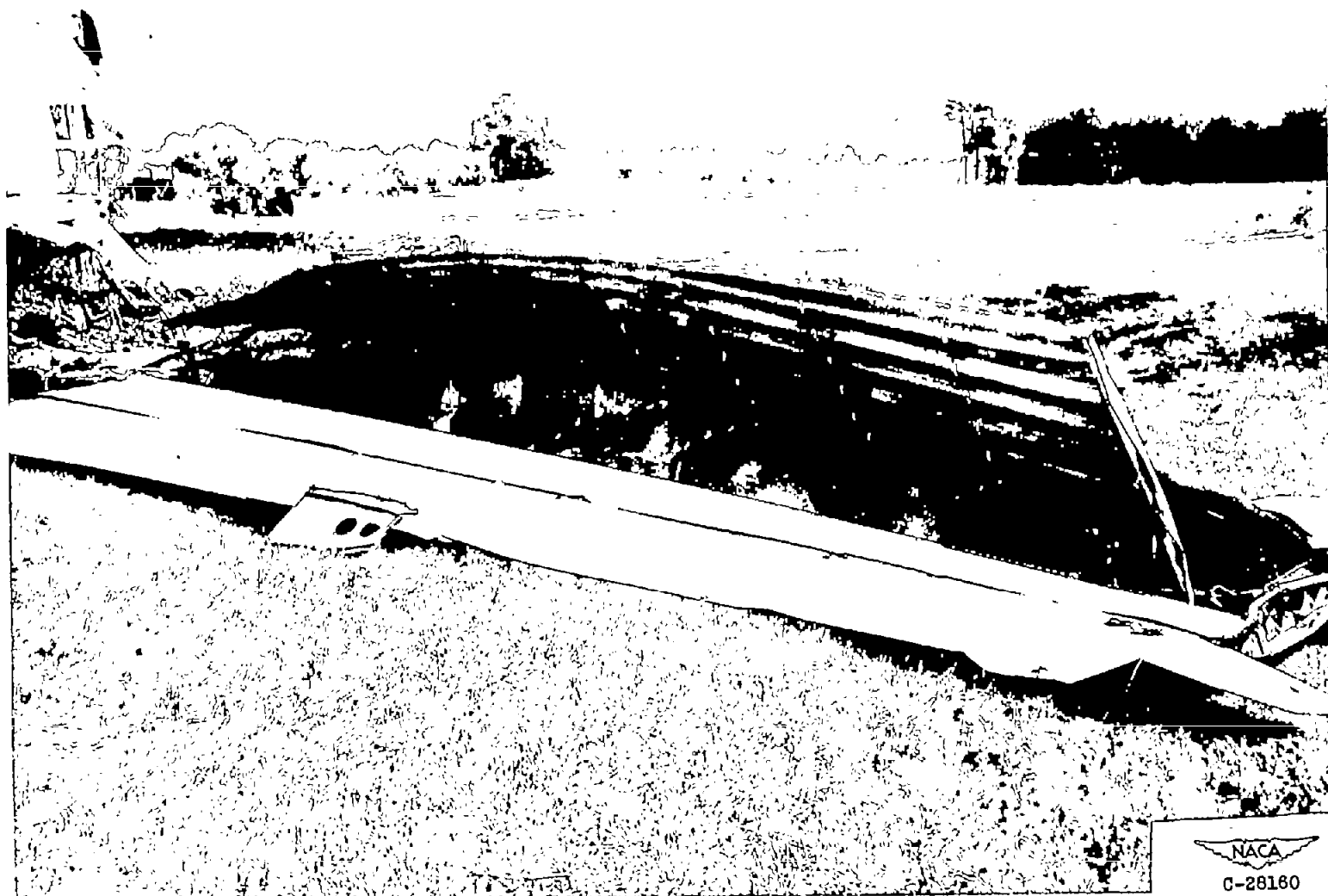


Figure 35. - Wing damage resulting from internal explosion that occurred several minutes after original fire was in progress. Explosion caused by ignition of fuel-air mixture trapped in wing.

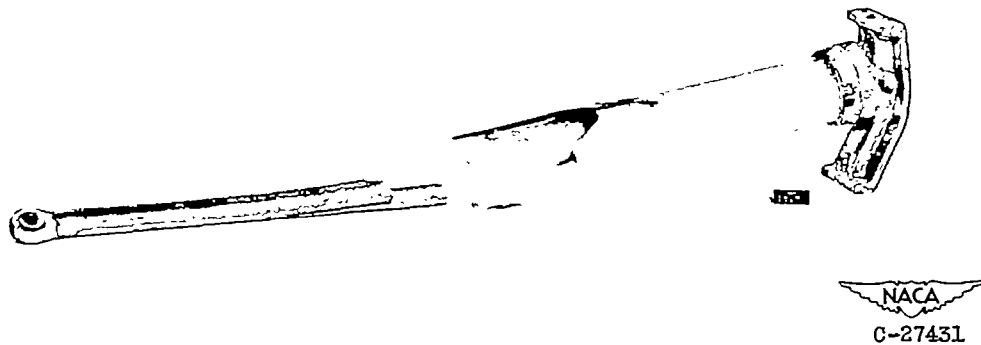


Figure 36. - Damage resulting when hydraulic shock strut was heated by aircraft fire and exploded.

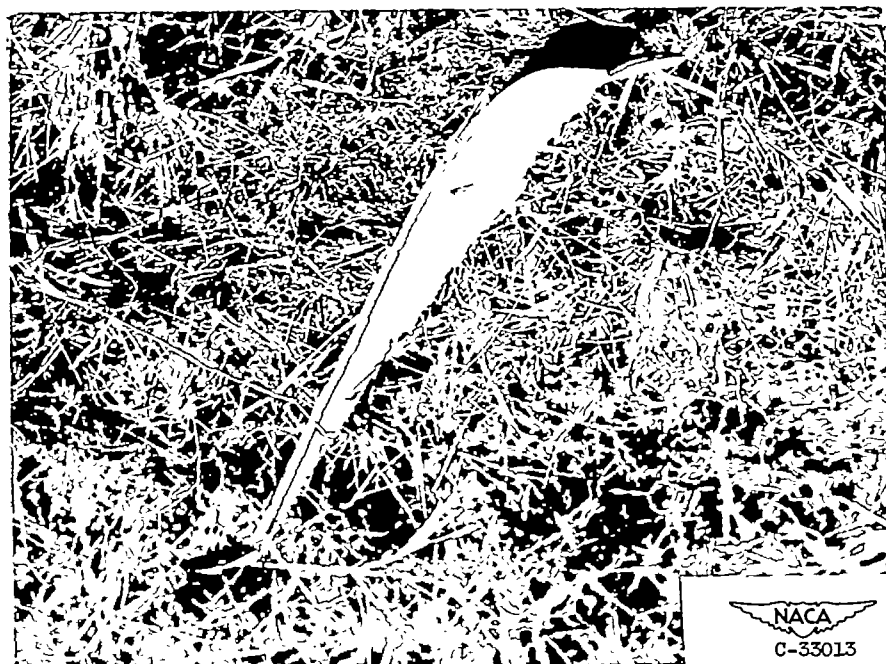


Figure 37. - Fragment of hydraulic shock strut cylinder found 150 feet from airplane after shock strut exploded because of fire.



Figure 38. - Insignificant damage to floor structure of low-midwing, twin-engine type aircraft resulting from simulated take-off accident. Cabin floor lies along indented joint line between two curved sections of fuselage.

NACA  
C-28140

NACA TN 2996

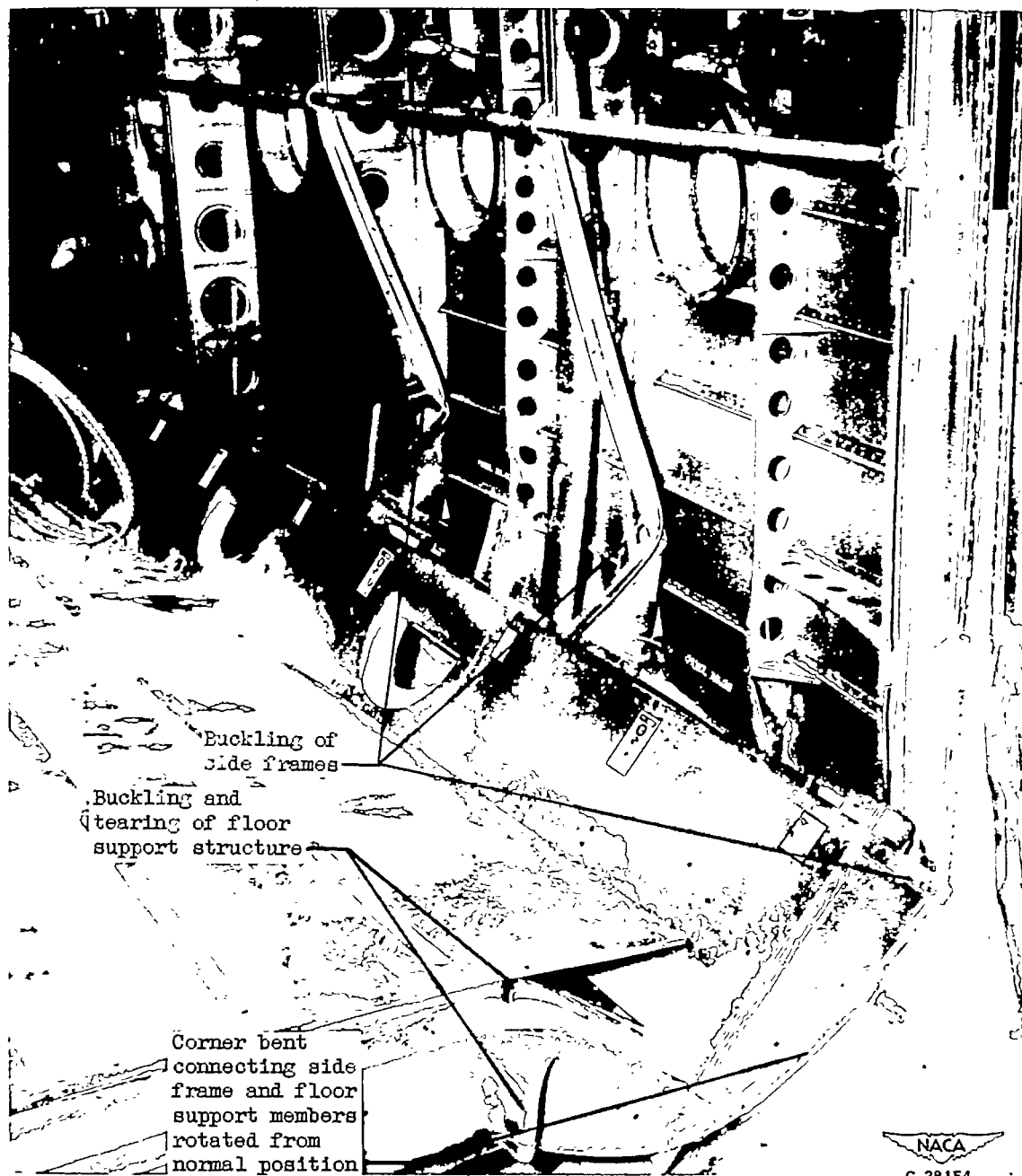


Figure 39. - Damage to packet-type cargo airplane floor structure and side framing resulting from vertical impact and sliding friction on hard ground surface.

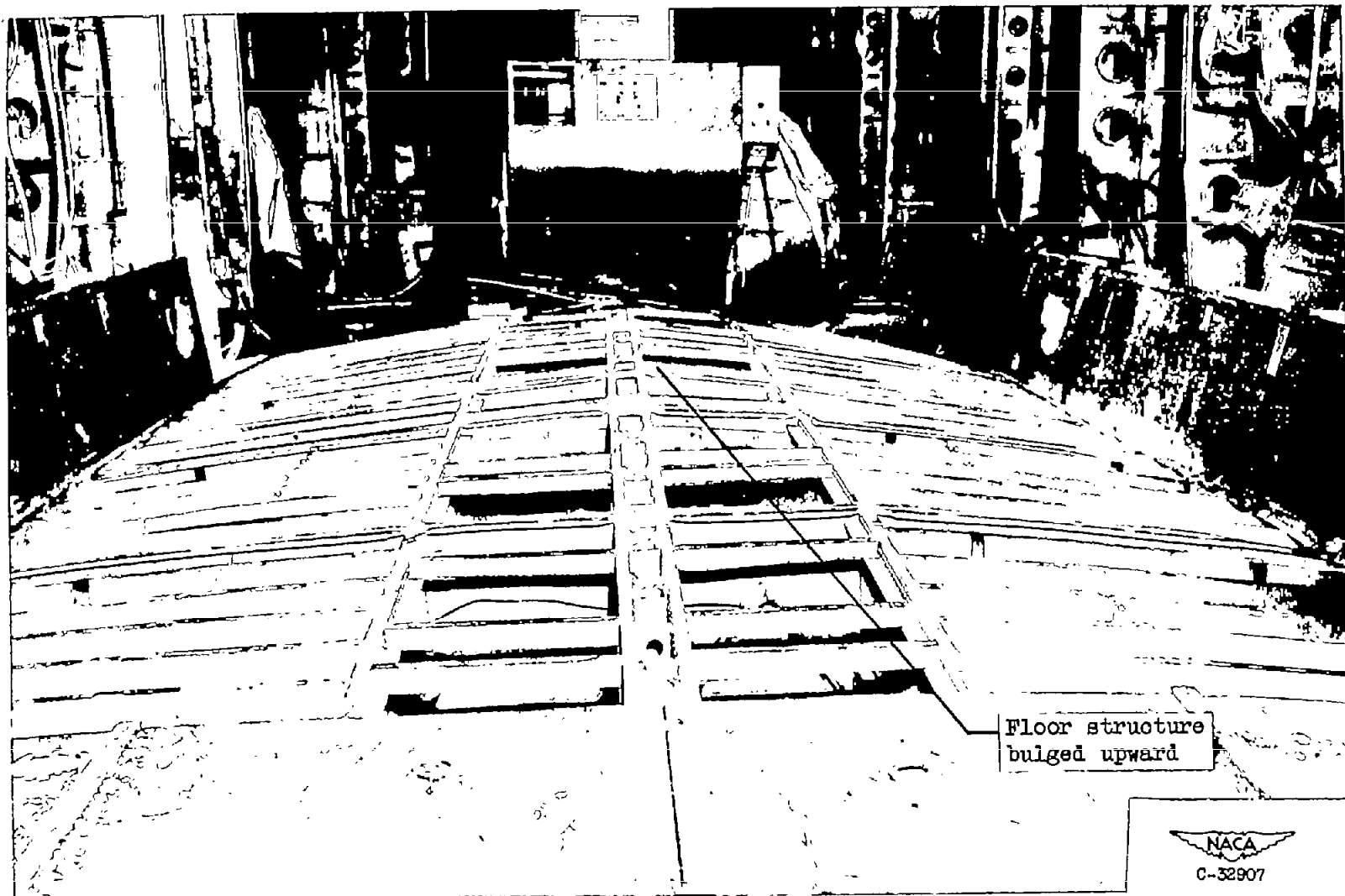


Figure 40. - Floor support structure of cargo-type airplane bulged slightly upward as a result of nose-wheel damage and landing impact upon hard dirt surface.

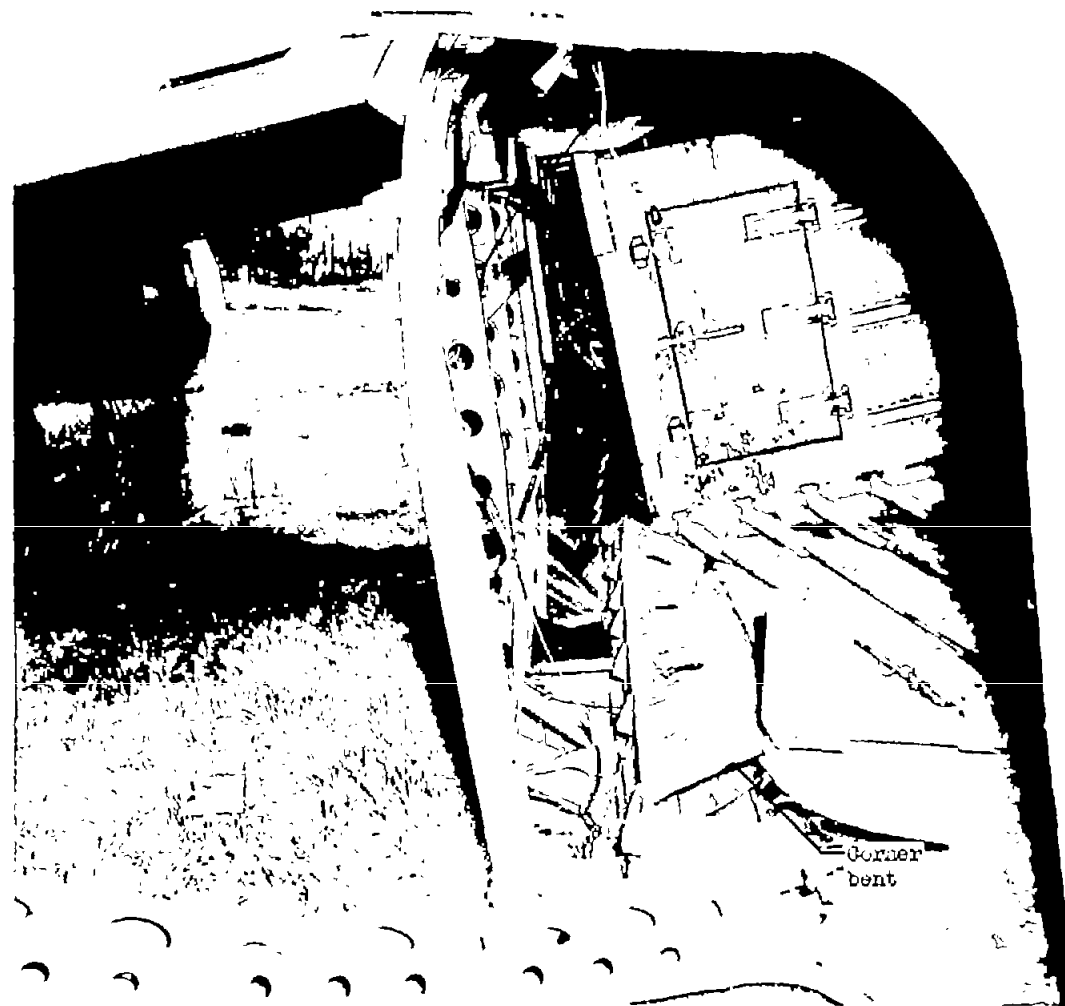
Floor structure  
bulged upward

NACA  
C-32907



NACA  
O-32908

Figure 41. - Floor structure of cargo-type airplane severely damaged and bulged upward as a result of nose-wheel damage and landing upon a mud surface.



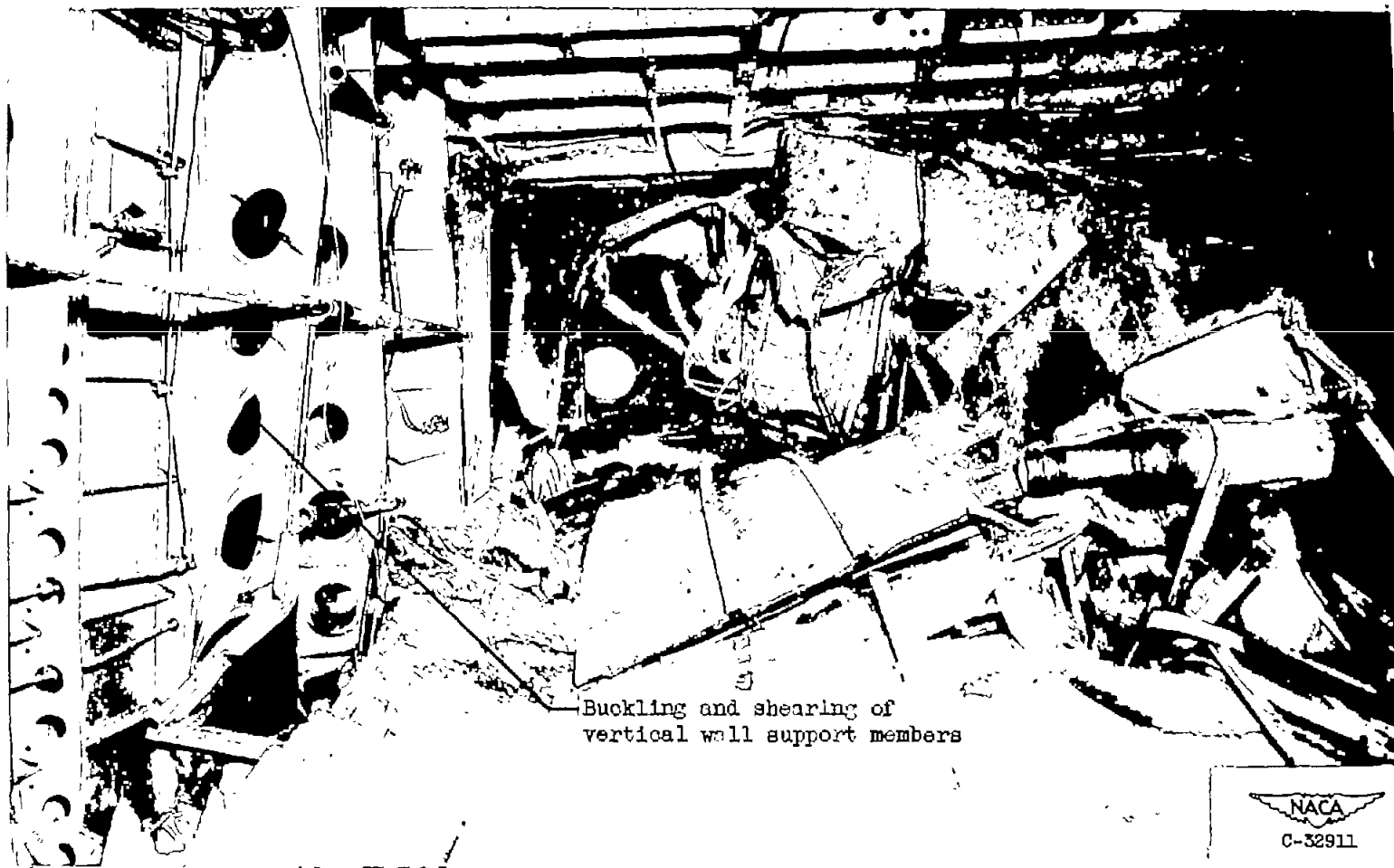
NACA  
C-32909

Figure 42. - Corner bent rotated from  $90^{\circ}$  to about  $120^{\circ}$  from its normal position by combined lateral and vertical forces caused by ground loop.



(a) Side members separated from ceiling members.

Figure 43. - Incipient lateral collapse of rectangular-type fuselage framing from lateral load imposed by ground-loop crash.



(b) Buckling and shearing of vertical wall members.

Figure 43. - Continued. Incipient lateral collapse of rectangular-type fuselage framing resulting from lateral load imposed by ground-loop crash.



(c) Buckling of side frame structure.

Figure 43, - Continued. Incipient lateral collapse of rectangular-type fuselage framing resulting from lateral load imposed by ground-loop crash.



(d) Fractured connection between side frame and ceiling members.

Figure 43. - Continued. Incipient lateral collapse of rectangular-type fuselage framing resulting from lateral load imposed by ground-loop crash.



(e) Side of fuselage bulged.

figure 43. - Concluded. Incipient lateral collapse of rectangular-type fuselage framing resulting from lateral load imposed by ground-loop crash.

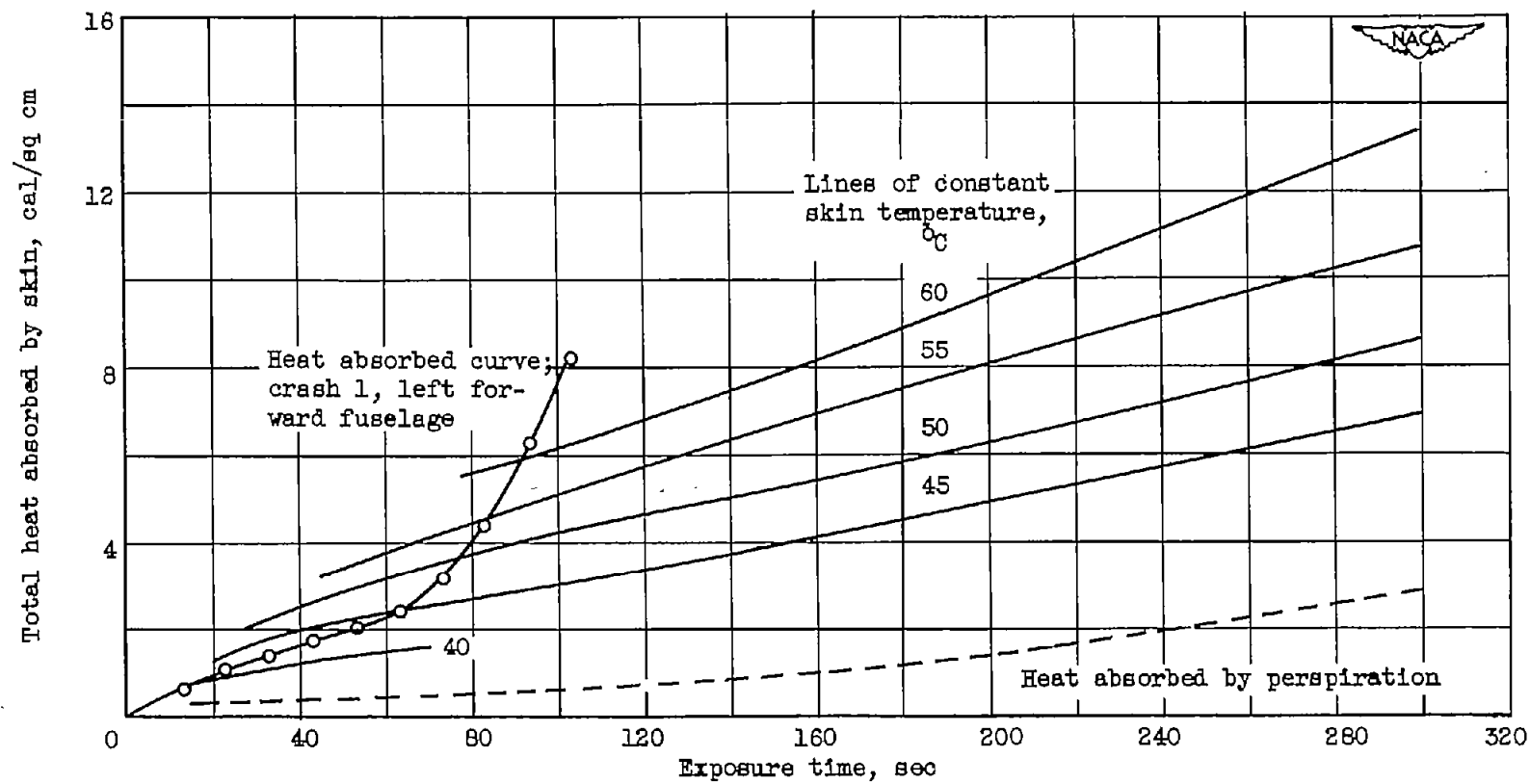


Figure 44. - Diagram showing temperature of human skin resulting from absorption of heat shown by ordinate during time interval shown by abscissa. (Diagram based on data from refs. 4 and 15.)

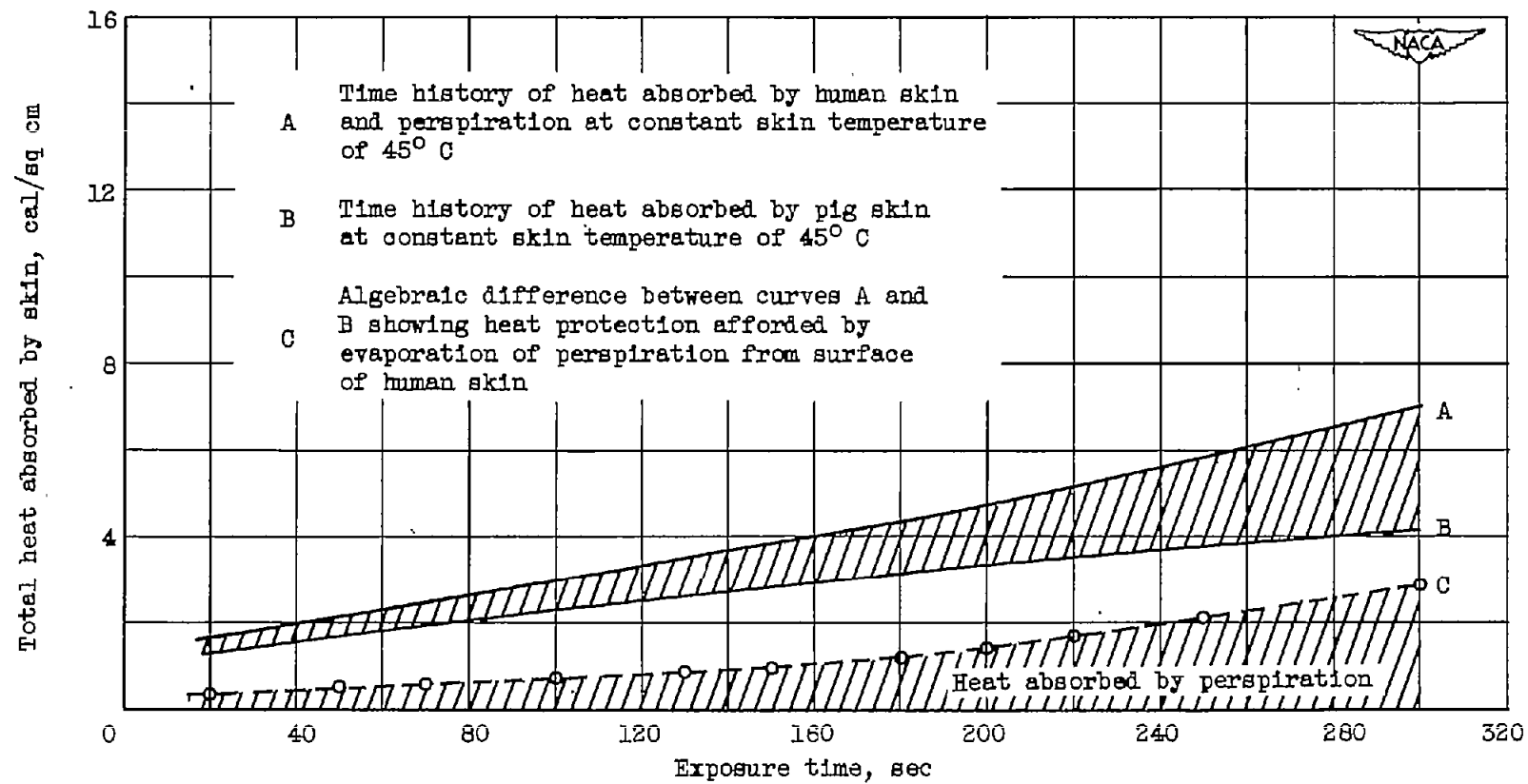


Figure 45. - Differences in heat absorption by human and pig skin attributable to perspiration.

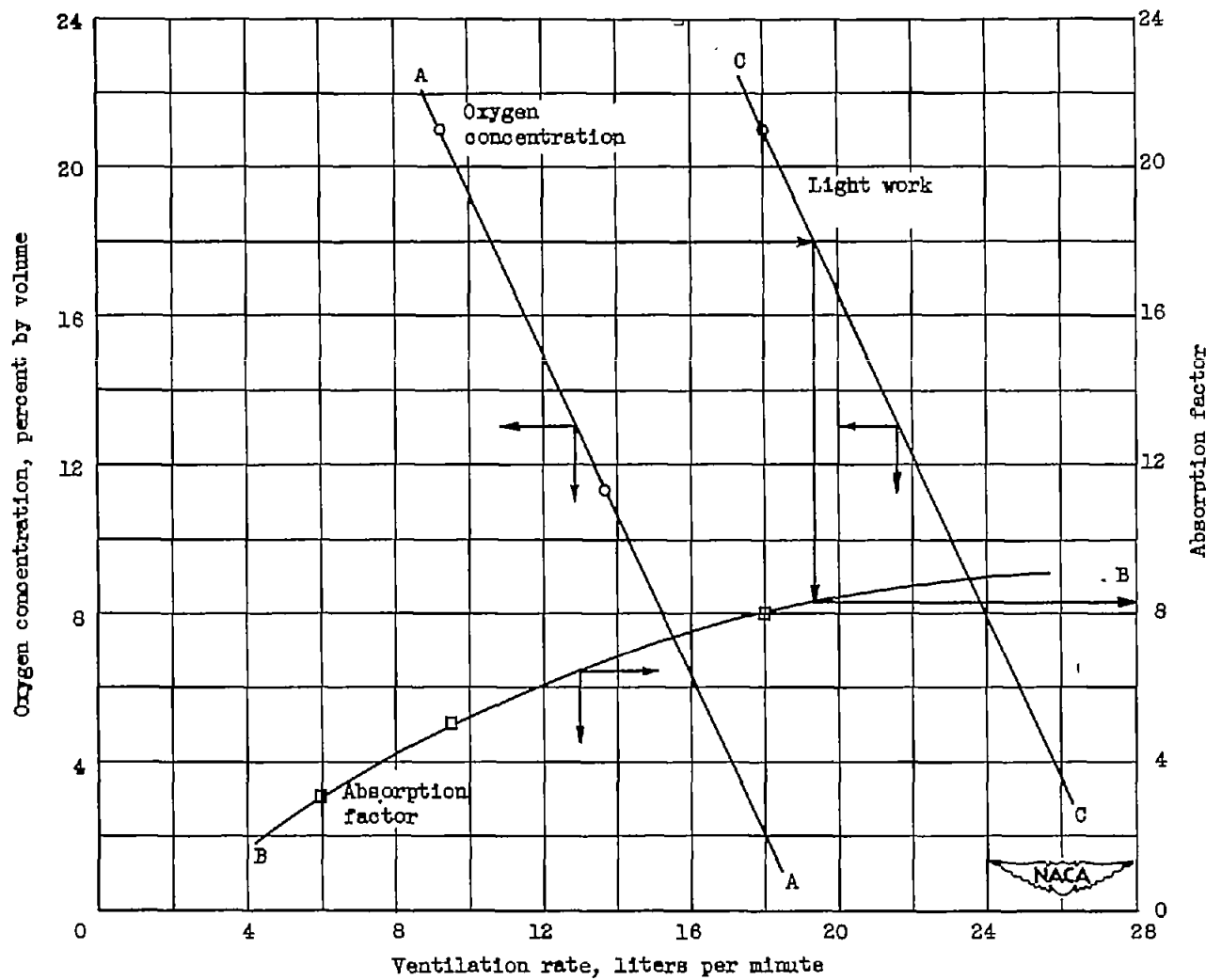


Figure 46. - Diagram for determining carbon monoxide absorption factor for a subject doing light work in various oxygen concentrations. (Based upon data presented in ref. 8.)